AD-A047 981 MARYLAND UNIV COLLEGE PARK INST FOR FLUID DYNAMICS --ETC F/G 4/2
ENVIRONMENTAL CONDITIONS IN A TROPICAL FOREST REGION IN THAILAN--ETC(U)
NOV 74 H E LANDSBERG, O E THOMPSON DAAK02-72-C-0287
UNCLASSIFIED BN-799 ETL-0129 NL

1 OF 2
ADA047 981

ETL-0129

INSTITUTE

for

FLUID DYNAMICS

and

APPLIED MATHEMATICS

Technical Note BN 799

November 1974

ENVIRONMENTAL CONDITIONS IN A TROPICAL FOREST REGION IN THAILAND

by

Helmut E. Landsberg
Owen E. Thompson
Robert E. Kaylor
Rachel T. Pinker

Preliminary Final Report: Contract DAAK02-72-C-0287, U.S. Army Engineer Topographic Laboratory, Ft. Belvoir, Virginia; H. E. Landsberg, Principal Investigator

Publication #109, Graduate Program in Meteorology

UNIVERSITY OF MARYLAND
College Park

REVERSE OF FRONT COVER

Destroy this report when no longer needed.
Do not return it to the originator.

The findings in this report are not to be construed as an official Department of the Army position unless so designated by other authorized documents.

The citation in this report of trade names of commercially available products does not constitute official endorsement or approval of the use of such products.

ETL-0129

Technical Note BN 799 November 1974

ENVIRONMENTAL CONDITIONS IN A TROPICAL FOREST REGION IN THAILAND

by

Helmut E. Landsberg
Owen E. Thompson
Robert E. Kaylor
Rachel T. Pinker

Preliminary Final Report: Contract DAAK02-72-C-0287, U.S. Army Engineer Topographic Laboratory, Ft. Belvoir, Virginia; H. E. Landsberg, Principal Investigator

Publication #109, Graduate Program in Meteorology

Approved For Public Release
Distribution Unlimited

UNCLASSIFIED

SECURITY CLASSIFICATION OF THIS PAGE (When Data Entered)

(19) **REPORT DOCUMENTATION PAGE**

READ INSTRUCTIONS BEFORE COMPLETING FORM

(18) 1. REPORT NUMBER: ETL-0129	2. GOVT ACCESSION NO.
3. RECIPIENT'S CATALOG NUMBER	
(6) 4. TITLE (and Subtitle): Environmental Conditions in a Tropical Forest Region in Thailand	(9) 5. TYPE OF REPORT & PERIOD COVERED: Contract Report.
6. PERFORMING ORG. REPORT NUMBER: 109	
(10) 7. AUTHOR(s): Helmut E. Landsberg, Owen E. Thompson, Robert E. Kaylor, Rachel T. Pinker	(15) 8. CONTRACT OR GRANT NUMBER(s): DAAK 02-72-C-0287
9. PERFORMING ORGANIZATION NAME AND ADDRESS: Institute for Fluid Dynamics & Applied Mathematics, University of Maryland, College Park, Maryland 20742	10. PROGRAM ELEMENT, PROJECT, TASK AREA & WORK UNIT NUMBERS
11. CONTROLLING OFFICE NAME AND ADDRESS: U.S. Army Engineer Topographic Laboratories, Fort Belvoir, Virginia 22060	(11) 12. REPORT DATE: November 1974
	13. NUMBER OF PAGES: 171
(12) 186 p.	15. SECURITY CLASS. (of this report): Unclassified
	15a. DECLASSIFICATION/DOWNGRADING SCHEDULE

16. DISTRIBUTION STATEMENT (of this Report)

Approved for public release; distribution unlimited

(14) BN-799, PUB-199

17. DISTRIBUTION STATEMENT (of the abstract entered in Block 20, if different from Report)

18. SUPPLEMENTARY NOTES

19. KEY WORDS (Continue on reverse side if necessary and identify by block number)

Climatological	Relative Humidity
Infra-red Radiation	Richardson Gradient Number
Micro[illegible]orological	Solar Radiation
Monso[illegible]	Thailand
Rain[illegible]	Tropical Forest

20. ABSTRACT (Continue on reverse side if necessary and identify by block number)

Major results of a two year project to study the climatological and micrometeorological conditions in a tropical evergreen forest region and summarized in this report. The study has been under the sponsorship of the U. S. Army Engineer Topographic Laboratory. The forest area under study is in the interior of Thailand and is influenced by a cool, dry northeast monsoonal flow from November to March and a warm, moist southwest monsoonal flow from May to September. Measured information were collected during a three

DD FORM 1 JAN 73 1473 EDITION OF 1 NOV 65 IS OBSOLETE

179 450

UNCLASSIFIED

SECURITY CLASSIFICATION OF THIS PAGE (When Data Entered)

Block #20 cont'd

year field program sponsored by the U. S. Army Natick Laboratories and included ground station temperature, relative humidity, precipitation, evaporation, hours of sunshine, and tower measurements of temperature, dew point temperature, and wind speed, incoming and reflected solar radiation, incoming and outgoing infra-red radiation and sub-surface temperature profiles in the forest and in a cleared area within the forest region.

The results discussed here include a climatological survey of the experimental site as well as a comparison of the monsoonal cycles at a number of widely dispersed sites in Southeast Asia; an analysis of the profiles of temperature and wind speed in the forest and cleared area; diurnal variations of static stability and Richardson number representative of several different periods of the year; a summary of calculations of the roughness characteristics of the forest canopy and the variability thereof; spectral analyses of kinetic energy above and within the forest canopy during both monsoonal flow regimes; estimates of the albedo of the forest and the net fluxes of radiational energy for several periods of the year; estimates of sensible and latent heat fluxes above the forest canopy.

ABSTRACT

Major results of a two year project to study the climatological and micrometeorological conditions in a tropical evergreen forest region are summarized in this report. The study has been under the sponsorship of the U. S. Army Engineer Topographic Laboratory. The forest area under study is in the interior of Thailand and is influenced by a cool, dry northeast monsoonal flow from November to March and a warm, moist southwest monsoonal flow from May to September. Measured information were collected during a three year field program sponsored by the U. S. Army Natick Laboratories and included ground station temperature, relative humidity, precipitation, evaporation, hours of sunshine, and tower measurements of temperature, dew point temperature, and wind speed, incoming and reflected solar radiation, incoming and outgoing infra-red radiation and sub-surface temperature profiles in the forest and in a cleared area within the forest region.

The results discussed here include a climatological survey of the experimental site as well as a comparison of the monsoonal cycles at a number of widely dispersed sites in Southeast Asia; an analysis of the profiles of temperature and wind speed in the forest and cleared area; diurnal variations of static stability and Richardson number representative of several different periods of the year; a summary of calculations of the roughness characteristics of the forest canopy and the variability thereof; spectral analyses of kinetic energy above and within the forest canopy during both monsoonal flow regimes; estimates of the albedo of the forest and the net fluxes of radiational energy for several periods of the year; estimates of sensible and latent heat fluxes above the forest canopy.

TABLE OF CONTENTS

LIST OF FIGURES

LIST OF TABLES

SECTION I - INTRODUCTION

This Technical Note serves as a final report on Contract DAAK-02-72-C-0287 from the U. S. Army Engineer Topographic Laboratory, Ft. Belvoir, Virginia, to the Graduate Program in Meteorology, University of Maryland. The scope of the research under this contract was to prepare a scientific analysis of the climatological and micro-meteorological data obtained during a scientific field program called TREND (Tropical Environmental Data). The TREND field experiment was under the sponsorship and management of the Earth Sciences Laboratory, U. S. Army Natick Laboratories (Dr. Paul Dalrymple: Project Supervisor) and carried out by the Applied Scientific Research Corporation of Thailand in collaboration with several agencies of the Thai Government. The experiments were conducted during the years 1967-70 as an interdisciplinary study of a tropical dry evergreen forest environment and embodied surveys of micrometeorological conditions; hydrologic factors; soil, vegetation, and biological surveys. Meteorological data from the TREND experiments, which serve as the source of information for the scientific analysis in this report, were provided by USAETL in the form of raw data tapes recorded at the TREND site and certain computer printouts prepared during the field experiment.

Personnel participating in the processing, analysis and interpretation of the TREND meteorological data were as follows: Dr. Helmut E. Landsberg, Principal Investigator; Dr. Owen E. Thompson, Co-Investigator; Mr. Robert E. Kaylor, Computer Systems Specialist; Mrs. Rachel T. Pinker, Mr. David K. Lee, Dr. Hassan El-Sayed, Miss Jae K. Eom, Project Research Assistants; Mr. Mark Rodney, Technician; Mrs. Syvia Epstein, clerical assistant.

The study site for the TREND experiment is the Sakaerat Forest, an area of about 80 square kilometers in Thailand situated on the Korat Plateau at approximately 14°31'N, 101°55'E which is about 60 km south-southwest of Khorat (Nakhon Ratchasima) and about 190 km northeast of Bangkok. (See Figure 1) Meteorological data were taken along two towers approximately 50 m high and 450 m apart, one tower penetrating the forest, the other erected in a small clearing and both based at about 535 m above sea level on a tilted slightly dissected sandstone plateau which slopes from southwest to northeast. Figure 2 shows the forest area under consideration and the two towers mentioned above. The forest includes good stands of dry evergreen forest, dry dipterocarp forest and clearings in various stages of regeneration. The immediate vicinity of the towers is comprised of a two-storied forest. The top story consists almost exclusively of Hopea ferrea, with a scattering of Shorea sericeiflora, with dense and continuous crown canopy with tree tops ranging from 20-35 m high. The second story consists of the species Hydrocarpus ilicifolius, Walsura trichostemon, Aglaia pirifera, Lagerstroemia, and Memecylon ovatum with tops ranging from 5-17 m high. The forest floor was well covered with thick undergrowth.

The experimental design for the micro-meteorological survey called for the collection and processing of temperature, dew point temperature, wind speed and direction at numerous levels along both towers, various radiation fluxes at the tops of the towers and near the ground, and sub-surface temperature profiles near both towers. Six satellite ground stations

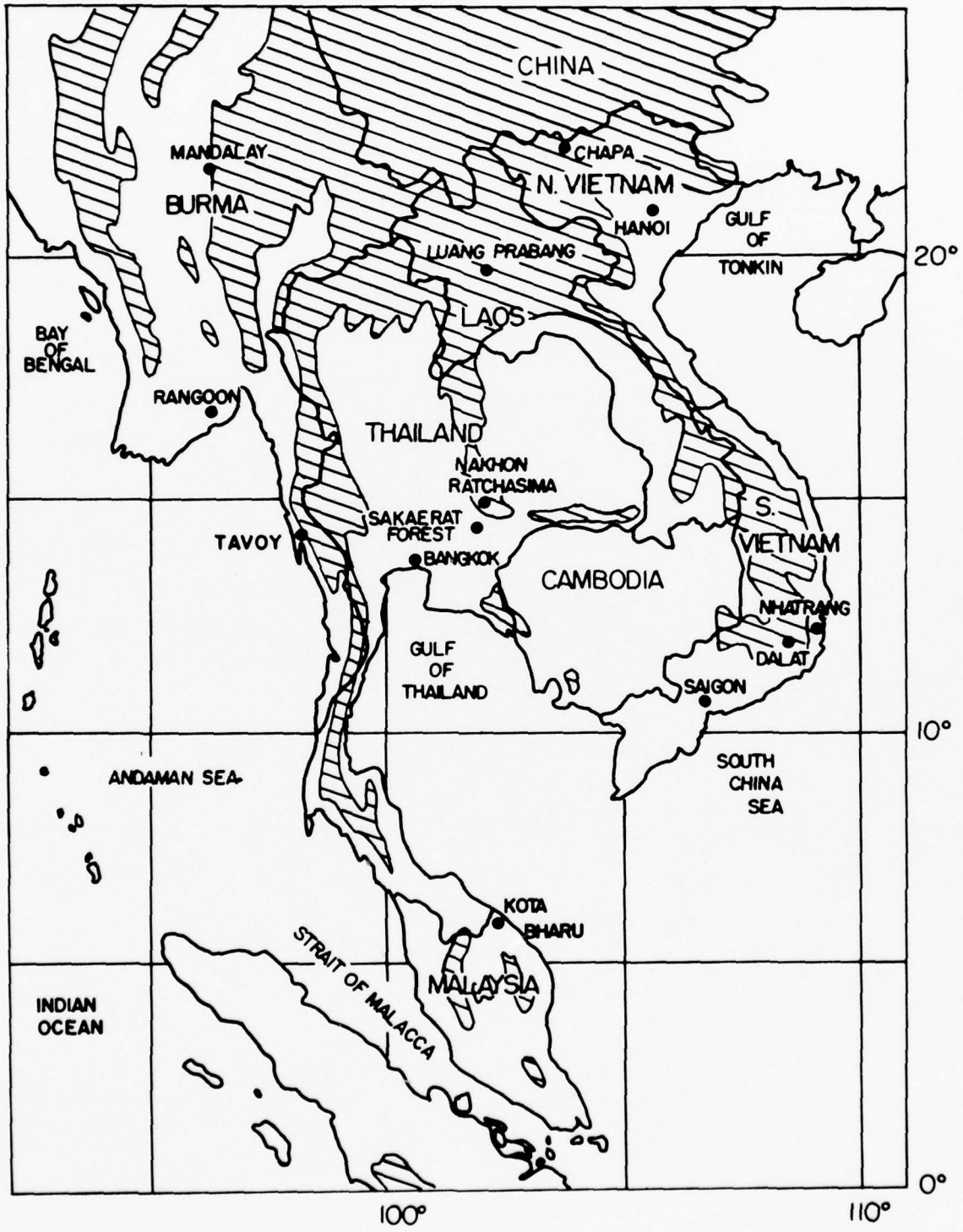

Figure 1. Map of Southeast Asia Showing the Location of the TREND Experimental Site and the Configuration of Highland Areas

Figure 2. The Sakaerat Forest Area Looking Northeast from Over the Tower in the Forest With Tower in the Clearing in the Center of the Photograph

recorded temperature, humidity, precipitation and potential evaporation. Two base stations, each within about 2.5 km of the towers, also had sunshine recorders, additional rain gauges and evaporation gauges. Figure 3 shows, schematically, the location of the various measuring instruments along each tower. A general account of the instrumentation and monitoring procedures is given in ASRCT (1969). Briefly, the data logging system [Hewlett Packard] ~~is comprised of~~ comprises two systems combined into one, capable of analogue and digital recording. The digital system records the 42 values of temperature and 16 values of wind speed, along with date and time. The analogue system records the various radiation measurements, wind direction, precipitation, dew point temperature and station pressure. The frequency of scanning in both systems is of the order of once per half-minute. In what is to follow, data recorded on the digital system is referred to as "D-tape data", that on the analogue system as "A-tape data".

The harshness of the tropical climate--heat,moisture, mildew, etc.--made maintenance of the measuring systems very difficult. In particular, the dew point sensors frequently malfunctioned so that the accuracy and reliability of dew point temperatures in the data record must always be suspect.

The results presented in this report emanate from efforts at the University of Maryland to extract useful climatological and micro-meteorological information from the raw data available to us from Project TREND. Section II serves as an outline of the extensive development of data reduction schemes which were necessary to convert the raw data material into a

TEMPERATURE: ALL LEVELS
DEW POINT: ALL LEVELS EXCEPT 16
WIND SPEED, DIRECTION: LEVELS WITH SOLID LINES
PRECIPITATION: LEVELS 1, 16
SUBSURFACE TEMPERATURE: 5,10,20,50,100 CM

RADIATION:

FOREST	CLEARING
LEVEL 1: R_S(DIRECT)	LEVEL 14: $R_L\uparrow$, $R_S\uparrow$
LEVELS 1, 14: $R_L\downarrow$, $R_L\uparrow$	
$R_S\downarrow$, $R_S\uparrow$, R↓(SPECTRAL)	
R↓(UV) , ILLUMINATION	

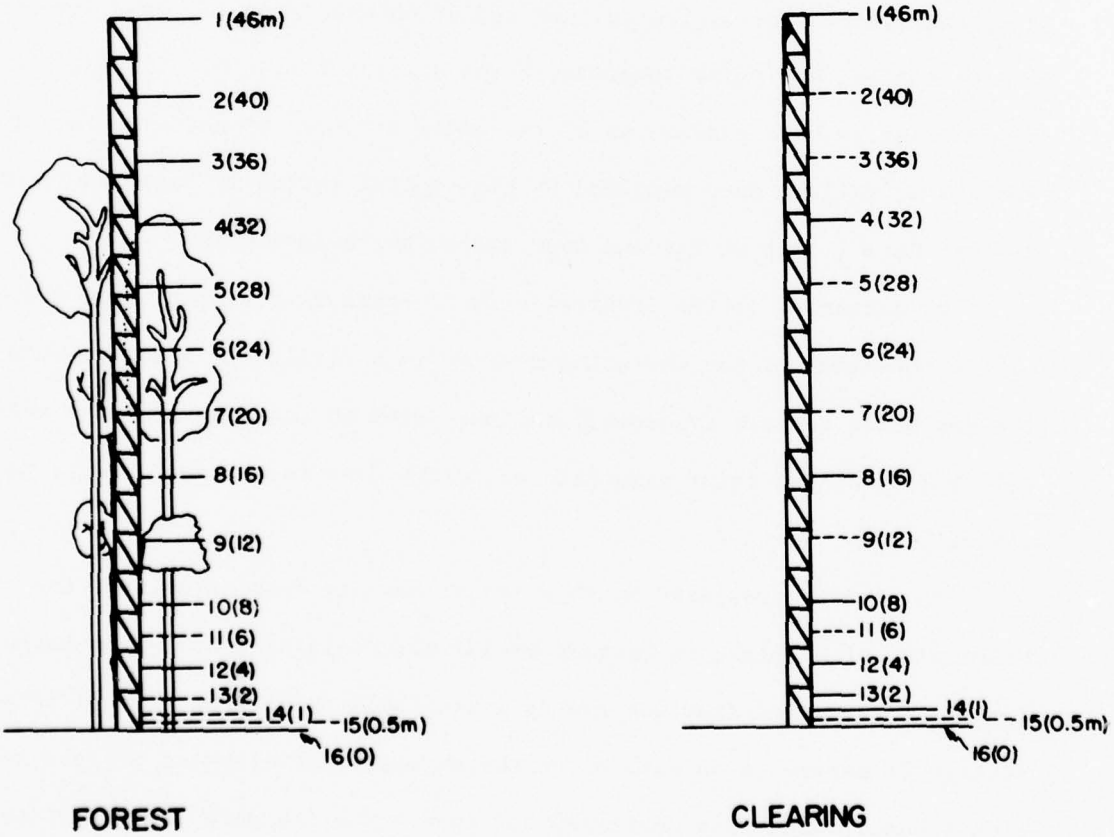

Figure 3. MEASUREMENT LEVELS ALONG THE TOWERS IN THE FOREST AND CLEARING.

data resource useful for analysis. Section III summarizes the climatological conditions at the TREND experimental site while at the same time placing this into perspective with regard to the monsoonal cycle in Southeast Asia. Section IV summarizes results of a careful analysis of the wind speed and temperature distributions in the forest environment. Section V summarizes the behavior of various energy fluxes in and above the forest canopy.

SECTION II - PROCESSING OF TREND EXPERIMENT RAW DATA AND CURRENT DATA AVAILABILITY

A considerable fraction of the effort during this project was devoted to the preparation of the raw micro-meteorological data for computer processing. This proved to be a formidable task because of the condition of the raw data tapes and the manner in which data are recorded on those tapes. Computer techniques were developed for the reading of raw "D" tapes, on which the basic wind and temperature profile data are recorded, and repacking the information on magnetic tape in a form convenient for high speed processing on a Univac 1108 machine but also compatible with Control Data Corporation hardware. The following discussion summarizes the procedure. In the discussion, the term "word" refers to a 36 bit, Univac 1108 computer word.

On the raw D-tapes from the TREND Field Experiments, the time, wind speed and temperature data were recorded every 10 seconds in a 'BCD' format on an incremental tape recorder. Each scan consists of 1 digit for the year, 3 digits for the day and 2 digits each for the hours, minutes and seconds. Following this are 42 temperature points each consisting of a s ign, channel number, and 4 digits of temperature. The last group consists of 3 digits of wind speed, every other one starting with the letter 'F'. One scan requires 102 words or 612 6-bit bytes. There are 1024 words per tape record, (6144 bytes), or roughly 10.04 scans per record. At 556 bytes per inch recording density, plus 0.75 inches for the inter-record gap, each record is about 11.8 inches long. The major problem in reading

these tapes is that the incremental recorder used tended to stretch the tape, resulting in poor spacing between characters. On a modern tape drive system (Univac, IBM, CDC, etc.) this spacing is interpreted as an inter-record gap, resulting in loss of data or loss of position on the tape drive. The amount the tape was stretched can be seen from the fact that one of the unreadable tapes has 2739 records, which requires almost 2700 feet of tape, but a normal reel only contains 2400 feet of tape!

After considerable experimentation, it was concluded that an older tape drive could read these tapes better than a more advanced tape drive. The University of Maryland still owns two IBM 1401 systems which seem to be well-suited for this copy work. Because the 1401 has only 8000 bytes of memory, and the input record requires 6144 bytes, the copy program was made as simple as possible.

The program functions by first clearing the core, then reading in a record. The record is accepted regardless of parity errors, abnormal frame counts, input-output checks, etc. Then 1024 words (36 bit, Univac 1108 word) are written on a temporary tape in even parity, 800 bytes to the inch. If the input record is shorter than this it is padded with BCD 'Z's. If for some reason it is longer, it is chopped to this length. The program will generally recover and recopy 90% or so of the data on the original raw "D" tapes obtained from the TREND site recorders.

The next step in the procedure is to repack the data from the temporary tapes, obtained from the 1401 processing routine, onto permanent storage tapes in a compressed format compatible with Univac 1108 and CDC 6600, 7600

hardware. These final storage tapes then represent the data base for all subsequent computer processing for TREND micro-meteorological studies. The compression factor is about 5 to 1. The following is a summary of the program labeled 'PACK' which produces permanent storage tapes from the temporary copy tapes.

PROGRAM 'PACK' FOR CONVERSION OF TEMPERATURE AND WIND DATA TAPES,

INTRODUCTION

THIS PROGRAM ACCEPTS FIVE RAW DATA TAPES AS INPUT AND PACKS THEM ONTO ONE OUTPUT TAPE. THE RAW INPUT TAPES ARE IN EVEN PARITY, BCD CODE, AND 556 BPI DENSITY; THE OUT-PUT TAPES ARE ODD PARITY, BINARY, AND 800 BPI DENSITY. ALL TAPES ARE 7-TRACK. THE PACKING CONVERTS EACH DATA ITEM TO AN EIGHTEEN BIT QUANTITY AND STORES TWO ITEMS PER COMPUTER WORD (36-BIT, 1108 COMPUTER).

THIS PROGRAM HAS BEEN DESIGNED SPECIALLY FOR THE UNIVAC 1108 COMPUTER; IN PARTICULAR, THE 18 BIT ITEM LENGTH WAS SELECTED TO TAKE ADVANTAGE OF THE PART-WORD TRANSFERS AVAILABLE ON THIS MACHINE. HOWEVER, THE FINAL RECORD LENGTH WAS ADJUSTED BY PADDING SO THAT EACH RECORD IS AN EXACT MULTIPLE OF SIXTY BITS AND THEREFORE IS COMPATIBLE WITH THE CDC 6600 OR 7600 SERIES COMPUTERS.

AN ATTEMPT HAS BEEN MADE TO RECOVER AS MANY OF THE BAD INPUT RECORDS AS SEEM ECONOMICALLY FEASIBLE; A SAMPLE RUN WITH A POOR INPUT TAPE RECOVERED ABOUT 94% OF THE DATA. WHENEVER A TIME SCAN CANNOT BE RESOLVED, THE SCAN IS 'FLAGGED' AND THE PROPER TIME UNITS INSERTED WITH ZERO FILL FOR THE DATA UNITS. IF THE TIME GAP IS OVER 60 SECONDS, NO FLAGGING OR FILLING IS DONE; THE RECORD CONTINUES WITH THE NEW TIME.

ALL ITEMS ARE CARRIED AS FIXED POINT INTEGERS. THE TEMPERATURE DATA HAS OCTAL 300,000 ADDED TO ALLOW FOR THE POSSIBILITY OF NEGATIVE TEMPERATURES;

WHEN THIS QUANTITY IS SUBTRACTED, THE ORIGINAL DATA IS RECOVERED EXACTLY. THE WIND SPEEDS ARE IN PULSES PER SECOND, AND MUST BE DIVIDED BY 31.87 AND A CONSTANT OF 0.52 ADDED TO THE RESULT TO OBTAIN MILES PER HOUR. THE FACTORS 3187 AND 52 ARE PACKED WITH THE DATA. NO CHANNEL NUMBERS ARE PACKED ONTO THE OUTPUT, BUT THE DATA IS ALWAYS WRITTEN IN THE SAME ORDER AS THE INPUT DATA: TEMPERATURE CHANNEL NOS. 101, 201, 301, . . ., 114, 214, 314; THEN WIND CHANNELS 1, 2, . . ., 16.

INPUT TAPES

FIVE TAPES ARE WRITTEN SERIALLY ONTO ONE OUTPUT TAPE. THE PROGRAM ASSUMES THAT THESE FIVE TAPES ARE IN ORDER AND FOLLOW EACH OTHER IN TIME. IF THE LAST RECORD ON THE FIFTH TAPE DOES NOT END WITH A COMPLETE SCAN, THIS LAST SCAN WILL PROBABLY BE LOST. THE INPUT TAPES MUST BE ASSIGNED WITH FORTRAN NUMBERS 10, 15, 20, 25, 30 IN THAT ORDER (EXEC. II UNIT NOS. "D", "I", "N", "S", "X"). IF MORE THAN ONE OUTPUT TAPE IS TO BE WRITTEN, EACH INPUT UNIT MAY BE RELOADED AS SOON AS THE PROGRAM FINISHES WITH IT. THE PROGRAM WILL REWIND THE TAPE UNITS AS THEY ARE FINISHED. NOTE THAT THE PROGRAM EXPECTS FIVE INPUT TAPE UNITS TO BE ASSIGNED TO IT, RATHER THAN ONE MULTI-REEL UNIT.

EACH INPUT TAPE UNIT MUST BE ASSIGNED WITH EVEN PARITY, 800 BPI DENSITY (FOR 1401 COPY TAPES), HARDWARE TRANSLATE TO FIELD-DATA, AND PARITY ERROR OPTION IF AVAILABLE. ESTIMATED TIME PER INPUT TAPE IS BETWEEN TWO AND THREE MINUTES, DEPENDING ON THE NUMBER OF RECORD ERRORS. INPUT IS COMPLETELY BUFFERED SO THAT VERY LITTLE TIME IS LOST ON TAPE READS.

OUTPUT

OUTPUT TAPES ARE ASSIGNED FORTRAN NUMBERS 12 AND 14, IN THAT ORDER. (EXEC. II UNITS "F" AND "H"). IF MORE THAN TWO OUTPUT TAPES ARE TO BE WRITTEN, THE TWO UNITS ARE RELOADED AS NECESSARY. THE PROGRAM WILL REWIND EACH UNIT AS IT IS FINISHED.

AGAIN, THE PROGRAM EXPECTS TWO PHYSICAL UNITS TO BE ASSIGNED, RATHER THAN ONE MULTI-REEL UNIT. THESE UNITS MUST BE ASSIGNED WITH ODD PARITY, 800 BPI DENSITY, NO TRANSLATE. EACH OUTPUT TAPE REQUIRES ONE CARD AS DATA INPUT; THIS IS THE REEL NUMBER AND MUST BE A THREE DIGIT INTEGER BETWEEN '001' AND '511'(OCTAL 777). (FORTRAN FORMAT I3). THERE MUST BE ONE DATA CARD PER OUTPUT TAPE FOLLOWED BY ONE CARD WITH '000' TO STOP THE PROGRAM. IF THIS LAST CARD IS LEFT OUT, THE PROGRAM WILL EXIT BY 'ERRS' RATHER THAN THE NORMAL EXIT, BUT OTHERWISE NOTHING DRASTIC WILL HAPPEN.

LOADING

'PACK' IS AN ASSEMBLY LANGUAGE PROGRAM WHICH SHOULD COMPILE WITH ANY 1108 ASSEMBLY LANGUAGE COMPILER. IT REQUIRES LIBRARY ROUTINES 'NWDU$', 'NTRAN', 'NSTOP$', 'NRDU$', 'NIO1$', 'NIO2$', AND 'NINTR$'. IF THIS LAST ROUTINE IS NOT AVAILABLE, IT MAY BE ELIMINATED BY DELETING CARDS 98 AND 99 WITHOUT AFFECTING THE PROGRAM. IF ANY OF THE OTHER ROUTINES ARE LABELED DIFFERENTLY, REFER TO THE REFERENCE TABLE AND CHANGE THE PROPER CARDS. THE PROGRAM ALSO REQUIRES ONE PROCEDURE, 'AXR$' WHICH DEFINES REGISTERS, IMMEDIATE OPERATIONS, PART WORD TRANSFERS, ETC. THIS PROCEDURE IS VITAL TO THE OPERATION OF THE PROGRAM.

'PACK' IS WRITTEN IN UNBLOCKED BCD CARD IMAGES, EVEN PARITY, 800 BPI DENSITY, ON A TAPE LABELED 'PACK TEMP. PROGRAM'. IT SHOULD BE COPIED TO DRUM AND ANY REVISIONS HANDLED ON THE DRUM COPY, LEAVING THE TAPE COPY IN THE ORIGINAL FORM. IN THE PRESENT FORM, THE PROGRAM REQUIRES OVER 6500 LOCATIONS FOR INSTRUCTIONS AND OVER 6600 FOR DATA (INCLUDING ALL LIBRARY ROUTINES).

OUTPUT TAPE FORMAT

PACK WRITES AN OUTPUT TAPE WITH 755 WORDS (36 BITS) PER RECORD, AT 800 BPI DENSITY AND ODD PARITY. EACH RECORD THEREFORE OCCUPIES 5.6625 INCHES OF TAPE, PLUS 0.75 INCHES FOR IRG, FOR A TOTAL OF 6.4125 INCHES PER RECORD. EACH INPUT TAPE HAS ABOUT 2400 RECORDS WITH 8.98246 SCANS PER RECORD, SO FIVE INPUT TAPES HAVE ABOUT 107,790 SCANS. EACH OUTPUT RECORD HAS 25 SCANS, SO THE OUTPUT TAPE WILL CONTAIN ABOUT 4315 RECORDS, USING APPROXIMATELY 2,306 FEET OF TAPE.

THE FIRST 5 WORDS OF EACH RECORD CONTAIN CONSTANTS AND FACTORS:

RECORD WORD 1	BITS 1 - 9	REEL NUMBER
	BITS 10 - 18	TAPE TYPE
	BITS 19 - 36	RECORD NUMBER
RECORD WORD 2	BITS 1 - 9	YEAR (9 OR 0)
	BITS 10 - 18	DAY
	BITS 19 - 36	OCTAL 300000
RECORD WORD 3	BITS 1 - 18	FACTOR 3187
	BITS 19 - 36	FACTOR 52

RECORD WORD 4: SAME AS SCAN WORD 1 FOR THE FIRST SCAN IN THE RECORD.

RECORD WORD 5: SAME AS SCAN WORD 1 FOR THE LAST SCAN IN THE RECORD.

FOLLOWING THE FIVE HEADER WORDS ARE 25 SCANS OF DATA, ALL CODED THE SAME, WITH 30 WORDS PER SCAN.

SCAN	WORD 1	BITS 1 - 6	FLAG
		BITS 7 - 18	DAY
		BITS 19 - 24	HOUR
		BITS 25 - 30	MINUTES
		BITS 31 - 36	SECONDS
SCAN	WORD 2	BITS 1 - 18	FIRST TEMPERATURE
		BITS 19 - 36	SECOND TEMPERATURE
SCAN	WORD 22	BITS 1 - 18	41 ST. TEMPERATURE
		BITS 19 - 36	42 ND. TEMPERATURE
SCAN	WORD 23	BITS 1 - 18	FIRST WIND
		BITS 19 - 36	SECOND WIND
SCAN	WORD 30	BITS 1 - 18	15 TH WIND
		BITS 19 - 36	16 TH WIND

(NOTE: BITS ARE NUMBERED FROM LEFT TO RIGHT)

THE FLAG IS SET TO "1" FOR A NORMAL SCAN; IF A SCAN IS MISSING OR IN ERROR, THE FLAG IS SET TO "2", THE PROPER TIME FILLED IN AND ALL DATA POINTS SET TO ZERO. IF THE LAST INPUT SCAN FROM THE FIFTH INPUT TAPE DOES NOT RESULT IN A COMPLETE OUTPUT RECORD, THE PROGRAM ZERO FILLS THE REST OF THE RECORD, INCLUDING FLAG AND TIME BITS.

WHEN THE FIVE INPUT TAPES ARE FINISHED, THE PROGRAM WRITES AN EOF, THEN WRITES A TRAILER: TRAILER WORD 1: SAME AS RECORD WORD 2 FOR THE FIRST RECORD ON THE TAPE.

TRAILER WORD 2: SAME AS SCAN WORD 1 FOR THE FIRST SCAN ON THE TAPE.

TRAILER WORD 3: SAME AS RECORD WORD 2 FOR THE LAST RECORD ON THE TAPE.

TRAILER WORD 4: SAME AS SCAN WORD 1 FOR THE LAST SCAN ON THE TAPE.

TRAILER WORD 5: SAME AS RECORD WORD 1 EXCEPT WITH TOTAL RECORD COUNT.

THE PROGRAM THEN WRITES TWO MORE EOF'S.

SAMPE RECORD:

WORD 1	9 REEL	9 TYPE	18 RECORD NO.	9 YEAR	9 DAY	18 OCTAL 300,000	2
3	18 DECIMAL 3187		18 DECIMAL 52	SAME AS WORD 6			4
5	SAME AS WORD 726			6 FLAG	12 DAY	6 HOUR / 6 MIN / 6 SEC	6
7	18 TEMP.CHAN 101		18 TEMP.CHAN. 201	18 TEMP.CHAN.301		18 TEMP.CHAN.102	8
27	18 TEMP.CHAN.214		18 TEMP.CHAN 314	18 WIND CHAN 1		18 WIND CHAN 2	2B
35	18 WIND CHAN 15		18 WIND CHAN 16	6 FLAG	12 DAY	6 HOUR / 6 MIN / 6 SEC	36
751	18 WIND CH. 7		18 WIND CH. 8	18 WIND CH. 9		18 WIND CH. 10	752
753	18 WIND CH. 11		18 WIND CH. 12	18 WIND CH. 13		18 WIND CH. 14	754
755	18 WIND CH. 15		18 WIND CH. 16	INTER-RECORD GAP (IRG)			

EACH RECORD STARTS WITH THE FIVE WORD HEADER: THE TRAILER RECORD IS WRITTEN ONLY ONCE PER TAPE, FOLLOWING AN END-OF-FILE MARK.

TRAILER RECORD

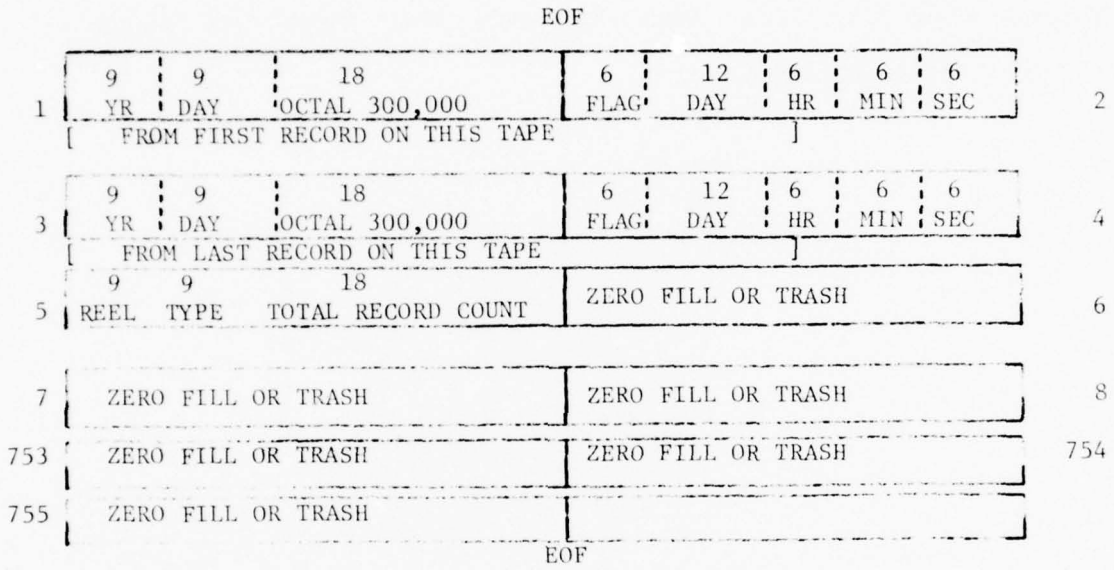

EOF

TO CONVERT THE DATA TO USABLE FORM, SUBTRACT OCTAL 300,000 FROM EACH TEMPERATURE POINT AND MULTIPLY BY 0.01. EACH WIND POINT MUST BE MADE INTO A FLOATING POINT NUMBER, DIVIDED BY 31.87, AND THE RESULT ADDED TO 0.52 TO OBTAIN MILES PER HOUR. AS MANY OPERATIONS AS POSSIBLE SHOULD BE DONE IN THE FIXED POINT REPRESENTATION SINCE DIVIDE IS AN EXPENSIVE OPERATION.

NOTE ON READING TAPES ON CDC 6600

EACH RECORD CONTAINS 453 WORDS (60 BIT), WITH 18 WORDS PER SCAN. THE RECORD SHOULD BE BUFFERED INTO AN UNPUT ARRAY, THEN TRANSFER TO AN ASSEMBLY PROGRAM. SINCE FIVE '1108' WORDS EQUAL THREE '6600' WORDS, THE PROGRAM CAN WORK IN UNITS OF THREE WORDS.

In trying to implement this program on the National Bureau of Standards' UNIVAC 1108 under EXEC 2, several problems were encountered. The program would have tied up six tape drive units during execution but only two at a time are actually used, so the systems staff at NBS suggested using one multi-reel file for input rather than five. After this change was made, the program would not execute properly. The problem was finally traced to the 'NTRAN'tape swapping routine which works properly under EXEC 8 but not in EXEC 2. The systems staff at NBS was very helpful but none of their suggestions resolved the difficulty. Therefore, the only alternative was to write the tape swapping section directly in assembly language. However, this would have tied the program to EXEC 2 since the tape routines differ between the two versions of EXEC. Since NBS was in the process of converting to EXEC 8, a more logical procedure was to use EXEC 8 and not try to make the program compatible with EXEC 2. Due to various logistics problems involved with D-tape data reduction and processing off campus, a decision was made during the fourth quarter to perform this task at the University of Maryland Computer Center rather than at the National Bureau of Standards.

Another problem came from the 1401 tape copies of the original data tapes. For some reason, the copied tapes had dropped bits and some evidence of "print through" or bleeding of bits was indicated. The 'NTRAN' routine was not able to handle these problems economically, so a hardware-level routine was inserted for the'NTRAN' read routine and direct assembly routines used for tape swapping and output.

A section was added to the input routine to make possible direct reading of fairly good tapes without going through the 1401 copy process.

This routine will work with most tapes as long as there are no end-of-files except at the beginning and end of the tape. However, the initial tests with poor tapes showed that the 1401 could recover more of the data than the 1108.

A program was written to process the output tapes from 'PACK'. The program computes half-hour average temperatures and wind speeds centered at the half-hour and hour. Since one tape provides about two weeks of data, longer averages are also possible without tape swapping routines. The analysis in Section IV makes use of such 30-minute averaged profiles except for certain of the spectral analyses.

Considerable progress was made during this project in converting the raw TREND data tapes into usable information. This progress was not without its problems and delays, as noted before. The efficiency of data reduction increased with the transfer of all processing to the University Computer Center although the unanticipated extra expense of preliminary IBM 1401 copying and Univac 1108 repacking was borne by this contract account. This ultimately made it necessary to terminate these preprocessing activities before all the raw D-tapes were repacked. In retrospect, however, we are quite pleased to have salvaged as much data as we have.

Table 1 provides a documentation of the D-tape data processing. The set of remaining raw input tapes is "rough" enough to cause minor problems in any future attempts to complete the preprocessing of the TREND project data record. For example, certain raw D-tapes (e.g.: #322,388) are missing so that there will be gaps in the data coverage unless they are found. Other input tapes (e.g.: #340) yielded far less data than expected after processing.

TABLE 1. SUMMARY OF PROCESSED D-TAPE DATA (Both 7-track and 9-track output tapes)

Reel Number	Input Tapes	Dates of Data Coverage	Input Records	Output Records	Total Scans	Bad Scans	% Bad Scans
240	237, 238, 240, 241, 243	(9/25/69) - (10/8/69)	12,112	4314	107,850	1073	1.0
275	273, 274, 275, 277, 278	(12/1/69) - (12/12/69)	10,871	3879	96,975	110	0.11
287	285, 286, 287, 288, 290	(12/26/69) - (1/8/70)	10,717	3850	96,250	8	0.01
293	291, 292, 293, 295, 296	(1/8/70) - (1/19/70)	10,617	3814	95,350	10	0.01
301	298, 299, 301, 302, 304	(1/19/70) - (2/15/70)	10,938	3946	98,650	409	0.41
308	305, 306, 308 309, 311	(2/15/70) - (2/28/70)	12,006	4306	107,650	79	0.07
316	312, 314, 316, 317, 318	(2/28/70) - (3/14/70)	11,962	4240	106,000	273	0.26
331	328, 330, 331, 333, 334	(4/6/70) - (4/20/70)	12,048	4311	107,775	134	0.12
338	335, 337, 338, 340, 341	(4/20/70) - (5/5/70)	11,092	3862	96,550	617	0.64
354	351, 352, 354 355, 356	(5/24/70) - (6/6/70)	12,127	3355	83,875	16,121	19.2
363	363, 365, 366, 367, 369	(6/19/70) - (7/2/70)	11,750	4096	102,400	1,271	1.24
374	371, 372, 374, 375, 376	(7/2/70) - (7/24/70)	10,749	3862	96,550	38	0.04
380	377, 378, 380, 381, 383	(7/24/70) - (8/11/70)	12,000	4287	107,175	?	?
395	393, 394, 395, 397, 398	(8/29/70) - (9/13/70)	11,981	3972	99,300	21,729	21,88
14	70		160,970	56,094	1,402,350	41,872	2.99%

TOTALS

REMARKS:
Input tape 278 is short.
Input tape 295 is short.
Input tape 298 covers the period (1/19/70) - (1/21/70) then skips to (2/5/70)
Input tapes 322 and 388 are missing.
Input tape 323 has nothing recorded on it.
Input tape 340 is short.
Input tapes 358, 362', 362" have special problems.
Input tapes 384, 385, 389 have "noise" problems related to simultaneous recording of A-tape data.
Input tape 393 yielded only 3 good scans.
Input tape 394 yielded about 13,000 of 19,000 scans.

Such tapes had to be recopied and reprocessed a second time to obtain more nearly the full amount of data. Further, at least one raw input tape (#323) was found with no data on it at all. Some input tapes (e.g.: #384, 385, 389) presented repacking problems due to "noise" which was generated by simultaneous A-tape recording on site. On the more encouraging side, some raw input tapes were repacked without the preliminary IBM 1401 copy work. Of the 40 input tapes that have been fully processed thus far, 810,075 scans have been recovered of which only about 2-1/4% are bad or unusable scans. Overall, our experience with the data reduction indicates that a large faction of the TREND project micro-meteorological tower data can be salvaged from the raw data tapes by the processing routines developed by our research group provided proper care and time is given to the effort.

It should be mentioned that final output tapes are written in both 7-track and 9-track versions. Since it is difficult to make 7-track copies of 9-track tapes, this dual output was done in order to preserve the unique TREND data as a universal data source for future analysis and research. Hence, any future requests for copies of the TREND micro-meteorological data can be handled using output tapes of the same format as requested.

It was virtually impossible to prepare analyzable data tapes from the analogue (A) tapes partly due to extra financial squeeze and partly due to insufficient information regarding the original preparation of A-tapes.

Certain radiation, dew point temperature and wind direction information for limited periods have been keypunched from data printouts made from some of the A-tapes during the original TREND field experiments. These data are summarized later in this report. In addition, some data from the various ground stations in the TREND experimental area were made available to us by USAETL and these serve as the principle source of information for the climatological summary in the next section.

SECTION III - CLIMATOLOGICAL CONDITIONS IN THE SAKAERAT FOREST

1. CLIMATOLOGICAL SUMMARY OF THE EXPERIMENTAL AREA

To place the micrometeorological studies of the forest into proper climatological context, data from the principal surface station were summarized over the nearly three years of record to construct a climatology of the area. Computer printouts of hourly values of temperature, relative humidity, precipitation, pan evaporation and hours of sunshine were available from the original field experiment. The data were averaged over each month of the record from November, 1967, to September, 1970. Using the average air temperature and relative humidity values for each month, values of "effective temperature" were obtained in conventional fashion (Landsberg, 1970). Basically, the effective temperature takes into account the combined effect of temperature and humidity on a person's comfort. Effective temperature is

defined as a sensation in which, for a given air temperature and humidity, the state of comfort is equal to that experienced for an environment at a lower temperature with saturated conditions. That is, air would have an effective temperature of 20°C if it feels the same as air at 20°C and 100% relative humidity. For example, this would be the case for air at 22.5°C and 50% relative humidity or at 25°C and 10% relative humidity. Averages of hourly values of effective temperature were compared with values computed from daily averages of temperature and relative humidity for three test days -- December 14, 1967; April 19, 1970; August 13, 1970 -- to see if one could obtain reasonably close values with the lesser computation frequency.* The mean daily effective temperature for these three days were, respectively, 14.3°C, 27.1°C and 24.7°C. Corresponding values of effective temperature computed from the daily mean temperature and relative humidity were, respectively, 14.6°C, 27.4°C and 25.1°C. These are tolerably representative values so the summaries incorporate values computed on this latter basis.

Precipitable water, U, in the atmospheric column over Sakaerat Experiment Station were computed using the method of Smith (1966) with empirical (λ) values taken from Lettau (1970). These were computed using monthly average values of temperature and relative humidity. Values of the storage of water vapor in the atmospheric column were computed by taking the differences of precipitable water from month to month, ΔU. The advection, A,

---

* See Section III.6 for further documentation.

of water vapor into the atmospheric column was computed as a residual in the balance equation,

$$\text{Storage} = \text{Evaporation} - \text{Precipitation} + \text{Advection}$$

$$\Delta U = E - P + A$$

Table 2 gives values of climatological elements for each month of the record at Sakaerat Forest.* Figure 4 shows a representative annual variation of each element determined by further averaging overall corresponding months in the record. The figures on the number of hours of daylight were taken from the Smithsonian Meteorological Tables on Duration of Daylight for the 15th of each month.

The cool, dry northeast monsoon, associated with high pressure over the Asian continent, is evident in each year of record in Table 2 during November to February as well as in the annual summary. During these periods, the temperatures and relative humidities are comparatively low. The temperature values indicate that the northeast monsoon was less vigorous during 1968-69 than the other two years in the record. The average temperature during these four months of 1968-69 was 25.4°C as compared with 21.7°C for 1967-68 and 22.2°C for 1969-70.

The representative annual cycles of temperature and effective temperature show maximum values (27.5°C, 24.9°C) during the transitional month of March and minimum values (21.5°C, 20.0°C) in December. The annual average temperature at Sakaerat was 25.0°C and annual average effective temperature was 23.5°C, with only a 5-6C° variation in either during the year.

---

* These data are plotted in Figure 9.

TABLE 2. Monthly Values of Climatological Elements at Sakaerat Experiment Station, Thailand.

Month	T (°C)	R.H. (%)	$\bar{T}_{eff}$ (°C)	Hours Sun-shine	Hours Day-light	Precipitation (mm) Total	Precipitation (mm) Daily	Evaporation (mm) Total	Evaporation (mm) Daily	U (mm)	ΔU/Δt (mm)	A (mm)
11-67	22.74	85.0	21.8	6.4	11.43	92.4	3.1	-	-	37.7	-	-
12-67	19.13	77.0	18.2	7.6	11.25	00.0	0.0	-	-	27.0	-10.7	-
1-68	21.12	68.8	19.9	7.7	11.33	00.0	0.0	-	-	27.4	+ 0.4	-
2-68	22.82	67.4	22.4	7.8	11.67	2.1	<0.1	-	-	33.6	+ 6.2	-
3-68	26.36	70.8	24.3	7.7	12.03	23.2	0.75	-	-	38.4	+ 4.8	-
4-68	25.38	78.6	23.9	6.3	12.47	138.7	4.6	-	-	40.2	+ 1.8	-
5-68	26.09	82.8	24.8	6.3	12.83	227.2	7.3	-	-	44.2	4.0	-
6-68	26.28	82.4	25.0	4.4	13.00	81.0	2.5	-	-	48.4	4.4	-
7-68	26.58	78.8	25.3	5.5	12.93	32.5	0.9	147.56	4.76	47.1	- 1.3	-116.4
8-68	26.59	77.3	24.9	4.9	12.63	50.9	1.5	137.70	4.59	46.1	- 1.0	- 87.8
9-68	25.43	78.5	24.4	5.2	12.22	138.3	4.6	111.00	3.70	41.1	- 5.0	22.3
10-68	23.47	85.0	22.5	6.3	11.82	89.4	2.9	95.48	3.08	39.7	- 1.4	- 7.5
11-68	24.37	79.2	23.0	7.9	11.43	4.9	0.1	125.70	4.19	39.1	- 0.6	-121.4
12-68	24.95	67.3	22.8	8.1	11.25	0.0	0.0	145.08	4.68	33.9	- 5.2	-150.3
1-69	25.12	68.9	23.0	6.5	11.33	15.3	0.5	122.45	3.95	34.9	1.0	-106.2
2-69	27.24	60.3	23.4	8.1	11.67	0.0	0.0	183.40	6.55	34.6	- 0.3	-183.7
3-69	27.58	65.5	24.9	6.9	12.03	152.9	5.0	175.15	5.65	38.2	3.6	- 18.7
4-69	27.53	68.3	25.0	7.5	12.47	74.1	2.5	187.20	6.24	39.6	1.4	-111.7
5-69	27.02	76.2	25.1	5.6	12.83	110.1	3.7	150.04	4.84	42.9	3.3	- 36.6
6-69	26.53	82.1	25.2	4.6	13.00	146.0	4.9	137.70	4.59	48.7	5.8	14.1
7-69	25.71	82.6	24.5	4.1	12.93	110.3	3.5	122.14	3.94	46.8	- 1.9	- 13.7
8-69	25.62	80.9	24.3	5.4	12.63	169.6	5.5	107.88	3.48	45.5	- 1.3	60.4
9-69	25.02	85.0	24.0	4.2	12.22	370.1	12.3	72.60	2.42	43.8	- 1.7	295.8
10-69	24.48	85.0	23.5	5.3	11.82	151.4	4.9	84.94	2.74	42.2	- 1.6	64.9
11-69	21.59	81.6	20.6	6.2	11.43	57.4	1.9	76.80	2.56	34.0	- 8.2	- 27.6
12-69	20.36	70.3	19.0	7.4	11.25	missing		121.83	3.93	26.6	- 7.4	-
1-70	21.70	69.5	20.1	7.4	11.33	18.8	0.6	127.41	4.11	28.7	2.1	-106.5
2-70	25.29	63.3	22.8	8.2	11.67	10.3	0.4	172.20	6.15	32.5	3.8	-158.1
3-70	28.45	65.5	25.6	7.2	12.03	71.5	2.3	213.28	6.88	40.2	7.7	-134.1
4-70	26.89	73.3	24.8	7.1	12.47	136.3	4.6	149.40	4.98	41.0	0.8	- 12.3
5-70	27.21	76.9	25.4	6.1	12.83	177.4	5.7	141.40	4.55	43.8	2.8	38.8
6-70	26.62	79.5	25.1	5.1	13.00	139.8	4.7	113.40	3.78	47.4	3.6	30.0
7-70	25.98	79.6	24.5	4.5	12.93	90.7	2.9	129.27	4.17	45.9	- 1.5	- 40.1
8-70	25.26	81.5	24.0	4.9	12.63	146.0	4.7	100.75	3.25	45.1	- 0.8	44.5
9-70	25.11	83.1	24.0	5.0	12.22	248.3	9.2	95.10	3.17	42.8	2.3	155.5

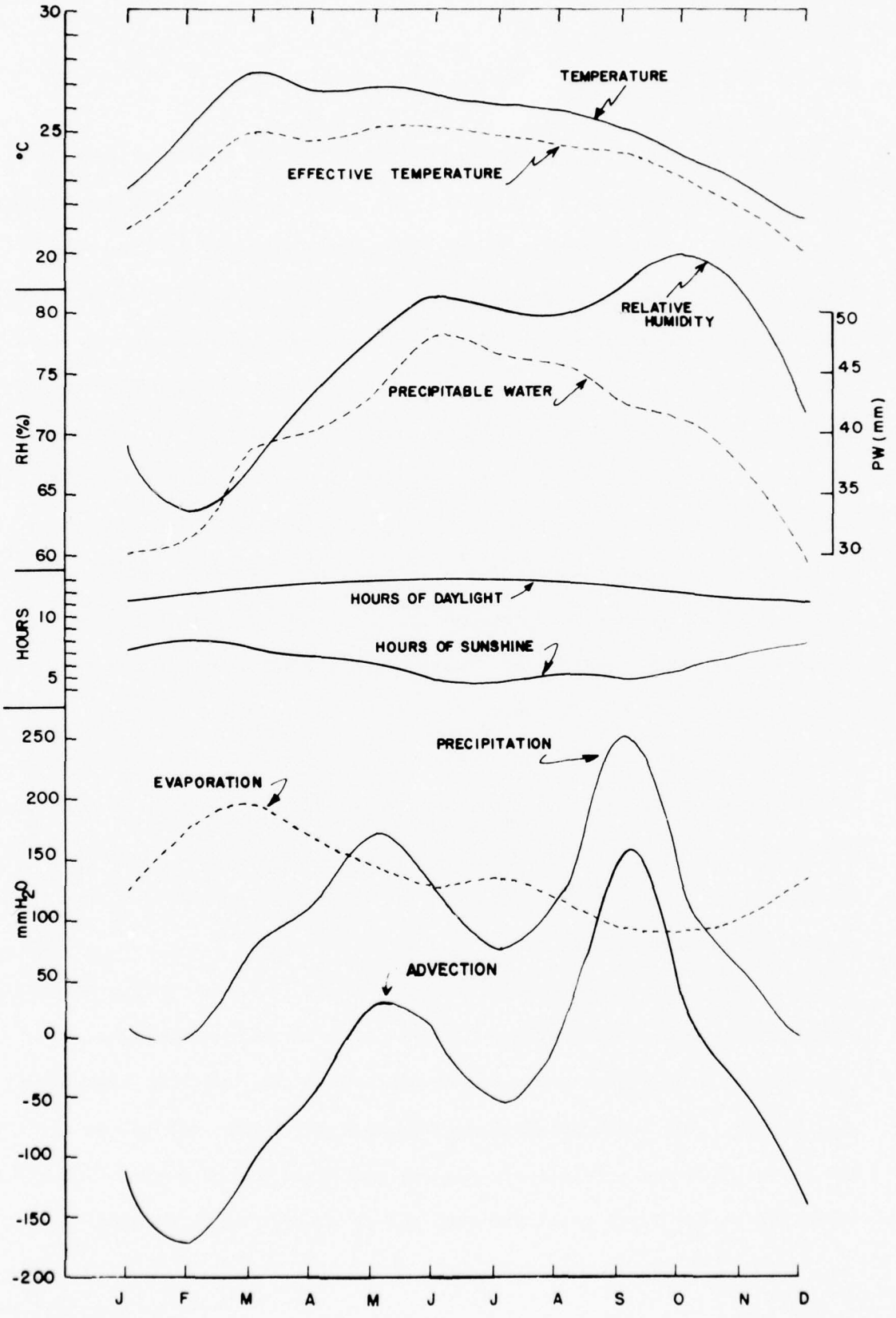

Figure 4. Annual Variation of Climatological Conditions at Sakaerat Forest

The relative humidity generally falls during the monsoonal period reaching a minimum value in February. The period minimum value was slightly more than 60% during February, 1969, the warmest February in the record. The relative humidity is generally largest in October, with an annual average value of 85%, and smallest in February with annual average value of about 64%. The largest difference between air temperature and effective temperature occurred during February, 1969 when the relative humidity reached its period low value. The average air temperature during that month was 27.2°C while the effective temperature in the relatively cool dry monsoonal air was only 23.4°C, almost 4C° cooler. In fact, the effective temperatures during the 1968-69 northeast monsoon and continuing through the first six months of 1969 were considerably cooler than air temperatures due to a long spell of relatively dry air associated with that season's monsoon.

The northeast dry monsoon occurs during a period of relative minimum daylength yet the sunshine recorders measured relative maximum amounts of sunshine during this period which indicates smaller amounts of cloud cover. The precipitation traces are also small averaging generally less than 1 mm/day during the northeast monsoon.

The warm and moist southwest monsoon generally occurs during the period April to September corresponding to the months of maximum daylight. The temperature, precipitation and relative humidity are generally high during this period. The total rainfall during these six months was 980 mm for 1969, 939 mm for 1970 and a relatively smaller amount of 669 mm during 1968. Contributing to the large total for 1969 was an average daily rainfall during

September of that year of nearly 12 mm/day. The double maxima in precipitation during the southwest monsoon, shown in Figure 4, is also evident in a summary of Bangkok climatological data for the period 1943-1952 from the Royal Thai Navy which was prepared by Lettau (1970). This will be discussed further in the next section.

The relative humidities are high during these monsoonal periods yet the effective temperatures are lower than the air temperatures by a greater amount than during the dry northeast monsoon where the air temperatures are much lower. The humidity generally increases during the southeast monsoon period achieving its maximum toward the end of the period, although there was an intrusion of drier air during July-September of 1968 which modified this trend.

The higher degree of cloudiness associated with the southwest monsoon is reflected in the sunshine recordings where relatively smaller amounts of sunshine occur each day than during the northeast monsoonal period. In fact, the monsoon cycle is well illustrated by the sunshine recording which is roughly 180° out of phase with the cycle of daylight duration.

The precipitable water record tends to parallel the relative humidity record over the whole period. The effect of temperature on the precipitable water is best shown for September-November, 1968 where the lowering air temperature maintains a lowering precipitable water value in the face of a large peak in relative humidity values. The evaporation tends to respond to the solar radiation available at the surface but is also controlled by the ambient relative humidity and air temperature. The evaporation is generally largest when air temperatures are high and ambient humidity is low, and generally smallest during periods of higher ambient humidity, falling temperatures and fewer hours of sunshine. Similar temperature effects

occur during the same months of 1969 and 1970 and seem somewhat characteristic of the monsoonal climate.

The water vapor storage term is generally small throughout the period with values within ± 10 mm/month and is not shown in Figure 4. The advection term shows the large monsoonal influx of moist air feeding the rainfall systems of May and September with outfluxes of moist air from the region during periods of evaporation excess over precipitation during the northeast monsoon. Average rainfall during May and September is 172 mm/month and 252 mm/month respectively separated by three months of lesser rainfall with local minimum during July of 78 mm/month. The precipitation drops to near zero during the northeast monsoon season of December, January and February. For the rainfall peak of May, about 90% (146 mm) is contributed by evaporation, 17% (29 mm) is contributed by advection with 3.3 mm added to storage. During September, 62% (156 mm) is contributed by advection, 37% (93 mm) is contributed by evaporation and 1.2% (3.0 mm) is contributed by storage. During the relative minimum of July, there is a fairly vigorous advection of about 43% (57 mm) of the evaporated water out of the region leaving only about 78 mm to rain out. During the dry months of December, January and February nearly all the evaporated water is advected out of the column with little precipitation and only minor changes in storage.

2. DIURNAL VARIATION OF CONDITIONS AT SAKAERAT FOREST

Data from four different months of the year were analyzed for their diurnal variations. Figures 5a, b, c, show the corresponding values of temperature, relative humidity and precipitation on an hourly basis for the

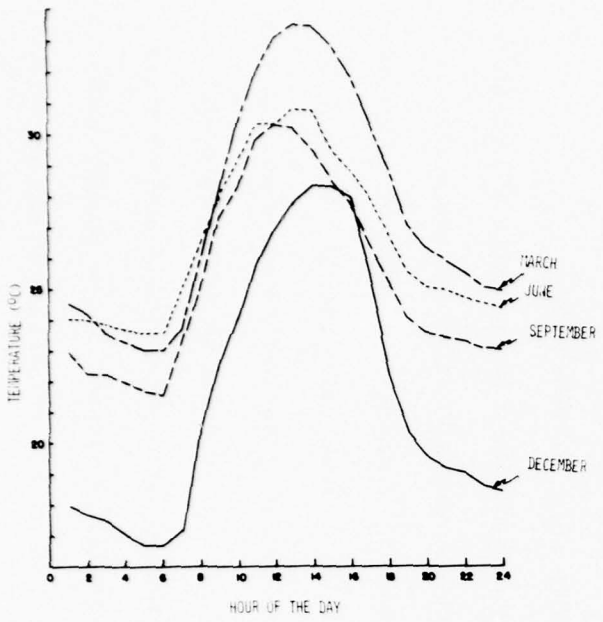

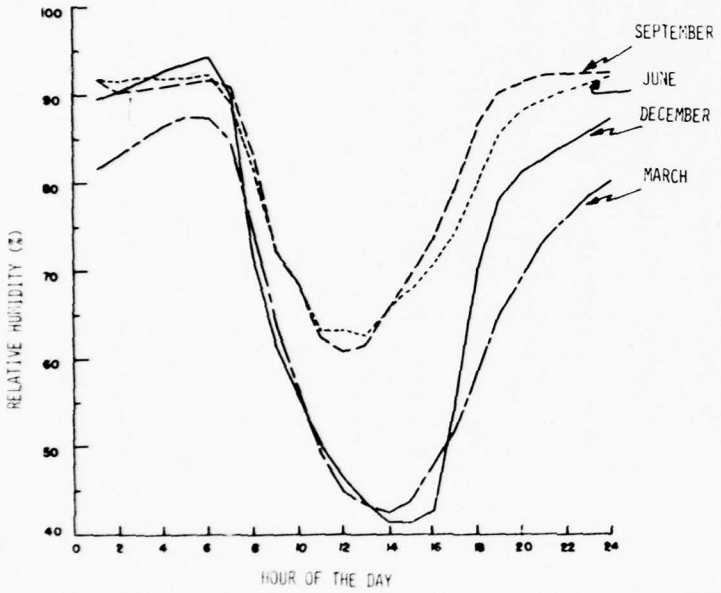

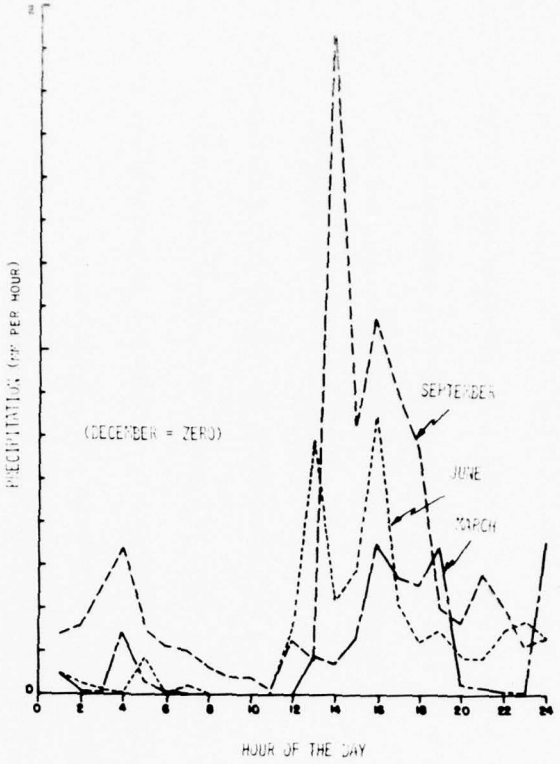

FIGURE 5. DIURNAL VARIATION OF CONDITIONS AT SAKAERAT FOREST. a) TEMPERATURE b) RELATIVE HUMIDITY c) PRECIPITATION.

months of March, June, September and December. Directing attention first to the temperature, Figure 5a shows its diurnal variation for each of these months. Temperature maxima generally occur around 1300 LST-1400 LST. The diurnal variation for the month of September shows a maximum somewhat earlier than this. Referring for the moment to the precipitation record in Figure 5c, it is seen that the rainfall during September has a maximum at 1400 LST with much lower values during the preceding two hours but maintaining high values throughout the afternoon. This characteristic of the diurnal rainfall cycle effectively shifts the temperature maximum to an earlier hour by cooling the air during those rainy hours when the temperature would ordinarily be expected to achieve its maximum value if skys were clear.

As was apparent in the monthly temperature summary, the temperature is highest during the transitional month of March when there are more hours of sunshine near the surface. Temperatures are lowest during December when the solar cycle yields the shortest daylight period. For each of the months shown, temperatures have their minimum values around 0600.

The relative humidity during the southwest monsoon months is considerably higher than during the transitional month of March and the month of December during the dry northeast monsoon. During the months of March and December, relative humidity reaches its minimum value around 1400-1500 LST, the minima during June and September occurring earlier, about noon. In each month, the minima in relative humidity tend to occur in association with maximum temperatures when saturated mixing ratio values would achieve their maxima also. Relative humidity is generally largest in the predawn hours coinciding with the time of minimum temperature and saturated mixing ratio.

The precipitation during December is virtually zero at all hours. Afternoon maxima are evident in each of the other months shown with September and June showing the largest values. There appears to be something of a short periodic cycle in the afternoon rainfall, although we did not statistically test for this. During the rainy season, September shows three local peaks in the afternoon occurring at 1200, 1400, and 1600 and June shows local peaks at 1300, 1600 and 1900. This suggests a 2-3 hour cycle in the afternoon monsoonal convection. Each of the three months of significant rain also show nocturnal maxima; a peak occurring in the early evening between 2000 and 2400, depending on the month, and an early morning maximum a few hours before dawn. All of the months show relatively small amounts of rainfall between dawn and noon.

3. INTERDIURNAL TEMPERATURE VARIATIONS

The change of temperature from day to day is a good measure of climatic conditions. It gives a good index of restlessness of the local atmosphere. A frequency distribution of this element for Sakaerat Forest is shown in Table 3. The table shows that the frequency of rises and falls of temperature from day to day is nearly symmetrically distributed around zero. The lack of prominent synoptic disturbances is exemplified by the fact that 90% of the interdiurnal changes are less than 2°C. These are essentially imperceptible and characterize a monotonous bioclimate without stimuli. In the whole period of record there were only 8 cases when rises and falls between days equalled or exceeded 4°C. Six of these were falls and are minor cold

outbreaks which once in a while even befall these low latitudes. By middle latitude standards one would hardly notice them, considering the fact that the mean interdiurnal temperature variations on the U. S. Great Plains in November to April is about 5°C and that values of 3°C are very common (Landsberg, 1966).

The monotony of the climate is also borne out by an iteration analysis (see Yule, 1950). This consists of a check on the length of period for which the same sign of interdiurnal variation persists. Table 4 gives the number of cases for rises and falls of temperature of varying length in days, due allowance being made for missing data. There is a tendency for rise periods to be somewhat longer than the falls, indicating that any cooling trend is more apt to be short lived than warming trends.

The iteration test yields the results of Table 5. Even without any further test it is immediately noted that the quick iterations from falls to rises are considerably less than statistically expected and the long intervals without iteration in sign of temperature trend quite inflated. In fact, a chi-square test indicates a probability of 0.005 that the observed distribution could be produced by chance and deviate this much from the expected. The statistical test confirms formally the earlier statement that day-to-day changes tend to persist in sign and also that this is more pronounced for rises than falls of temperature. If one compares this type distribution with conditions in higher latitudes, especially in winter, one encounters there a great many cases in the 1-day category with sign changes in the short duration category overwhelmingly common. Instead of the tendency for persistence of trend, as at the tropical station, there is a distinct pattern of oscillation. The period of observation at Sakaerat Forest is too short to attempt a seasonal breakdown. Similarly the data are

Table 3. Percent Frequency of Interdiurnal Temperature Change at Sakaerat Forest.

°C	0	0-0.9	1.0-1.9	2.0-2.9	3.0-3.9	≥4
% rises	4	32	13	4	1	1
% falls	0	28	13	3	1	0

(976 cases)

Table 4. Lengths of Intervals with the Same Sign of Interdiurnal Temperature Variation: Sakaerat Forest.

Days	1	2	3	4	5	6	7	8	9	10	N
Falls	123	87	35	17	3	1	0	0	0	0	(496)
Rises	126	67	33	23	7	3	1	0	0	1	(521)

Table 5. Iteration Test Applied to Data of Tables 3,4 .

Periods (length)		1	2	≥3 Days
Falls	Expected	205	90	33
	Observed	123	87	56
Rises	Expected	215	95	34
	Observed	126	67	68

not adequate to perform an harmonic analysis in the search for possible rhythms in weather patterns.

4. COMPARISON BETWEEN SAKAERAT FOREST AND OTHER SOUTHEAST ASIAN LOCATIONS

Data presented by Anstey (1966) for several locations in Southeast Asia were compared with that at Sakaerat Forest to determine certain geographic differences as well as differences due to forest exposure of instrumentation. Table 6 shows the geographic configuration of all stations and the annual total rainfall of each. Table 7 and Figure 6 show the comparison of basic elements at four of these stations which are at about the same latitude.

The temperature record at Sakaerat Forest closely parallels that for Bangkok, which is about 190 km away from the *TREND site*. There is a fairly consistent difference in temperature between these two locations which averages 2.5°C through the year, Bangkok showing the warmer temperatures. This difference is due largely to differences in elevation, instrument exposure between the two locations and the city influence. Subtracting this annual average difference of 2.5°C from Bangkok values leave remainders which are within 1.1°C of the Sakaerat readings for virtually every month of the year. This is so even though the data for Bangkok are from different years than those for Sakaerat Forest. The main differences in the annual variation in temperature from the Bangkok summary and the Sakaerat Forest data occurs during April and May, at the beginning of the moist, southeast monsoon season. The correlation of temperature data at Sakaerat Forest with those at Nhatrang and Tavoy are generally worse, especially with Tavoy showing a much different annual cycle of temperatures.

TABLE 6. GEOGRAPHICAL CONFIGURATION OF SOUTHEAST ASIAN LOCATIONS RELEVANT TO THE CLIMATOLOGICAL SUMMARIES OF TABLE 7, FIGURES 6, 7, 8.

Location	Elevation (M)	Latitude (N)	Longitude (E)	Annual Total Rainfall (CM)
Bangkok (Thailand	2	13°44'	100°30'	1400
Chapa (N. VietNam)	1641	22°22'	103°52'	2860
Dalat (N. VietNam)	1501	11°57'	108°26'	1803
Hanoi (N. VietNam)	7	21°03'	105°52'	1808
Kota Bharu (Malaya)	6	6°08'	102°15'	3147
Luang Prabang (Laos)	340	19°53'	102°08'	1308
Mandalay (Burma)	76	21°59'	96°06'	846
Nhatrang (S. VietNam)	6	12°15'	109°12'	1440
Rangoon (Burma)	6	16°47'	96°13'	2507
Saigon (S. VietNam)	11	10°47'	106°40'	1974
Sakaerat Forest (Thailand)	550	14°31'	101°55'	1133
Tavoy (Burma)	6	14°05'	98°12'	5291

TABLE 7. Annual Variation of Conditions at Sakaerat Experiment Station and 3 Other Southeast Asian Locations

Month	Temperature (°C)				ΔT(°C)	ΔT-	Precipitation (mm)				ΔP(mm)	ΔP-	Relative Humidity (%)				ΔRH(%)	ΔRH-
	Sak.	Bang.	Nhat.	Tav.	Bang.- Sak.	$\Delta T_{avg.}$	Sak.	Bang.	Nhat.	Tav.	Bang.- Sak.	$\Delta P_{avg.}$	Sak.	Bang.	Nhat.	Tav.	Bang.- Sak.	$\Delta RH_{avg.}$
1	22.6	25.0	23.9	25.6	2.3	-0.2	11.4	7.6	58.4	5.1	- 3.8	-25.8	69.1	68	79	75	- 1	8
2	25.1	26.7	24.4	26.7	1.6	-0.9	4.1	20.3	22.9	12.7	16.2	- 5.8	63.7	60	80	76	- 4	5
3	27.5	28.9	25.6	27.8	1.4	-1.1	82.5	35.6	43.2	33.0	-46.9	-68.9	67.3	63	81	74	- 4	5
4	26.6	29.4	27.2	28.9	2.8	+0.3	116.4	58.4	22.9	86.4	-58.0	-80.0	73.4	62	82	75	-11	-2
5	26.8	29.4	28.3	27.8	2.6	+0.1	171.6	198.1	66.0	502.9	26.5	4.5	78.6	65	82	85	-14	-5
6	26.5	28.9	28.3	26.1	2.4	-0.1	122.3	160.0	45.7	1104.9	37.7	15.7	81.3	69	81	92	-12	-3
7	26.1	28.3	28.3	25.6	2.2	-0.3	77.8	160.0	45.7	1242.1	82.2	60.2	80.3	68	80	93	-12	-3
8	25.8	28.3	28.9	25.6	2.5	0.0	122.2	175.3	20.8	1143.0	53.1	31.1	79.9	66	81	92	-14	-5
9	25.2	27.8	27.8	26.1	2.6	0.1	252.2	304.8	170.2	828.0	52.6	30.6	82.2	73	84	92	- 9	0
10	24.0	27.2	26.7	27.2	3.2	0.7	120.4	205.7	340.4	264.2	85.3	63.3	85.0	74	85	86	-11	-2
11	22.9	26.1	25.6	26.1	3.2	0.7	51.6	66.0	383.5	58.4	14.4	- 7.6	81.9	68	84	80	-14	-5
12	21.5	25.0	24.4	25.0	3.5	1.0	0.0	5.1	188.0	5.1	5.1	-16.9	71.5	67	81	73	- 5	4
Avg.	25.05	27.2	26.7	26.7	2.5								76.2	67	82	83	- 9	
Total							1132.5	1397.0	1440.2	5290.8	22.0							

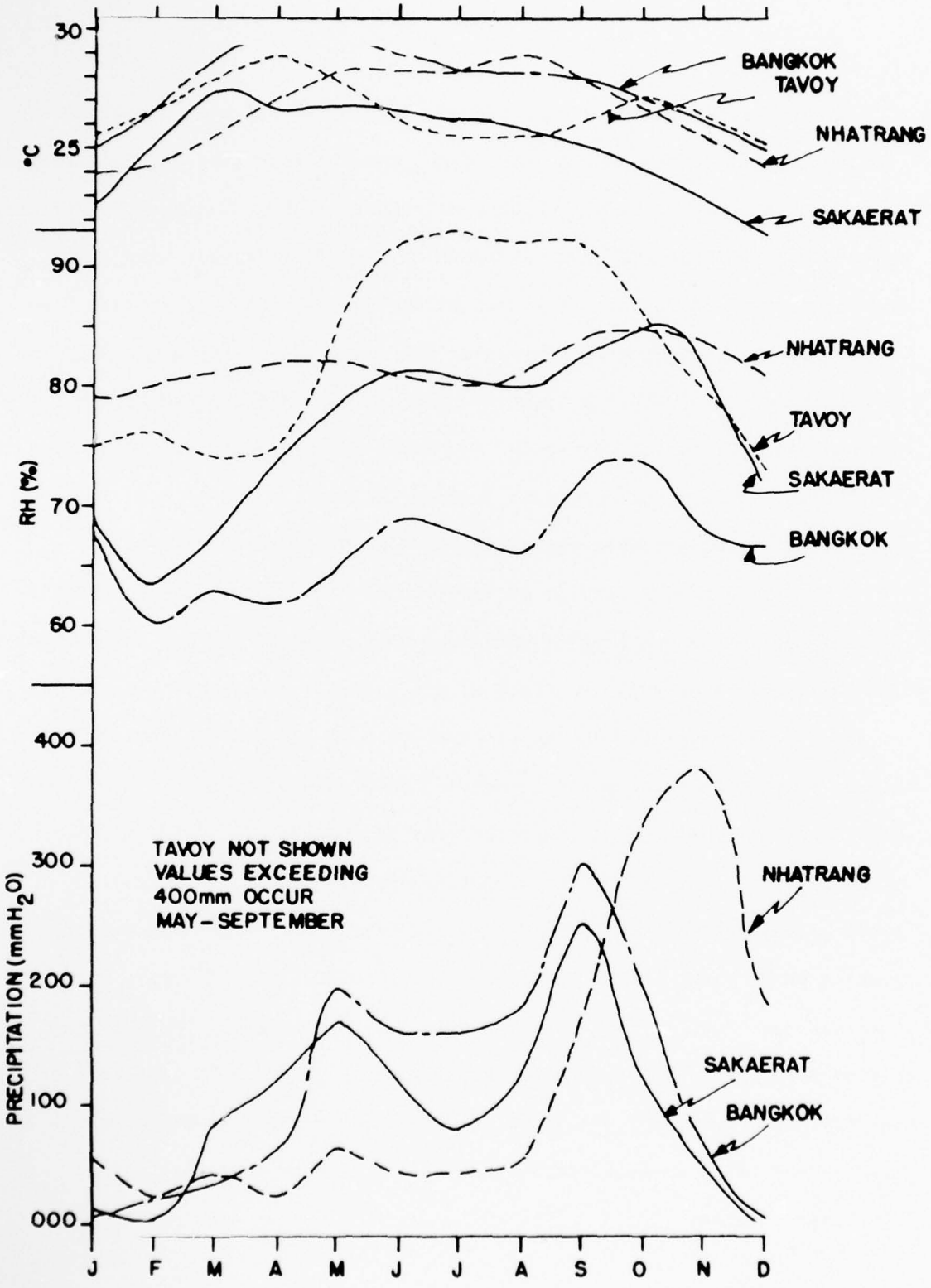

Figure 6. Annual Variation of Conditions at Sakaerat Forest and Three Other Southeast Asian Locations

The record of relative humidity at Sakaerat Forest most closely resembles that of Bangkok but in this case, the discrepancies are much larger. Over the year, the relative humidity at Sakaerat Forest averages 9 percentage units higher than Bangkok but the month to month differences vary from 1 percentage unit in January to 14 percentage units in May, August and November. The differences in climatic regimes at the other two locations is again in evidence in the relative humidity records with Nhatrang exhibiting a somewhat similar regime during the southwest monsoon season but departing considerably during the northeast monsoon and spring transition. Tavoy, once again, shows a completely different type of annual variation.

The precipitation records of Bangkok and Sakaerat Forest show similar regimes during the entire year with monsoonal peaks during May and September, with an interceding relative minimum, and a comparatively dry winter. Averaged over the year, monthly precipitation at Bangkok is about 22 mm higher than at Sakaerat Forest, however, the range of monthly differences for individual months throughout the year is from 85 mm to -58 mm. The precipitation at Nhatrang shows a large monsoonal surge from August to December peaking in November and a substantially smaller, early season peak in phase with that in Thailand. The precipitation at Tavoy, Burma, which is not shown in Figure 6, exhibits only a single surge during the period April to November with a maximum monthly rainfall of 1242 mm occurring in July. The comparatively large values at Tavoy are presumably due to the lack of mountains or continental area on its windward side during the southwest monsoon.

Since some but not all stations in Anstey's summary exhibit double maxima in precipitation, a further comparison of the rainfall regimes of these locations was made in search of a consistent pattern. Figures 7a-e show a normalized [percent of annual total] annual variation of precipitation for selected stations chosen to illustrate the various monsoonal regimes. The data have also been normalized to equivalent months of 30.4 days duration. The normalization of the data tends to suppress certain systematic influences of station elevation and latitude.

The coastal stations of Tavoy and Rangoon, Burma shown in Figure 7a exhibit only a single, advectively fed surge of rainfall. All other stations have some continental fetch to the southwest and show evidence of an earlier season, evaporatively fed surge as well. The northern inland stations of Hanoi, Chapa and Luang Probang are the nearest to being in phase with the monsoon cycle exhibited at Tavoy but show some distortion attributed to early season evaporation from the land. Mandalay, Bangkok and Sakaerat Forest all show an early season, evaporatively fed rainfall maximum in May with a significant depression of rainfall from June to August, the months of peak rainfall along the coast of Burma. This suppression of rainfall is undoubtedly due to the screening effect of the mountains and highlands at the windward reaches of these stations. The monsoonal rains do not reach their maximum at these locations until September. Saigon and Dalat exhibit similar effects but are farther removed from the drying influence of the Burmese and Malayan mountain ranges and are also influenced by extensive flow over the Gulf of Thailand during the southwest monsoon. Nhatrang and Kota Bharu both show significant

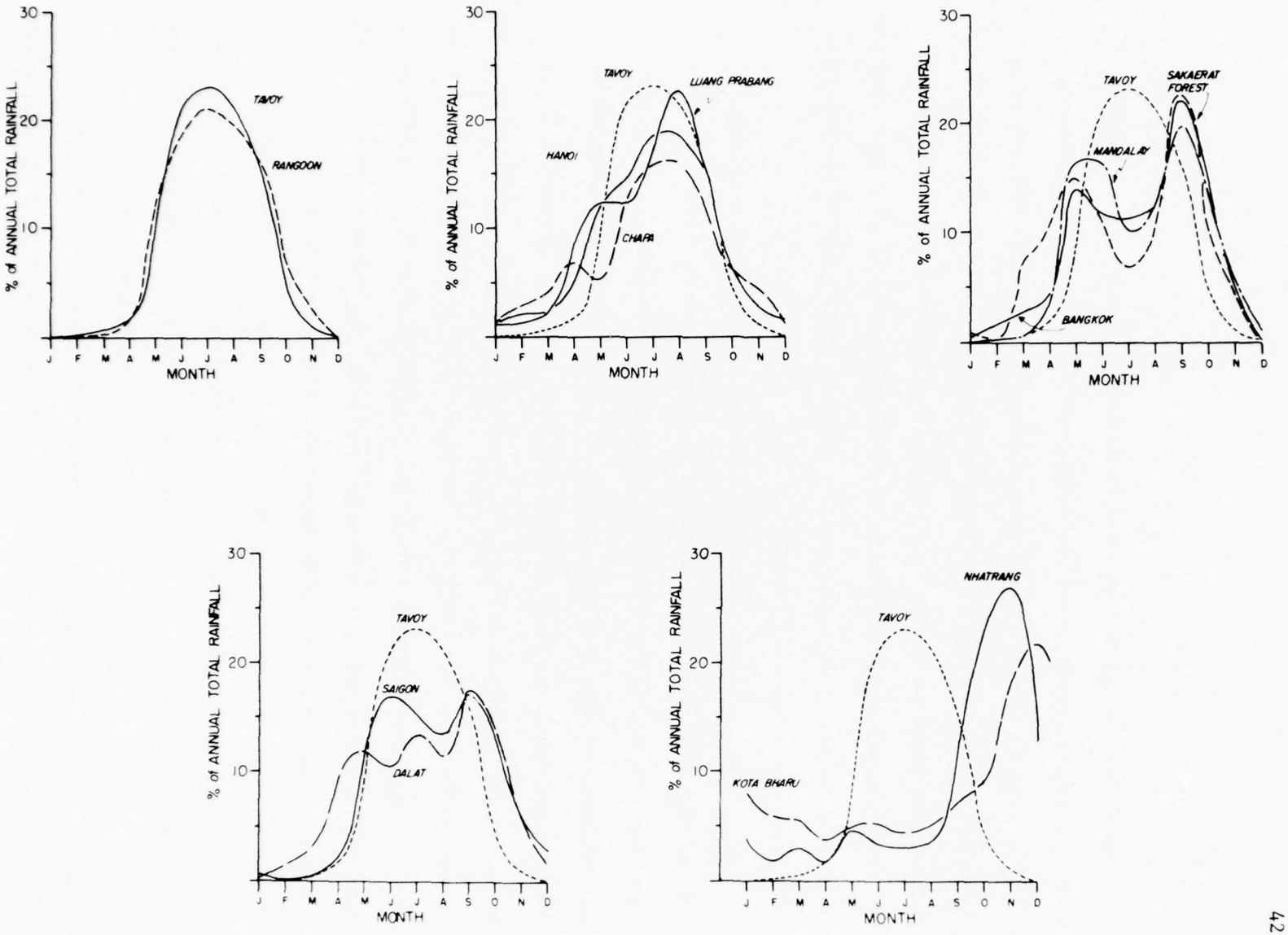

Figure 7. Normalized Annual Variation of Precipitation for Stations Listed in Table 6

phase differences from the other locations. Kota Bharu, being on the southwestern shore of the Gulf of Thailand with a highland area to its south and southwest, shows generally low rainfall during the entire period of the southwest monsoon but a maximum during the early months of the northeast monsoon when it is leeward of the gulf. Nhatrang exhibits a similar seasonal delay of its precipitation maximum since it has a large continental fetch during the southwest monsoon and is just leeward of highlands near the east coast of Vietnam but is subject to the maritime influence of the South China Sea in the later months of transition to the northeast monsoonal flow.

Figures 8a-d show the complex monsoon cycle of Southeast Asia in a geographic perspective. The surfaces represent the percent of annual total rainfall which falls in each of four particular months chosen to illustrate the phase relationships over the area. Kota Bharu data is not included in these figures due to its unique situation relative to the distribution of water and land. The normalization again tends to suppress some systematic elevation and latitude effects but differences in fetch and orography contribute to the complexity of the distributions. Significant variations are apparent between the higher latitude, interior stations, which are the farthest from the tropical waters of the Andaman Sea and Gulf of Thailand, and the stations in Thailand and at Mandalay which are closer to but protected from the sea by the mountain ranges to the southwest. The opposing coastal stations of Tavoy, Burma and Nhatrang, Vietnam illustrate the dramatic phase differences in monsoonal rains across the region. The southwest monsoon seems to be best illustrated by the coastal stations of Tavoy and Rangoon, Burma where the monsoonal rains begin to build during May and June reaching a maximum in

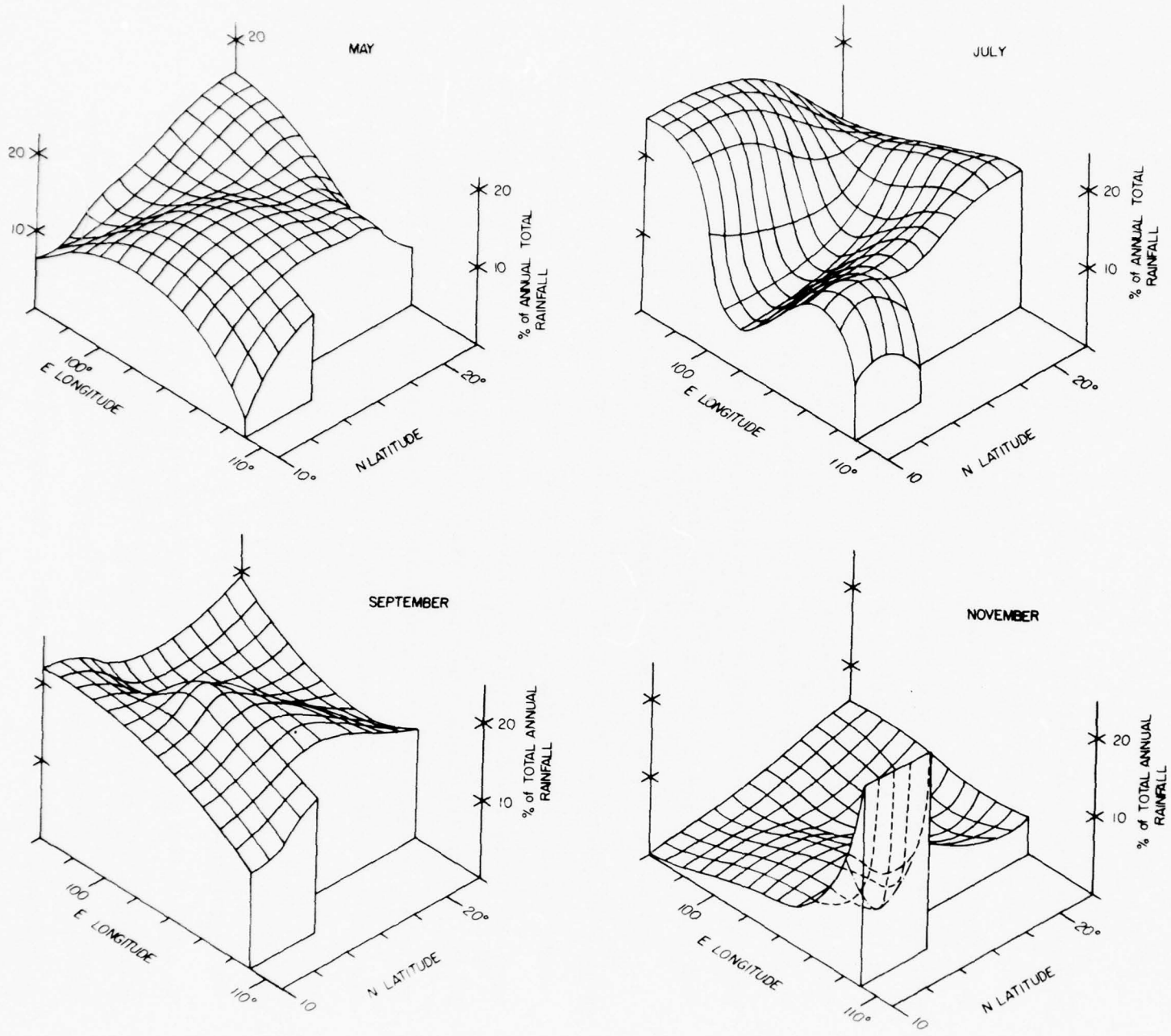

Figure 8. Geographical Perspective Representation of the Complex Monsoon Cycle of Southeast Asia

July. The evaporation from land areas is relatively high during the early months so that interior locations also show an early season surge. However, locations such as Mandalay, Burma and Bangkok and Sakaerat Forest in Thailand, being leeward of the coastal mountain ranges of Northern and Southern Burma and Malaysia, show a decline in rainfall during June and July, the months of maximum rainfall on the windward side of these mountain ranges. These stations do not fully exhibit the monsoonal effect until August and September. The higher latitude inland stations of Chapa, Hanoi and Luang Prabang are more nearly in phase with the coastal stations of Tavoy and Rangoon. The stations along the southeast coastline show a significant delay of the monsoonal rains with Nhatrang, for example, experiencing maximum rainfall in October and November when the transition from the southwesterly monsoon regime to the northeasterly monsoon regime impends.

5. SUMMARY AND CONCLUSIONS

The characteristics of the climate of Sakaerat Forest, Thailand, have been discussed in this paper. The area is influenced by a cool, dry northeast monsoonal flow generally off the Asian continent during the period from November to February and by a warm, moist southwest monsoonal flow off the Andaman Sea and the Gulf of Thailand during the period from April to September. This latter period is characterized by two distinct rainfall surges in May and September separated by a period of lesser rainfall during June and July. The climatic regime at Sakaerat Forest is somewhat similar to that at Bangkok, 190 km to the southwest. However, differences in elevation and significant differences in the heat and moisture balance in the forest yields a consistent cool bias of about 2.5°C in the Sakaerat Forest and a more complicated interruption of the annual cycle of relative humidity compared with Bangkok. Both stations exhibit lowering temperatures and

relative humidities during the cool northeast monsoon. The evaporation increases during this period due to low humidity values. The divergent flow around the Asian continental high pressure cell suppresses the precipitation, however, and leads to an advective flux of moisture out of the Thailand region and relatively low precipitable water values.

During the warm, moist southwest monsoon, the temperature, relative humidity, precipitable water and precipitation are all relatively high at Sakaerat Forest. Sakaerat, Bangkok and several other stations in southeast Asia show double maxima in precipitation during the season, the first surge during spring being supported largely by high amounts of evaporation but the second and larger surge during late summer and fall being supported by a large advection of moisture into the region from maritime sources to the south and southwest. Tavoy and Rangoon, Burma, on the eastern and northern shores of the Andaman Sea, show single and very large monsoonal rainfall effects extending from May to September and peaking in July, about two months earlier than the surge in Thailand. Nhatrang, Vietnam, and other eastern coastline stations in Southeast Asia, show relatively weak early season rainfall surges and the late season precipitation maximum comes one to two months later than the surge in Thailand.

Thus, the precipitation cycles in Southeast Asia seem to be a complex function of the seasonal shift of the circulation pattern in relation to the distribution of sources of maritime air, and windward reaches of the warmed land evaporation sources. Forest cover, such as that at Sakaerat Forest, further modifies the local heat, momentum and moisture budgets so that exchanges of these properties between the earth and atmosphere, and

mean values of properties, are generally different than at urbanized but otherwise comparable locations in Southeast Asia.

6. SUPPLEMENTAL INFORMATION

In this Section, various supplementary results are included which further characterize the climatological conditions at the TREND experiment site.

In Section III.1, mention was made of a comparison between daily average values of hourly effective temperature and effective temperature computed from daily mean temperature and relative humidity for three particular days. Table (8) shows the details of this comparison for December 14, 1967; April 19, 1970; and August 13, 1970.

Table (9) gives the effective temperature distribution for daily mean values. The entries are the period average values of the number of days in each month with daily mean effective temperature in the intervals shown. The entries in parentheses are percentages of the total number of days of that particular month during the period of record at Sakaerat. The effective temperature gives a reasonable first approximation to heat stress problems in tropical countries. It can furnish guidelines for clothing to be worn and to levels of physical labor that can be tolerated. Effective temperature is a fairly good measure of sultriness. This is, of course, a subjective sensation and, for non-indigenous individuals, a matter of degree of acclimatization.

Table 8. Daily mean of hourly effective temperatures compared with values determined using daily average temperature and daily average relative humidity.

Time	Dec. 14 1967		Effective	April 19, 1970		Effective	August 13, 1970		Effective
	Temp.	R. H.	Temp.	Temp.	R. H.	Temp.	Temp.	R. H.	Temp.
0100	13.5°C	83%	13.0°C	27.7°C	78%	25.8°C	24.0°C	94%	23.5°C
0200	12.7	92	12.5	27.1	78	25.3	24.0	94	23.5
0300	12.0	86	11.7	27.0	75	25.1	24.0	94	23.5
0400	11.2	92	11.0	27.0	71	24.9	24.0	92	23.4
0500	10.7	88	10.5	27.0	66	24.5	23.0	100	23.0
0600	11.3	86	11.0	26.9	66	24.4	22.9	98	22.7
0700	12.0	78	11.6	28.0	63	25.1	25.0	81	23.9
0800	13.4	72	12.9	30.0	58	26.3	26.0	80	24.7
0900	14.7	62	13.9	32.0	56	27.6	28.5	70	25.9
1000	16.7	56	15.5	34.0	52	28.8	30.5	59	26.7
1100	18.3	54	16.8	36.0	46	29.6	31.2	56	27.0
1200	19.5	50	17.5	37.0	38	29.4	33.0	56	28.4
1300	20.3	48	18.1	38.0	39	30.1	33.0	56	28.4
1400	21.8	47	19.3	36.3	42	29.4	31.9	70	28.9
1500	22.2	47	19.7	36.7	44	29.9	24.2	98	24.0
1600	21.2	48	19.0	35.0	48	29.2	25.1	98	24.9
1700	18.0	64	16.7	34.0	48	28.3	25.0	98	24.8
1800	15.0	83	14.5	32.1	54	27.5	25.0	93	24.6
1900	14.0	87	13.7	30.2	62	26.8	25.0	86	24.1
2000	13.3	88	13.0	30.3	60	26.7	25.0	88	24.3
2100	13.2	90	13.0	29.9	66	26.8	24.0	98	23.8
2200	12.9	89	12.7	29.2	70	26.6	23.9	100	23.9
2300	12.7	92	12.5	28.9	76	26.6	23.2	100	23.2
2400	12.5	86	12.2	28.2	80	26.6	23.9	98	23.7
Average	15.1	73.7	14.3	31.2	59.8	27.1	26.1	85.7	24.7
Effective Temperature determined from daily mean temperature and relative humidity			14.6			27.4			25.1

Table 9. Effective Temperature Distribution for Daily Mean Values

ET(°C)	JAN	FEB	MAR	APR	MAY	JUN	JUL	AUG	SEP	OCT	NOV	DEC	YEAR
14.1-16	5	0	0	0	0	0	0	0	0	0	0	4	9
	(5.6)	(0)	(0)	(0)	(0)	(0)	(0)	(0)	(0)	(0)	(0)	(4.4)	(0.1)
16.1-18	7	4	0	0	0	0	0	0	0	0	3	16	30
	(7.8)	(4.8)	(0)	(0)	(0)	(0)	(0)	(0)	(0)	(0)	(3.6)	(17.8)	(2.9)
18.1-20	20	8	0	0	0	0	0	0	0	0	8	27	63
	(22.5)	(9.5)	(0)	(0)	(0)	(0)	(0)	(0)	(0)	(0)	(9.7)	(30.0)	(6.3)
20.1-22	21	18	4	6	0	0	0	0	0	7	32	21	109
	(23.6)	(21.4)	(4.4)	(6.4)	(0)	(0)	(0)	(0)	(0)	(11.6)	(38.6)	(23.4)	(10.7)
22.1-24	30	19	16	17	11	5	12	26	40	39	31	22	268
	(33.8)	(22.6)	(17.8)	(19.2)	(13.3)	(5.5)	(13.3)	(28.7)	(46.6)	(65.0)	(37.3)	(24.4)	(26.2)
24.1-26	6	34	56	55	61	83	77	65	46	14	9	0	506
	(6.7)	(40.5)	(62.2)	(62.0)	(73.4)	(92.3)	(85.6)	(71.3)	(53.4)	(23.4)	(10.8)	(0)	(49.7)
26.1-28	0	1	14	11	11	2	1	0	0	0	0	0	40
	(0)	(1.2)	(15.6)	(12.4)	(13.3)	(2.2)	(1.1)	(0)	(0)	(0)	(0)	(0)	(4.0)
N	89	84	90	89	83	90	90	91	86	60	83	90	1025

The data for Sakaerat Experiment Station show that for persons from moderate latitude countries the period from April through October is uniformly in the "uncomfortable" range. December and January are the only months when most of the days are in the "comfortable" range and some, probably not more than one out of five, are definitely cool. The area of Table (9) between the dotted lines represents the comfort zone for lightly clad U. S. subjects.

On the other hand, the high stress limit of 30°ET is also rarely exceeded. The few values that were noted were in mid-day in the pre-summer monsoon season. In such conditions heavy physical labor has to be avoided to reduce the risk of heat stroke.

Table (10) shows monthly average values of climatological elements averaged over the period of record at Sakaerat Experiment Station. These data are plotted as Figure 4 of this report.

Data of Table 2 of this report are plotted in Figure 9.

Tables (11a,b,c,d) give values of temperature, relative humidity and precipitation on an hourly basis for the months of March, June, September and December. These data are plotted as Figures 5a,b,c, of this report.

Table 10 Monthly average values of climatological elements averaged over the period of record at Sakaerat Experiment Station.

onth	T	R. H.	Teff	Hours sun-shine	Hours day-light	Precipa-tation (mm)		Evapora-tion (mm)		U	ΔU/Δt	A*	A+
	(°C)	(%)	(°C)			Total	Daily	Total	Daily	(mm)	(mm)		
1	22.65	69.07	21.00	7.20	11.33	11.4	0.37	124.9	3.94	30.2	1.0	-112.6	-106.4
2	25.12	63.67	22.87	8.03	11.67	4.1	0.16	177.8	5.33	31.5	1.3	-172.4	-170.9
3	27.46	67.27	24.93	7.27	12.03	82.5	2.67	194.2	6.27	38.9	7.4	-104.3	-76.4
4	26.60	73.40	24.60	6.97	12.47	116.4	3.90	168.3	5.61	40.3	1.4	-505	-62.0
5	26.77	78.63	25.10	6.00	12.83	171.6	5.57	145.7	4.70	43.6	3.3	29.2	1.1
6	26.48	81.33	25.10	4.70	13.00	122.3	4.03	125.6	4.19	48.2	4.6	1.3	22.1
7	26.09	80.33	24.77	4.70	12.93	77.8	2.43	133.0	4.29	46.6	-1.6	-56.8	-56.7
8	25.82	79.90	24.40	5.07	12.63	122.2	3.90	115.4	3.77	45.6	-1.0	5.8	5.7
9	25.19	82.20	24.13	4.80	12.22	252.2	8.70	92.9	3.10	42.6	-3.0	156.3	157.9
10	23.98	85.00	23.00	5.80	11.82	120.4	3.90	90.2	2.75	41.0	-1.6	28.6	28.7
11	22.90	81.43	21.80	6.83	11.43	51.6	1.70	101.2	3.38	36.9	-4.1	-53.7	-74.5
12	21.48	71.53	20.00	7.70	11.25	0.0	0.00	133.5	4.31	29.2	-7.7	-141.2	-150.3
Avg.	25.0	76.2	23.5	6.3	12.1	94.4	3.11	133.6	4.30	39.6	0.0	-39.2	-40.1
Total						1132.5		1602.7			0.0	-470.2	-481.7

* esidual of Average Values: $\bar{P} - \bar{E} + (\Delta\bar{U}/\Delta t)$

+ Average of Residuals for the period 7-68 to 9-70 (See Table 2)

TABLE 11a. DIURNAL VARIATION OF CONDITIONS AT SAKAERAT EXPERIMENT STATION FOR MARCH.

Hour	Temperature (°C)				Relative Humidity (%)				Precipitation (mm)			
	3-68	3-69	3-70	3-Avg.	3-68	3-69	3-70	3-Avg.	3-68	3-69	3-70	3-Avg.
01	23.3	25.2	25.3	24.6	87.3	78.0	79.4	81.6	0.0	0.18	0.00	.060
02	22.9	24.8	25.0	24.2	89.4	83.2	79.8	83.1	0.0	0.03	[illegible]	.010
03	22.0	24.2	24.7	23.6	92.2	82.6	80.1	85.0	0.0	0.01		.003
04	21.6	24.0	24.4	23.3	93.6	83.3	82.0	86.3	0.5	0.02		.173
05	21.4	23.8	23.9	23.0	99.4	85.0	83.4	87.6	0.1	0.00		.033
06	21.5	23.7	23.8	23.0	95.1	84.8	84.0	87.3	0.0	0.00		.007
07	22.3	24.2	24.6	23.7	89.3	84.0	80.9	84.7	0.0	0.02		.007
08	25.0	26.0	26.7	25.9	77.8	74.1	71.7	74.5	0.0	0.00		.000
09	27.2	28.3	29.1	28.2	66.3	63.6	61.5	63.8	0.0	0.00		.000
10	29.2	30.3	31.3	30.3	57.3	56.0	55.1	56.1	0.0	0.00		.000
11	30.8	31.9	33.2	32.0	51.3	48.8	47.5	49.2	0.0	0.00		.000
12	31.8	33.0	34.4	33.1	46.5	44.3	43.8	44.9	0.0	0.00		.000
13	32.5	32.8	35.2	33.5	44.3	44.0	41.6	43.3	0.0	0.34		.113
14	32.2	33.1	35.0	33.4	44.2	43.0	40.4	42.5	0.0	0.24	0.01	.083
15	31.7	32.6	34.1	32.8	44.5	43.7	43.2	43.8	0.1	0.34	0.04	.160
16	30.5	31.6	33.2	31.8	48.8	49.0	45.9	47.9	0.0	0.86	0.45	.437
17	29.6	30.0	31.5	30.4	53.4	53.3	49.1	51.9	0.0	0.41	0.60	.337
18	28.0	28.7	29.8	28.8	59.8	58.2	57.1	58.4	0.0	0.03	0.92	.317
19	26.3	27.2	27.8	27.1	68.5	61.7	64.5	64.9	0.0	1.12	0.16	.427
20	25.3	26.5	27.2	26.3	73.3	69.6	69.7	69.2	0.0	0.02	0.06	.027
21	24.8	26.4	26.6	25.9	76.9	68.9	74.2	73.3	0.0	0.00	0.04	.013
22	24.3	25.9	26.2	25.5	79.5	72.0	76.3	75.9	0.0	0.00	0.02	.007
23	23.9	25.7	25.8	25.1	83.2	73.7	78.8	78.6	0.0	0.00	0.00	.000
24	23.5	25.5	25.6	24.9	85.3	75.3	79.9	80.2	0.0	1.33	0.00	.443

TABLE 11b. DIURNAL VARIATION OF CONDITIONS AT SAKAERAT EXPERIMENT STATION FOR JUNE.

Hour	Temperature (°C)				Relative Humidity (%)				Precipitation (mm)			
	6-68	6-69	6-70	6-Avg.	6-68	6-69	6-70	6-Avg.	6-68	6-69	6-70	6-Avg.
01	24.1	24.1	24.1	24.1	93.0	90.9	89.5	91.9	0.00	0.15	0.03	.060
02	24.0	23.9	24.0	24.0	93.8	91.6	89.5	91.6	+	0.07	0.02	.030
03	23.9	23.8	23.8	23.8	94.2	91.6	90.1	92.0		0.03	0.02	.017
04	23.7	23.9	23.6	23.7	93.8	91.1	90.9	91.9		0.00	0.02	.007
05	23.4	23.8	23.6	23.6	94.2	90.6	91.3	92.0	0.30	0.02	0.02	.113
06	23.5	23.8	23.5	23.6	94.6	90.6	92.0	92.4	0.00	0.00	0.00	.000
07	25.6	24.8	24.6	25.0	89.8	90.6	87.2	89.2	+	0.04	0.03	.023
08	26.7	26.1	26.4	26.4	81.3	83.6	78.6	81.2		0.02	0.00	.007
09	28.0	27.5	28.5	28.0	74.8	75.0	68.5	72.8	0.1	0.00	+	.003
10	29.1	28.7	29.5	29.1	70.7	70.2	65.1	69.7	0.00			.000
11	30.0	29.8	31.1	30.3	66.1	64.2	59.4	63.2	+			.000
12	29.3	30.7	31.0	30.3	64.7	63.3	62.0	63.3			0.58	.193
13	30.6	30.8	30.9	30.8	63.9	62.4	62.1	62.8	0.10	0.65	1.45	.733
14	29.9	31.8	30.5	30.7	68.2	65.0	63.5	65.6	0.00	0.14	0.67	.270
15	29.2	29.7	29.6	29.5	68.7	66.6	68.2	67.8	0.60	0.35	0.14	.363
16	28.3	28.9	29.3	28.8	71.2	71.5	69.3	70.7	1.10	0.98	0.33	.803
17	27.4	28.1	28.2	27.9	75.8	74.0	72.5	74.1	0.30	0.40	0.09	.263
18	26.3	26.9	27.0	26.7	81.3	79.8	79.5	80.2	0.00	0.14	0.31	.150
19	25.4	25.7	25.7	25.6	85.7	86.1	84.8	85.5	+	0.40	0.15	.183
20	25.1	25.2	25.0	25.1	87.5	89.2	87.7	88.1		0.08	0.25	.110
21	24.9	24.9	24.9	24.9	89.3	90.9	87.4	89.2		0.29	0.02	.103
22	24.7	24.7	24.6	24.7	90.4	92.1	88.4	90.3		0.19	0.36	.183
23	24.5	24.4	24.5	24.5	91.5	93.1	89.0	91.2		0.52	0.11	.210
24	24.4	24.2	24.3	24.3	92.3	93.9	90.1	92.1		0.41	0.08	.163

TABLE 11c. DIURNAL VARIATION OF CONDITIONS ATSSAKAERAT EXPERIMENT STATION FOR SEPTEMBER.

Hour	Temperature (°C)				Relative Humidity (%)				Precipitation (cm)			
	9-68	9-69	9-70	9-Avg.	9-68	9-69	9-70	9-Avg.	9-68	9-69	9-70	9-Avg.
01	23.3	22.8	22.7	22.9	91.4	92.4	91.6	91.8	0.2	0.25	0.07	.173
02	21.6	22.7	22.6	22.3	85.9	93.4	91.3	90.2	0.2	0.13	0.27	.200
03	21.5	22.6	22.4	22.2	86.7	93.2	92.4	90.8	0.8	0.49	1.20	.830
04	21.4	22.3	22.1	21.9	86.3	93.7	93.1	91.0	0.2	1.06	0.01	.423
05	21.1	22.2	21.9	21.7	86.0	94.1	94.1	91.4	0.2	0.33	0.03	.187
06	21.1	22.0	21.8	21.6	86.2	94.7	94.8	91.9	<.1	0.31	0.01	.157
07	23.7	22.9	23.0	23.2	88.8	93.5	90.4	90.9	<.1	0.28	0.02	.127
08	25.6	25.1	25.3	25.3	83.5	86.2	79.9	83.2	0.1	0.13	0.00	.077
09	27.3	27.0	27.6	27.3	71.1	76.7	69.4	72.4	<.1	0.05	↓	.050
10	28.7	28.5	28.8	28.3	66.6	70.8	65.9	67.8	<.1	0.05		.050
11	29.8	29.3	30.2	29.8	59.9	65.7	61.5	62.4	0.0	0.04		.013
12	30.6	29.5	30.7	30.3	56.4	66.2	59.8	60.8		0.47		.157
13	30.6	29.3	30.7	30.2	55.3	68.0	61.5	61.6	0.0	0.30	0.00	.100
14	30.0	28.9	29.3	29.4	58.3	70.9	67.9	65.7	<.1	2.02	3.63	1.917
15	29.0	28.2	28.4	28.5	61.8	73.3	72.1	69.1	0.2	1.31	0.79	.767
16	28.5	27.3	27.6	27.8	65.9	77.9	76.4	73.4	1.2	0.79	1.27	1.087
17	27.3	25.9	26.4	26.5	72.1	82.8	83.1	79.3	0.2	2.17	0.25	.873
18	25.9	24.7	25.1	25.2	81.8	88.8	88.5	86.4	0.7	0.27	1.19	.720
19	24.6	23.8	23.8	24.1	87.0	91.6	91.7	90.1	0.5	0.15	0.11	.253
20	24.2	23.4	23.3	23.6	89.1	93.1	91.9	91.4	0.2	0.33	0.10	.210
21	23.9	23.3	23.1	23.4	90.4	93.3	92.8	92.2	0.3	0.71	0.04	.350
22	23.7	23.2	23.0	23.3	91.2	93.5	92.6	92.4	0.3	0.39	0.06	.250
23	23.6	23.0	22.8	23.1	91.0	93.8	92.6	92.5	0.3	0.05	0.08	.143
24	23.4	22.8	22.7	23.0	91.0	93.8	92.3	92.4	0.2	0.24	0.06	.167

TABLE 11d. DIURNAL VARIATION OF CONDITIONS AT SAKAERAT EXPERIMENT STATION FOR DECEMBER.

	Temperature (°C)				Relative Humidity (%)				Precipitation (mm)			
Hour	12-67	12-68	12-69	12-Avg.	12-67	12-68	12-69	12-Avg.	12-67	12-68	12-69	12-Avg.
01	16.1	21.0	16.9	18.0	92.5	89.0	86.6	89.4	0	0	0	0
02	15.7	20.9	16.6	17.7	94.4	90.2	86.8	90.5	↓	↓	↓	↓
03	15.4	20.7	16.3	17.5	94.9	92.0	88.2	91.7				
04	15.0	20.4	15.9	17.1	96.1	93.1	89.2	72.8				
05	14.8	19.8	15.6	16.7	96.2	94.5	89.4	93.4				
06	14.5	20.0	15.5	16.7	96.9	95.8	90.1	94.3				
07	14.8	20.4	16.5	17.2	93.5	89.2	87.0	89.9				
08	17.4	24.4	19.3	20.4	79.4	66.9	68.7	71.7				
09	19.5	26.5	21.6	22.5	68.2	56.7	59.8	61.6				
10	21.0	28.4	22.9	24.1	63.1	49.2	54.8	55.7				
11	22.6	30.1	24.8	25.8	57.7	42.7	49.6	50.0				
12	23.9	31.0	25.8	26.9	53.7	38.9	46.5	46.4				
13	25.0	31.7	26.8	27.8	50.3	36.4	43.6	43.4				
14	25.7	31.9	27.2	28.3	46.9	35.1	42.5	41.5				
15	26.1	31.8	27.1	28.3	46.6	34.7	43.0	41.4				
16	26.0	31.2	26.4	27.9	42.9	35.2	44.9	42.7				
17	23.6	28.7	23.8	25.4	62.9	42.8	58.3	54.7				
18	19.9	25.7	20.9	22.2	79.7	58.0	72.1	69.9				
19	18.2	23.5	19.1	20.3	86.5	68.6	79.5	78.2				
20	17.4	22.9	18.5	19.6	88.3	74.2	81.0	81.2				
21	17.0	22.2	18.5	19.2	89.8	78.4	80.0	82.7				
22	16.8	21.8	18.3	19.0	90.6	82.2	80.4	84.4				
23	16.5	21.5	17.8	18.6	90.3	84.8	82.5	85.9				
24	16.2	21.4	17.5	18.4	90.9	86.6	84.0	87.2				

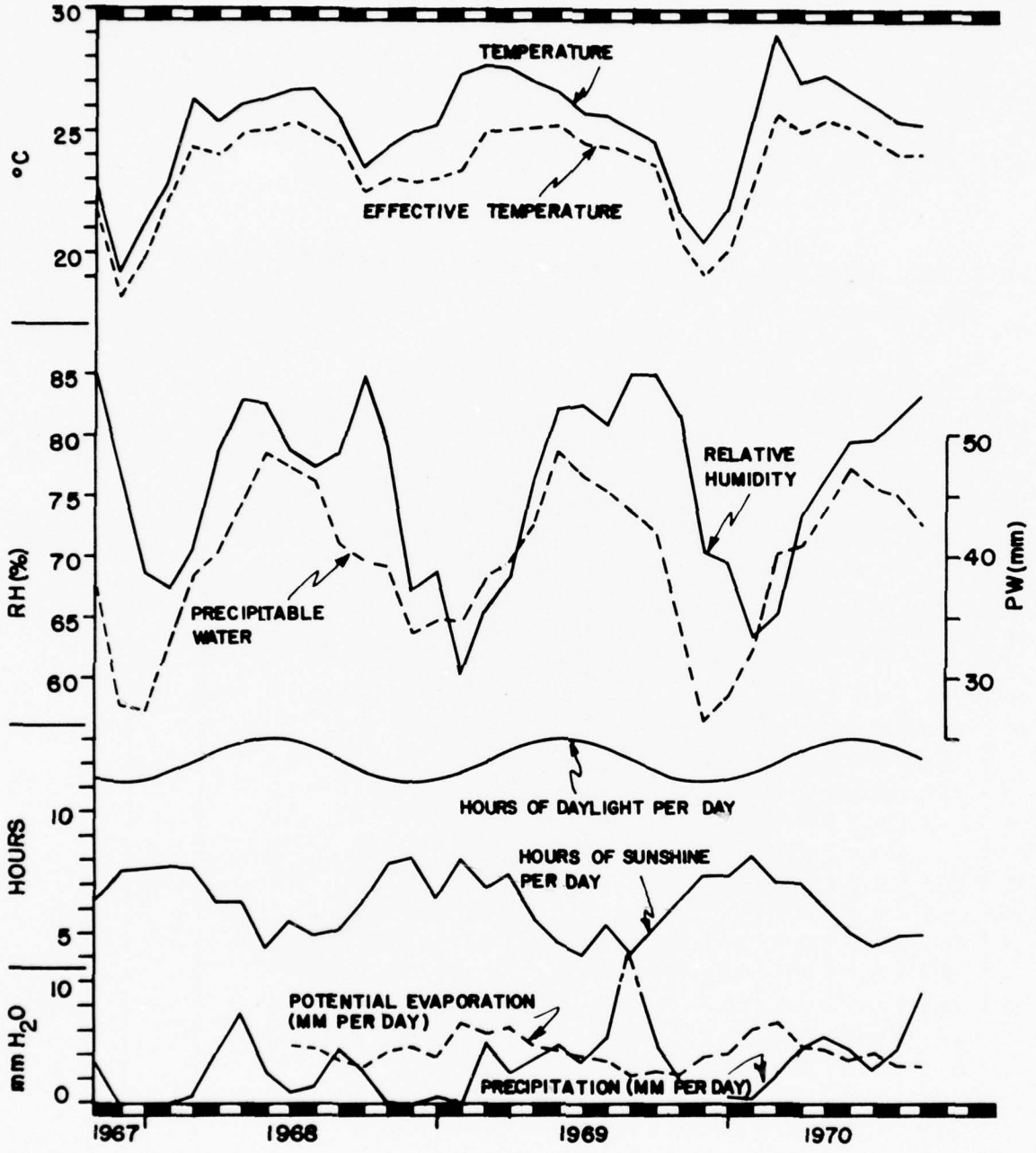

Figure 9. Monthly Variation of Climatological Conditions at Sakaerat Experiment Station. [See Table 2 for Tabulated Values.]

In order to guide the selection of short periods for intensive study of energy balances, turbulent fluxes, and the like, the entire period of record at Sakaerat Experiment Station was scanned to pick out days and/or periods of significant weather conditions.

Table (12) gives the dates of days with more than eight hours of sunshine. The number of hours of sunshine is also shown as well as a coded symbol for the precipitation events of each day. Thus, those days with a blank precipitation code represent clear days with no rain during the twenty-four hour period; dates with (*) or (+) are clear or mostly clear days but with rainfall amounting to less than an inch for the twenty-four hour period; etc.

Table (13) gives the dates of days with less than three hours of sunshine. Again, the number of hours of sunshine and the precipitation code are also shown for each day. Thus, entries with blank precipitation codes are cloudy days but days for which no precipitation fell in a twenty-four hour period; days with (++) are rainy days with more than an inch of precipitation in a twenty-four hour period; etc.

Finally, Table (14) gives dates of days with one full hour of sunshine at noon during the period of record at Sakaerat Experiment Station.

TABLE 12. DAYS WITH MORE THAN 8 HOURS OF SUNSHINE
DURING THE PERIOD OF RECORD AT SAKAERAT EXPERIMENT STATION
(Precipitation (P) Code: blank No rain, * between 0-10mm rain, + between 10-25mm rain, ++ greater than 25mm rain, M information missing)

Date	Hours Sunshine	P
1967		
11-17	8.8	
11-18	8.8	
11-19	8.6	
11-20	8.4	
12-4	8.1	
12-5	8.9	
12-6	8.9	
12-11	9.1	
12-14	8.2	
12-15	9.0	
12-16	8.9	
12-17	8.6	
12-18	8.1	
12-19	8.9	
12-20	8.7	
12-21	8.8	
12-22	8.7	
12-23	8.9	
12-24	8.7	
12-25	8.1	
12-26	8.6	
12-27	9.0	
12-28	8.9	
12-29	8.2	
12-30	8.3	
12-31	8.9	
1968		
1-2	8.9	
1-4	8.7	

Date	Hours Sunshine	P
1968		
1-5	8.9	
1-6	8.8	
1-7	9.0	
1-11	8.5	
1-12	9.0	
1-13	9.1	
1-14	8.5	
1-16	8.9	
1-17	8.4	
1-19	8.3	
1-20	8.6	
1-22	9.0	
1-28	8.9	
1-29	9.2	
1-31	9.0	
2-2	9.8	
2-3	9.9	
2-4	10.0	
2-5	10.0	
2-6	9.6	
2-7	10.1	
2-8	9.5	
2-9	8.9	
2-10	10.1	
2-11	9.9	
2-13	8.9	
2-15	9.4	
2-16	9.6	
2-18	9.2	
2-27	8.4	
2-29	8.5	

Date	Hours Sunshine	P
1968		
3-5	8.4	
3-6	8.5	
3-7	9.1	
3-10	9.2	
3-11	8.9	
3-14	9.3	
3-15	8.9	
3-17	9.0	
3-18	8.8	
3-19	8.4	
3-20	8.6	
3-26	8.7	
3-27	9.3	
3-28	8.5	
3-29	8.3	
3-30	8.7	
3-31	8.0	
4-1	9.7	
4-2	9.8	
4-3	10.1	
4-4	9.3	
4-15	8.4	
4-20	10.3	
4-27	8.5	
5-11	8.7	*
5-16	8.5	
5-20	9.3	
5-21	10.1	
5-23	10.4	
5-24	9.6	
5-25	8.3	

Date	Hours Sunshine	P
1968		
5-26	8.8	*
5-28	8.8	
6-19	8.1	
6-20	8.4	
6-21	8.4	
6-22	8.9	
6-23	8.9	
6-24	8.3	
7-7	8.0	
7-8	8.2	
7-19	9.5	
7-28	8.0	
8-7	8.5	*
8-19	9.4	*
8-20	9.4	*
8-24	8.6	
8-25	9.3	
8-26	8.8	
8-29	10.3	
9-9	8.7	
9-21	8.8	
9-22	8.3	*
9-27	8.0	+
9-30	8.1	
10-2	9.7	
10-3	9.1	
10-23	9.6	
10-24	9.7	
10-25	8.7	
10-26	8.7	
10-28	9.4	

Date	Hours Sunshine	P
1968		
10-29	9.5	
10-31	10.1	
11-1	9.6	
11-2	9.4	
11-3	9.5	
11-4	9.5	
11-5	9.4	
11-7	9.3	
11-8	8.5	
11-11	9.5	
11-12	9.3	
11-13	9.4	
11-16	9.0	
11-17	9.0	
11-18	9.3	
11-19	9.0	
11-20	9.1	
11-21	9.0	
11-22	9.2	
11-23	9.0	
11-24	8.1	
11-26	8.0	
11-28	9.0	
12-2	9.1	
12-3	8.9	
12-4	9.3	
12-5	9.1	
12-7	9.0	
12-8	9.2	
12-9	8.6	
12-11	9.1	
12-12	9.3	
12-13	8.9	
12-14	9.0	

Date	Hours Sunshine	P
1968		
12-15	9.2	
12-19	8.8	
12-20	9.2	
12-21	9.0	
12-22	9.1	
12-23	9.2	
12-24	9.0	
12-25	9.0	
12-26	8.4	
12-27	8.3	
12-28	8.5	
12-30	8.9	
1969		
1-1	8.6	
1-2	9.1	
1-3	9.2	
1-8	8.4	
1-10	8.8	
1-11	8.4	
1-20	8.4	
1-21	8.8	
1-23	8.3	*
1-26	8.2	
1-27	9.5	
1-29	9.3	
2-5	9.0	
2-6	8.6	
2-7	9.5	
2-8	9.7	
2-9	9.8	
2-10	9.4	
2-11	9.7	

Date	Hours Sunshine	P
1969		
2-12	10.0	
2-16	8.6	
2-17	9.1	
2-18	9.5	
2-19	9.8	
2-20	9.7	
2-21	9.8	
2-22	9.7	
2-23	9.3	
2-24	8.0	
2-25	8.0	
2-28	8.0	
3-2	8.7	
3-3	8.6	
3-4	8.9	
3-5	8.7	
3-8	9.3	
3-10	9.5	
3-20	8.2	
3-27	9.4	
3-28	8.5	
3-29	8.5	
3-30	8.7	
4-3	8.6	
4-6	9.0	
4-7	8.9	
4-8	9.5	
4-9	8.7	
4-13	9.1	
4-14	9.4	
4-15	10.0	
4-16	8.6	
4-17	9.7	
4-18	9.4	

Date	Hours Sunshine	P
1969		
4-21	10.5	
4-23	9.2	
4-24	8.2	
4-27	8.5	
5-3	8.0	*
5-5	9.1	
5-9	9.8	
5-12	8.9	
5-20	8.1	
5-21	8.3	
6-2	8.4	
6-29	9.0	*
6-30	8.0	*
7-5	9.5	
7-14	9.1	*
7-16	9.5	*
8-14	9.5	*
8-16	9.0	
8-19	8.8	*
8-27	9.4	*
8-31	9.0	
9-8	8.6	*
10-11	8.5	
10-16	8.0	*
10-17	8.5	+
10-18	9.0	
10-19	8.1	
10-20	8.0	*
10-28	8.0	
10-29	8.5	
10-30	8.0	+
11-9	8.8	
11-10	8.3	
11-11	9.6	

TABLE 12 (CONTINUED)

Date	Hours Sunshine	P
1969		
11-12	8.4	
11-13	8.7	
11-20	8.3	
11-21	8.8	
11-22	8.7	
11-27	9.1	
11-30	9.1	
12-1	9.0	M
12-2	8.7	M
12-3	8.9	M
12-4	8.9	M
12-5	8.9	M
12-6	8.7	M
12-7	8.9	M
12-8	8.9	M
12-10	9.1	M
12-11	9.3	M
12-12	9.2	M
12-14	8.6	M
12-18	8.1	M
12-21	8.9	M
12-22	8.9	M
12-23	8.9	M
12-24	8.9	M
12-26	9.2	M
12-27	8.8	M
12-29	9.2	M
12-30	9.9	M
12-31	8.8	M
1970		
1-1	9.0	
1-2	9.0	

Date	Hours Sunshine	P
1970		
1-3	10.0	
1-7	8.5	
1-8	9.0	
1-9	9.1	
1-10	9.1	
1-11	8.6	
1-12	10.0	
1-13	9.0	
1-14	8.4	
1-18	9.0	
1-19	9.3	
1-20	8.1	
1-21	8.4	
1-23	9.2	
1-24	8.7	
1-26	8.7	
1-27	9.3	
1-29	9.3	
1-30	8.9	
1-31	9.5	
2-1	8.7	
2-2	9.5	
2-3	9.4	
2-4	8.5	
2-5	9.5	
2-6	9.5	
2-7	10.0	
2-8	8.9	
2-9	9.7	
2-19	9.6	
2-20	10.7	
2-21	10.2	
2-22	9.9	
2-23	9.8	

Date	Hours Sunshine	P
1970		
2-24	9.7	
2-25	9.7	
2-26	9.8	
2-27	10.2	
2-28	10.1	
3-2	8.3	
3-3	8.4	
3-4	8.8	
3-5	8.2	
3-9	8.6	
3-10	8.1	
3-11	8.9	
3-12	8.8	
3-13	8.9	
3-14	8.9	
3-15	9.1	
3-16	9.1	
3-17	8.8	
3-18	8.8	
3-25	8.8	
3-28	8.3	
3-29	8.8	
3-30	8.6	
4-9	8.7	
4-10	9.6	
4-14	9.6	
4-15	10.3	
4-16	10.5	
4-17	9.9	
4-18	10.6	
4-19	10.1	
4-20	10.4	
4-22	8.1	*
4-29	8.0	*

Date	Hours Sunshine	P
1970		
4-30	10.0	
5-2	8.9	
5-3	8.3	*
5-8	9.4	
5-26	9.3	
5-27	9.1	
6-2	8.7	
6-10	9.4	
6-16	8.5	
6-24	9.2	*
6-29	8.3	*
7-2	8.0	
7-3	9.6	
8-9	9.1	
8-10	9.4	
8-30	10.2	
8-31	8.3	
9-4	8.5	*
9-8	9.2	
9-25	8.3	*
10-4	9.1	M
10-5	8.4	M
10-8	8.6	M
10-10	8.1	M
10-20	8.5	M
10-25	8.5	M
11-5	9.3	M
11-6	9.0	M
11-7	9.2	M
11-12	9.3	M
11-13	8.8	M
11-14	8.3	M
11-15	8.4	M
11-17	8.5	M

Date	Hours Sunshine	P
1970		
11-20	8.3	M
11-21	8.1	M
12-11	8.0	M
12-16	8.8	M
12-17	8.8	M
12-18	8.5	M
12-19	8.3	M
12-20	8.6	M
12-21	8.7	M
12-25	8.8	M

TABLE 13. DAYS WITH LESS THAN 3 HOURS OF SUNSHINE DURING THE PERIOD OF RECORD AT SAKAERAT EXPERIMENT STATION

(Precipitation (P) Code: blank, no rain, * between 0-10mm, + between 10-25mm, ++ greater than 25mm, M information missing)

Date	Hours Sunshine	P
1967		
11-27	0.9	
11-28	2.7	
12-8	1.8	
1968		
2-24	2.7	*
3.2	0.1	
4-5	2.3	++
4-19	1.7	*
4-26	2.2	
4-30	2.8	++
5-1	0.9	*
5-4	2.5	*
5-6	2.7	+
5-8	2.8	*
5-29	0.1	+
6-1	1.2	+
6-2	0.0	
6-3	0.1	*
6-4	1.7	+
6-5	0.2	
6-8	1.7	*
6-17	1.1	
6-27	1.6	*
6-29	1.1	*
6-30	1.3	*
7-5	1.8	
7-22	2.4	*
7-23	1.2	
7-26	0.9	
7-27	2.2	*

Date	Hours Sunshine	P
1968		
8-3	0.9	
8-4	2.1	*
8-5	0.4	+
8-10	0.1	
8-11	0.0	
8-12	0.4	*
8-13	0.0	
8-14	0.6	*
8-18	0.2	*
8-21	2.3	
9-2	2.8	
9-5	0.4	*
9-6	0.0	
9-7	0.0	
9-12	2.4	++
9-13	0.3	+
9-28	2.7	*
10-10	2.2	+
10-15	2.9	*
10-16	2.0	*
10-21	0.3	*
10-22	0.1	++
11-25	0.5	
12-6	1.9	
12-10	1.8	
1969		
1-6	0.0	*
1-25	1.9	*
2-2	1.6	
3-14	1.7	

Date	Hours Sunshine	P
1969		
3-17	1.8	++
3-18	0.0	*
4-5	0.0	++
4-26	0.0	+
4-28	1.8	+
5-7	0.0	
5-16	2.6	++
5-27	1.4	*
5-29	0.0	*
5-30	0.2	*
5-31	0.8	*
6-5	1.3	*
6-8	1.5	
6-12	2.3	*
6-13	1.7	+
6-18	0.0	
6-25	0.6	*
7-3	0.8	*
7-8	0.0	+
7-11	1.5	*
7-12	0.0	*
7-13	0.2	
7-18	2.4	+
7-19	0.0	+
7-20	1.5	
7-23	0.3	*
7-24	2.7	
7-26	2.8	
7-28	0.0	*
7-29	0.0	*
7-30	0.5	
8-5	0.7	

Date	Hours Sunshine	P
1969		
8-7	0.0	*
8-8	0.0	*
8-9	0.2	*
8-10	0.0	
8-11	0.7	
8-12	0.0	*
8-13	2.0	*
9-3	0.0	+
9-4	0.0	++
9-5	2.8	*
9-6	1.8	+
9-15	2.1	*
9-16	0.1	++
9-17	0.5	*
9-20	1.0	++
9-21	2.7	+
10-2	0.0	++
10-5	1.8	*
10-6	1.5	
10-7	0.6	
10-9	2.5	*
10-27	1.6	*
11-1	1.2	+
11-2	0.7	*
11-3	1.3	++
11-25	2.5	
11-29	1.9	
12-19	1.6	M
12-28	1.5	M

Date	Hours Sunshine	P
1970		
1-4	1.1	
1-5	0.1	
1-6	1.1	
1-15	2.5	+
1-16	1.2	
1-17	2.4	
2-11	1.3	
2-12	0.0	*
3-6	2.7	
3-23	0.0	
3-26	2.3	
4-4	2.6	*
4-13	1.5	++
4-26	1.4	*
5-15	2.6	++
5-16	1.5	
5-23	1.4	+
6-8	1.9	++
6-13	2.2	+
6-14	1.0	*
6-15	2.4	
6-21	0.5	*
6-27	2.5	*
6-28	1.3	*
7-5	1.7	*
7-8	2.5	
7-9	1.4	*
7-10	2.1	*
7-14	0.4	*
7-15	0.0	
7-16	0.4	
7-17	0.0	*
7-18	0.2	*

Date	Hours Sunshine	P
1970		
8-3	0.0	*
8-14	0.4	
8-18	0.0	*
8-19	2.7	
8-20	0.0	*
8-23	0.0	*
8-25	1.1	+
8-26	0.0	*
9-2	1.1	
9-9	1.5	*
9-10	1.1	+
9-11	2.1	*
9-17	1.3	++
9-27	2.8	M
9-29	2.8	M
10-11	1.5	M
10-12	2.9	M
10-16	0.0	M
10-19	0.4	M
10-26	0.1	M
10-27	2.1	M
10-29	1.7	M
10-30	0.0	M
10-31	0.0	M
11-1	0.6	M
11-8	0.8	M
11-10	1.6	M
11-11	0.2	M
11-29	0.0	M
11-30	0.7	M
12-1	0.5	M
12-3	2.1	M
12-4	2.9	M

Date	Hours Sunshine	P
1970		
12-5	0.0	M
12-10	2.4	M
12-14	0.1	M
12-22	2.5	M
12-29	2.8	M

TABLE 14. Days with One Full Hour of Sunshine at Noon during the Period of Record at Sakaerat Experiment Station

Month, Year	Days
11-67	17-21, 23-25, 30; no information before 11-16-67
12-67	3-6, 9-11, 14-31
1-68	1-17, 19, 20, 22, 28-31
2-68	1-9, 11, 13, 15-18, 20, 21,
3-68	3-19, 22-28, 30, 31
4-68	1-4, 7, 9-15, 17, 18, 20, 27-29
5-68	5, 7, 9, 13, 14, 16, 18-28, 31
6-68	6, 9, 12, 16, 20, 22, 23, 28
7-68	1, 2, 7, 8, 11, 14, 18-20, 30
8-68	2, 7, 8, 15, 19, 23-31
9-68	1, 3, 9, 11, 14, 21-25, 29, 30
10-68	2, 3, 5-7, 9, 11, 12, 18, 19, 23-31
11-68	1-5, 7, 8, 10-24, 27-30
12-68	1-5, 7-9, 11-31
1-69	1-4, 7-13, 15, 18, 21-23, 26-29, 31
2-69	1, 3, 5-13, 16-25, 28
3-69	1-11, 16, 20, 23, 26-31
4-69	1-4, 6-9, 11-25, 29, 30
5-69	1-3, 8-10, 13-15, 18-23, 25, 26
6-69	2-4, 7, 9, 11, 14, 15, 20-22, 26, 27, 29, 30
7-69	1, 4, 5, 7, 9, 10, 14, 16, 17, 31
8-69	2, 4, 14-16, 18-20, 24, 26, 27
9-69	1, 8, 9, 18, 23, 25, 26
10-69	1, 4, 10-20, 22, 23, 29-31
11-69	5, 9-15, 19-22, 26-28, 30
12-69	1-8, 10-12, 14, 15, 17, 18, 20-24, 26, 27, 29-31
1-70	1-3, 6-14, 18-31
2-70	1-10, 13, 14, 16-28
3-70	1-5, 8-18, 22, 24, 25, 27-31
4-70	1-3, 7, 9, 10, 14-20, 22, 24, 27, 29, 30
5-70	1-3, 5, 7, 8, 10-14, 19-21, 24, 26, 28, 29
6-70	2, 4, 5, 12, 16, 17, 19, 22, 30
7-70	3, 4, 13, 22, 25, 28
8-70	7, 9-14, 21, 24, 28, 29, 31
9-70	3, 5, 6, 8, 13-15, 18, 21, 23, 25
10-70	2-6, 8-10, 20, 23, 25
11-70	2-7, 12-15, 17-21, 26, 27
12-70	12, 15-21, 25-28

SECTION IV - ANALYSIS OF WIND AND TEMPERATURE PROFILE CHARACTERISTICS

1. PRELIMINARY ANALYSIS OF TEMPERATURE AND WIND PROFILES

Temperature and wind speed data from the two towers were subjected to preliminary analysis for three different periods of the year. Figures 3a,b,c show typical temperature and wind speed profiles for each tower during day and night periods for January 1-14, 1970, during the cool, dry northeast monsoonal flow; for June 20-30, 1970 and September 6-12, 1970 during the warm, moist southwest monsoonal flow. The profiles represent averages of all available profiles during the hours shown and over the periods mentioned above.

The cleared area generally maintains higher temperature and wind speed than the forest. There is an inversion of temperature just beneath the forest canopy in January during the daytime with strong lapse above.* The warmest temperature is at 30 m, generally near the canopy top. This warm layer tends to carry over into the clearing. Even though the temperature in January is lower than in June or September, this warming effect is more pronounced in January. This is because the cloud cover is less during the cool northeast monsoon than during the moist southwest monsoon and the sun shines on the forest for longer periods of the day in January than in June or September. [See Section III of this report.] The nocturnal profile of temperature for January also shows prominent radiational cooling at the canopy top level due, in part, to the low values of precipitable water in the air column above the forest region during the northeast monsoon.

---

* Baynton, et al. (1965) found similar behavior above a tropical forest.

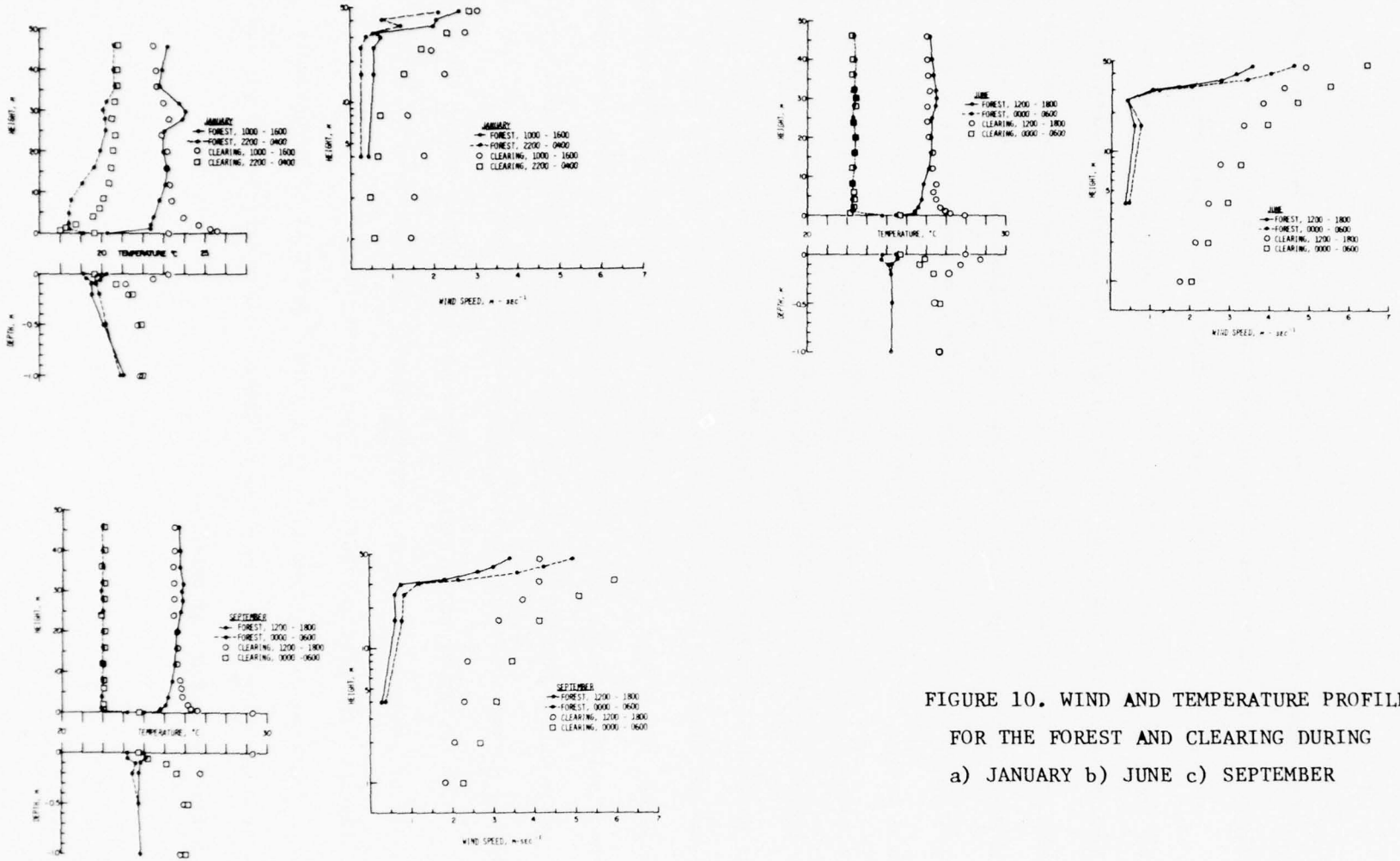

FIGURE 10. WIND AND TEMPERATURE PROFILES FOR THE FOREST AND CLEARING DURING a) JANUARY b) JUNE c) SEPTEMBER

The temperature of the forest floor in all three months is considerably cooler during the day than the surface in the clearing.

During the January daytime period shown, the surface temperature in the clearing was cooler than at 1 meter above the surface due to low shrub growth which was subsequently cleared -- the daytime temperature profiles in the clearing for June and September show maximum temperatures at the surface. Consistent with this, the surface temperature in the clearing during the night in January remained warmer than at 1 meter. This is due, in part, to the displacement of the effective level of radiational cooling to the top of the shrub growth and possibly also to a drainage cooling effect above the surface of the sloping terrain which is evident in the profiles for both the forest and the clearing. During June and September, the higher moisture content of the air tends to suppress any strong surface radiational cooling in the clearing during the nighttime hours. This leads to a diurnal change in the temperature profile which amounts to more of a shift to cooler temperatures at all levels during the night than a lapse reversal at low levels.

The nocturnal temperature profile in the clearing during the drier month of January also shows a rather strong inversion above 1 meter while the strongest inversions in the forest occur above the lower and upper stories of the forest. The nocturnal profiles of temperature in the clearing during June and September do not exhibit the prominent inverted structure of January.

The day-night temperature difference at 30 m, near the top of the forest canopy, is 4°C for all three months while at the surface the difference is only about 1°C or less. In contrast to this, in the clearing the differences are generally largest at the surface. Of course, such differences between six-hour averaged temperatures under-estimates the true diurnal variations in temperature. For example, in Section III of this report, we have established the mean diurnal variation of air temperature at Sakaerat Forest to be about 7°C in June, 8-9°C in September and 11-12°C in December.

The sub-surface temperature profiles show the clearing to remain always warmer than the forest soil even to a depth of 1 meter. The surface temperature undergoes a stronger diurnal variation in the clearing as expected. The temperature differences between the floors of the forest and clearing during the daytime period are about 3°C, 3.5°C and 5.3°C in January, June and September respectively while at night the differences are only about 1°C or less for all three months. At one meter depth, the differences in temperature between the forest and cleared area are about 1°C, 2.5°C and 2°C for January, June and September respectively with very little variation from day to night.

The wind speed profiles show the drag effect of the forest canopy in all seasons and at all times of the day. Above the forest canopy, the wind speed tends to show a logarithmic behavior while within the canopy, the wind speeds are low with rather unremarkable vertical variation. The anemometer at the 40 m level of the tower in the forest

had a bearing failure during January so that the values shown for 40 m are not representative of the winds at that level.* This anemometer was replaced shortly after the two week period represented by the January data and does not contaminate the profiles for June or September.

The day-night differences in the wind speeds indicate a nocturnal increase of wind speed at all levels in June and September during the southwest monsoon, but a daytime maximum of winds in January during the northeast monsoon. This is the case in both the forest and clearing.

The wind speed profiles in the clearing depart considerably from a logarithmic relation indicating that the cleared area is significantly influenced by the surrounding forest. It should be noted, however, that the data appear to define two distinguishable layers with the wind speed in the first 10 or so meters behaving differently than the data above. This is particularly evident in the June and September periods. Presumably, the wind characteristics at low levels are closely influenced by roughness and stability conditions near the floor of the forest while the forest canopy influences the wind behavior at upper levels along the tower.

---

* Personal communication with J. Zabransky, Field Experimenter during the TREND project.

2. Stability Characteristics of the Forest Area

For an assessment of the mean stability characteristics of the Sakaerat Forest area, values of the Richardson number were computed for several layers using wind and temperature profiles averaged for each thirty minute period of the day and further averaged over the periods in January, June and September represented by Figure 10. Figure 11 shows the diurnal variation of the various Richardson numbers for these three months. Richardson numbers are generally positive during nighttime hours changing to negative values during the day. The transition times are about 0700 and 1700. The major exception to this cycle is during the month of January where the daytime warm layer development above the canopy mentioned previously yields unstable conditions in the layer 32-36 m, but stable daytime conditions in the layer 36-46 m. The two layers show more consistency during June and September. The reader should take care to note the different scales in Figure 11a and Figures 11b,c.

Bulk Richardson gradient numbers were computed in the manner of Lettau (1957) for several conglomerate layers in the forest and clearing. The bulk Richardson gradient number is computed from local Richardson numbers as follows:

$$(Ri)_L = \sum_j (Ri)_j \; / \; \sum_j Z_j$$

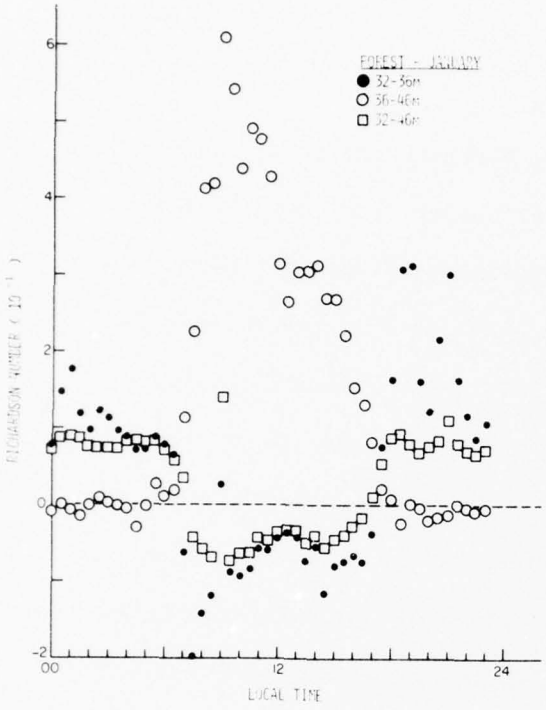

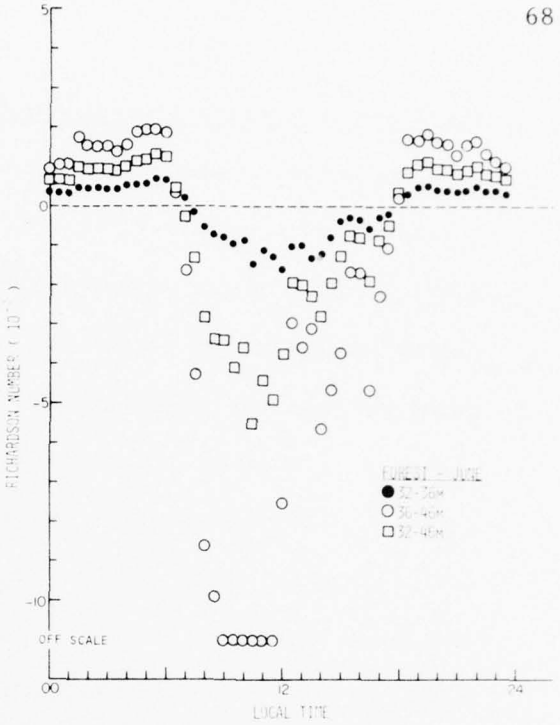

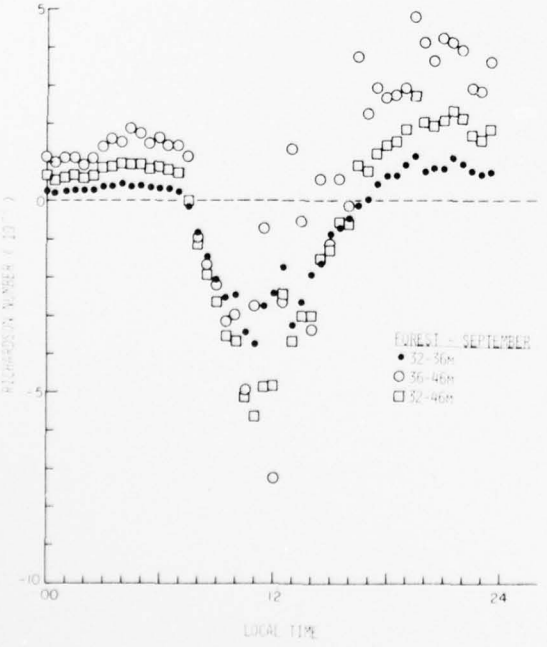

FIGURE 11. DIURNAL VARIATION OF RICHARDSON NUMBERS FOR VARIOUS LAYERS ABOVE THE FOREST CANOPY DURING a) JANUARY b) JUNE c) SEPTEMBER

where $(Ri)_j$ is the local Richardson number at a given geometric mean height Z_j and the sum is over the various sub-layers comprising a thicker layer whose stability is to be characterized. Lettau presents the stability classification shown in Table 15 for layers near the surface. Figure 12 shows values of $(Ri)_L$ for the layer 32m - 46 m above the forest canopy. The summation is carried out over the three geometric mean heights of 33.9 m, 40.7 m and 38.4 m. All values shown fall within the neutral classification of convective stability according to Lettau's classification. The values for January are all positive and exhibit an irregular diurnal variation due to the more complicated thermal structure as exemplified in Figures 10a and 11a. The values for June and September are smaller in magnitude and quite consistent with slight positive values at night and negative values during the day from about 0700 to 1700 local time.

Figures 13a,b show bulk Richardson gradient numbers for the layer 1-16 m in the clearing. Geometric mean heights for these computations are 1.41 m, 2 m, 4 m and 8 m. Note that the scale for January is two orders of magnitude larger than that for June and September corresponding to much greater extremes of stability and instability during the clear sky conditions of January. The diurnal variation during January is also much more irregular than during June or September although all three months show negative values during the day and positive values at night.

Figure 13c shows bulk Richardson gradient numbers for the layer 16-46 m in the clearing [geometric mean heights for these computations are 13.9 m,

TABLE 15. STABILITY CLASSIFICATION OF BULK RICHARDSON GRADIENT NUMBER (After Lettau, [1957])

Stability Class	$(Ri)_L, (10^{-3}/m)$	Stability Class	$(Ri)_L, (10^{-3}/m)$
L3 =Extreme Lapse	< than -15	I1 =Weak Inversion	5 to 6
L2 =Moderate lapse	- 15 to -10	I2 =Moderate Inversion	7 to 9
L1 = Weak lapse	- 9 to - 5	I3 =Strong Inversion	10 to 19
N = Neutral	- 4 to 4	I4 =Extreme Inversion	> 19

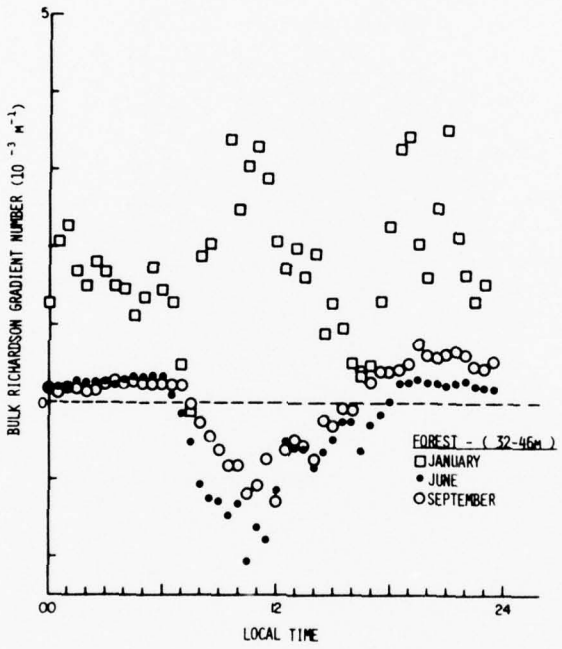

Figure 12. Bulk Richardson Gradient Number for the Microlayer Above the Forest Canopy for January, June and September

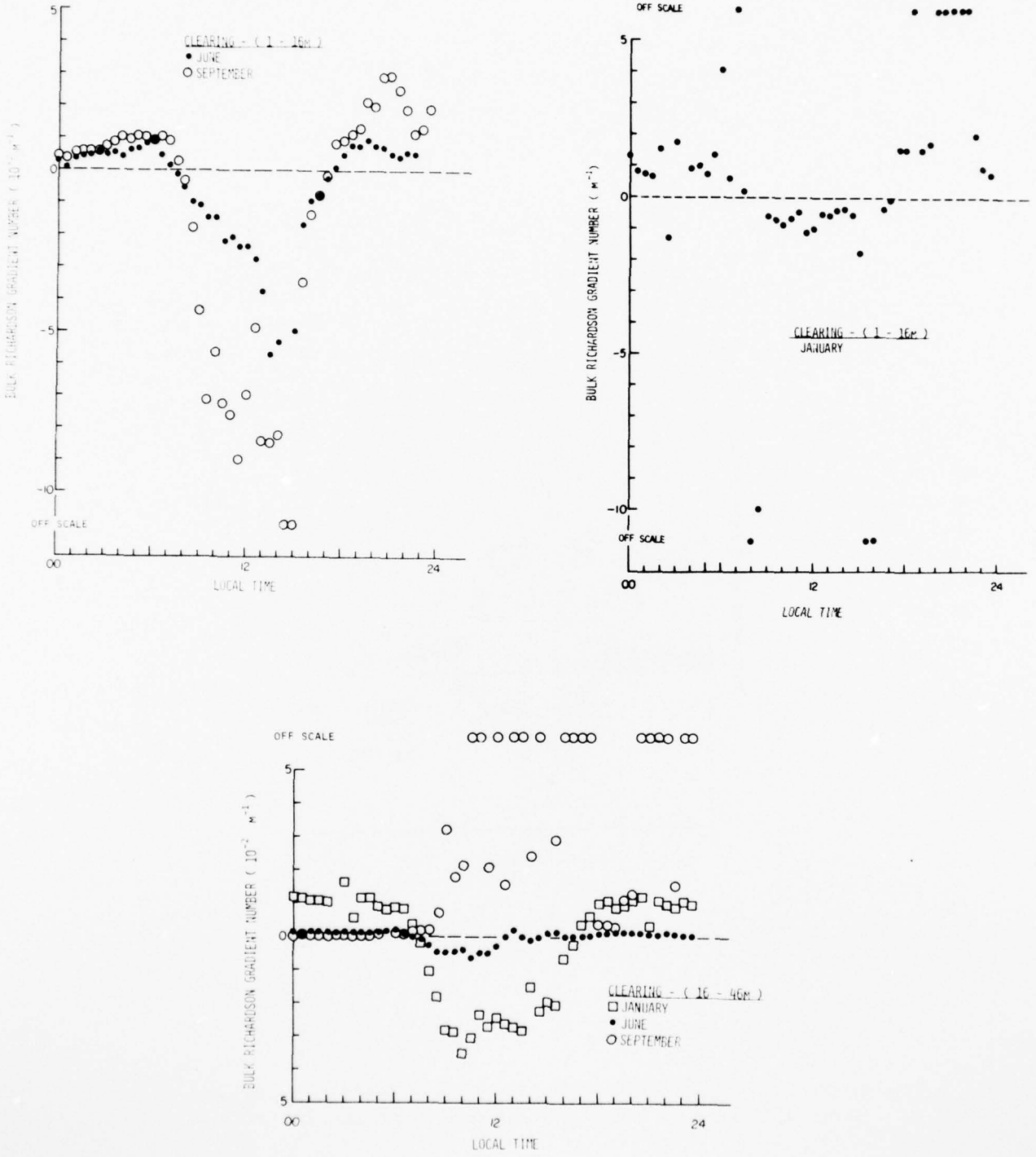

FIGURE 13. BULK RICHARDSON GRADIENT NUMBER FOR THE LOWER AND UPPER PORTIONS OF THE MICROLAYER IN THE CLEARING FOR JANUARY, JUNE AND SEPTEMBER.

22.6 m, 33.2 m, 38.4 m]. The scale is the same as Figure13b but, again, two orders of magnitude smaller than Figure 13a. Thus, the range of stability is much greater in the lower layer than the upper layer during January but comparable during June and September. The bulk Richardson gradient numbers are in the neutral category of Lettau from midnight to about 0730 during June and September but in an inversion class during these hours in January. January and June show a shift to negative values during the day but September exhibits stable conditions during the daytime hours. All months show neutral or stable values after about 1700 local time.

3. Roughness Characteristics of the Forest Area

Estimates of roughness parameter, z_o, datum displacement height, d, and friction velocity, u_*, were made for the forest canopy using a large sample of 30-minute averaged wind profiles occurring during near-neutral conditions in January, June and September. Computation of $(Ri)_L$ were first made for each individual 30-minute averaged wind and temperature profile for the periods January 8-10, 1970; June 20-26, 1970; and September 9-11, 1970 for the layer 30-46 m just above the forest canopy. The resulting values were used to screen the sample to extract only those profiles falling into the "N" category of Table 15. Since there was doubt about the wind speed measurements at 40 m in January, the data at this level were excluded for this period. For comparison, computations of $(Ri)_L$ were also made for the layers 1-16 m and 16-46 m in the clearing for the June and September periods.

A frequency distribution of the number of occurrences in each stability class is given in Table 16. Nearly all the cases sampled for the layer above the forest canopy during the moist, southwest monsoon period (i.e. those for June and September) fell into the near-neutral classification of Lettau. For the same layer in January, during the cool, dry northeast monsoon, about 41% of the cases exhibited near-neutral conditions with slightly less than 10% falling in various of the unstable categories and slightly less than half falling in various of the stable categories. For the clearing, the lower layer exhibits a wider variation of stability than does the upper layer for both June and September. Slightly less than 80% of the cases in June and about 69% of the cases in September show near-neutral conditions in the upper layer of the clearing; evidence of the modifying influence of the surrounding forest as noted earlier.

For near-neutral conditions, it is hypothesized that the wind speed variation with height above the forest canopy is represented by the logarithmic relation

$$u(z) = (u_*/k) \ln [(z - d + z_o) /z_o]$$

where u(z) is the wind speed, u_* is the friction velocity appropriate to the canopy, k = Von Karman's constant, z_o is the canopy roughness parameter and d is the datum displacement height. Of the various methods for estimating z_o, d and u_* which appear in the literature, the method adopted in this study is that described by Stearn's (1970), although comparisons will be made with other methods. In Stearn's method, the parameters z_o, d, u_*

TABLE 16. FREQUENCY DISTRIBUTION OF CONVECTIVE STABILITY CLASSES FOR PERIODS IN JANUARY, JUNE AND SEPTEMBER

Period Layer	No. of Cases	Stability Class							
		L3	L2	L1	N	I1	I2	I3	I4
Jan.8-10,1970 Forest-(30-46m)	144	3	2	9	59	6	6	6	52
June 20-26,1970 Forest-(30-46m)	336	0	0	0	336	0	0	0	0
June 20-22,1970 Clearing-(1-16m)	138	31	8	12	71	15	0	0	1
June 20-22,1970 Clearing-(16-46m)	138	1	7	16	108	3	0	3	0
Sept.9-11,1970 Forest-(30-46m)	144	0	0	1	140	3	0	0	0
Sept.9-11,1970 Clearing-(1-16m)	144	38	4	7	17	21	14	15	28
Sept.9-11,1970 Clearing-(16-46m)	144	0	0	0	99	6	8	5	26

are determined by an iterative procedure designed to minimize the mean square deviation $\sum_i E_i^2$ where

$$E_i = u(z_i) - (u_*/k) \ln [(z_i - d + z_o)/z_o]$$

The iteration procedure of Stearn's was applied to the ensemble of 30-minute averaged wind speed profiles in the layer 30-46 m above the forest canopy which fell in the "N" category of Table 16. The June data were further partitioned into a batch (A) of 201 cases for which the solar radiation impinging on the forest canopy was relatively steady, and a batch (B) of 72 cases during periods of comparatively rapid fluctuations of solar radiation. The iterative procedure converged for 273 of the 336 June cases but only 40 of 59 cases in January and 67 of 96 cases during September. The cases for which convergence was not obtained generally corresponded to values of $(Ri)_L$ which were negative and somewhat near the cut-off of the "N" classification of Table 15 suggesting that the limits of this cateogry should be narrower than as given in Table 15. Other investigators [for example, Lenschow and Johnson (1968)] have chosen to narrow the limits of the near-neutral category.

The resulting estimates of the averages and standard deviations of the parameters z_o, d, u_* are presented in Table 17. The roughness parameter varied considerably over the periods examined. The mean value for the January days was only 0.83 meters with a standard deviation more than half of the mean

TABLE 17. AVERAGE VALUES AND STANDARD DEVIATIONS OF ROUGHNESS PARAMETER, DATUM DISPLACEMENT HEIGHT, FRICTION VELOCITY AND CANOPY STRESS FOR THE SAKAERAT FOREST.

Period No. of Convergent Cases	$\bar{z}_o$(m) [σ_{z_o}(m)]	$\bar{d}$(m) [σ_d(m)]	$\bar{u}_*$(m-s^{-1}) [σ_{u_*}(m-s^{-1})]	$\tau(\bar{u}_*)$(dynes-cm^{-2})
January 8-10,1970 40 cases	0.83 [0.47]	29.53 [0.05]	0.33 [0.09]	1.31
June 20-26,1970(A) 201 cases	5.48 [1.66]	27.18 [0.69]	1.42 [0.45]	24.2
June 20-26,1970(B) 72 cases	5.62 [1.77]	27.16 [0.72]	1.26 [0.45]	19.1
Sept. 9-10, 1970 67 cases	3.61 [1.10]	28.09 [0.75]	1.07 [0.48]	13.7
Average (weighted by No. of cases)	4.69	27.58	1.21	18.97

value. The mean profiles of Figure 10 indicate lower wind speeds during January than during June and September. For June, the mean value of forest roughness parameter is about 5.5 m with standard deviation only a third of the mean value. The values of datum displacement height show more consistency over the three periods but are larger in January than in September or June. The friction velocity is smallest in January and largest in June.

Our results using Stearn's method were compared against various empirical formulae which have appeared in the literature. Stanhill (1969) gives a relationship between d and canopy height, h, as follows:

$$\log(d) = (0.9793)\log(h) - 0.1536$$

This relationship seems to be in excellent agreement with values reported in the literature for vegetation canopies of lower height. Szeicz, et al. (1969) found an empirical relationship between z_o and h as follows:

$$\log(z_o) = \log(h) - 0.98$$

Figure 14 shows estimates of d and z_o using these formulae for canopy height values of 29 m - 35 m along with our results using Stearn's method and a summary of several other studies given by Leonard and Federer (1973). The Stanhill formula yields a displacement height some 4 - 10 m smaller than the values estimated using Stearn's method. The Szeicz formula yields a

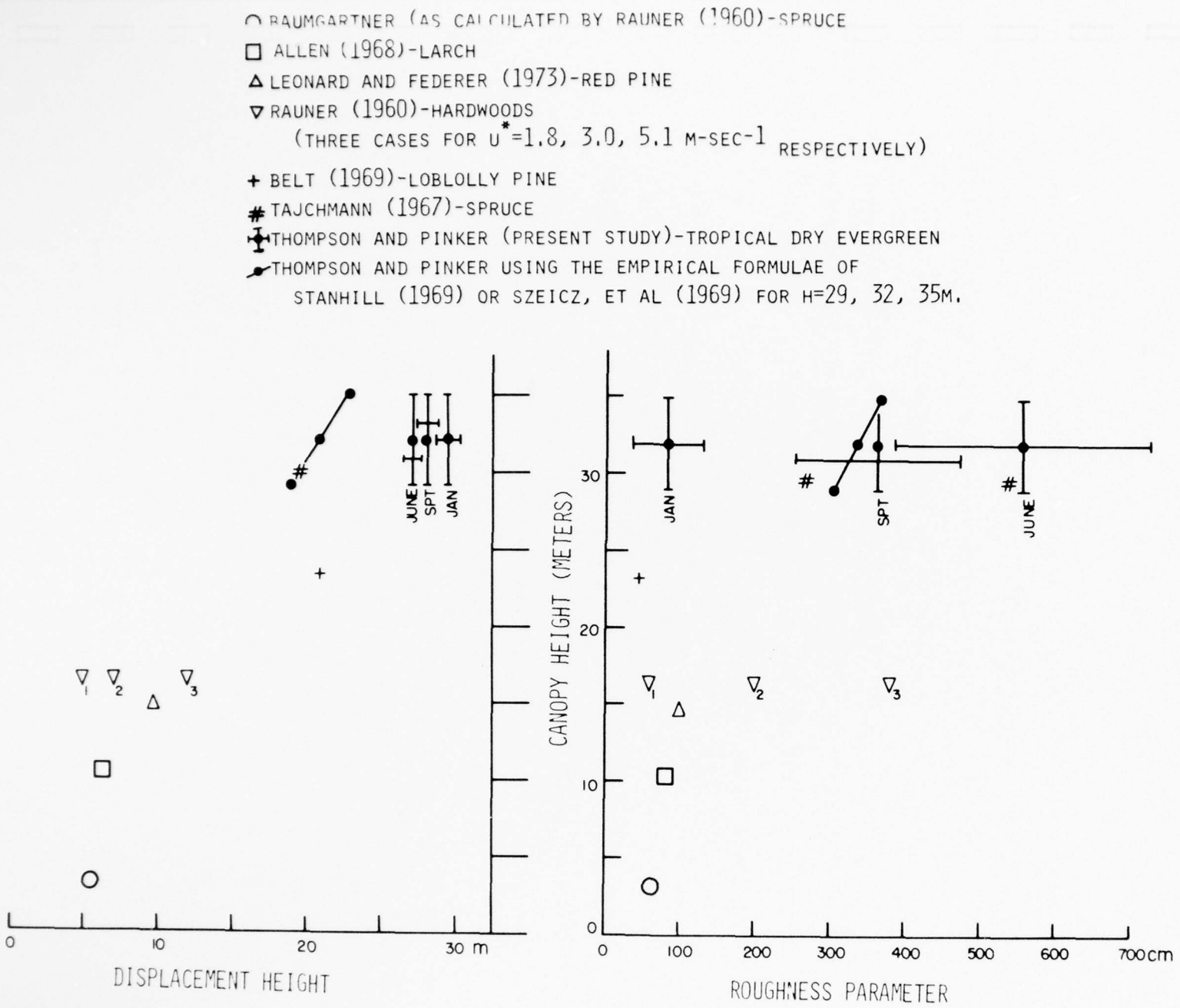

FIGURE 14. SUMMARY OF VARIOUS RESULTS ON THE RELATIONSHIP BETWEEN DATUM DISPLACEMENT LEVEL, ROUGHNESS PARAMETER AND CANOPY HEIGHT.

result which is consistent with the profile estimate for September but not for January or June.

A test was made for possible correlations between z_o and d with wind speed at the top of the tower (46 m). Rauner (1960) found that z_o increases and d decreases with increasing wind speed while Tajchmann (1967) found that z_o decreases and d remained constant as wind speed increased. Aller (1968) and Belt (1969) found no significant dependence on wind speed if d were allowed to be different for each computation of (z_o, d) but when a fixed value of d was used for an ensemble of profiles, z_o was found to decrease as wind speed increased but only for a particular wind direction. In the present study, the profiles were not partitioned according to wind direction, however, d and z_o were computed independently for each profile.

Table 18 shows the results of a simple correlation-regression analysis applied to the ensemble of 384 cases in January, June and September. It should be noted that the range of wind speeds above the forest canopy is not very large. Nonetheless, the roughness parameter is found to be an increasing function of wind speed and the datum displacement height a decreasing function of wind speed, which supports the findings of Rauner. Both parameters correlate best with the wind speed near the canopy (i.e. u(32)) but the correlation between d and u(46) is also significant at the 5% level. The correlation between roughness and wind speed is slightly better when the logarithm of z_o is used.

AD-A047 981 MARYLAND UNIV COLLEGE PARK INST FOR FLUID DYNAMICS --ETC F/G 4/2
ENVIRONMENTAL CONDITIONS IN A TROPICAL FOREST REGION IN THAILAN--ETC(U)
NOV 74 H E LANDSBERG, O E THOMPSON DAAK02-72-C-0287
UNCLASSIFIED BN-799 ETL-0129 NL

2 OF 2
ADA047 981

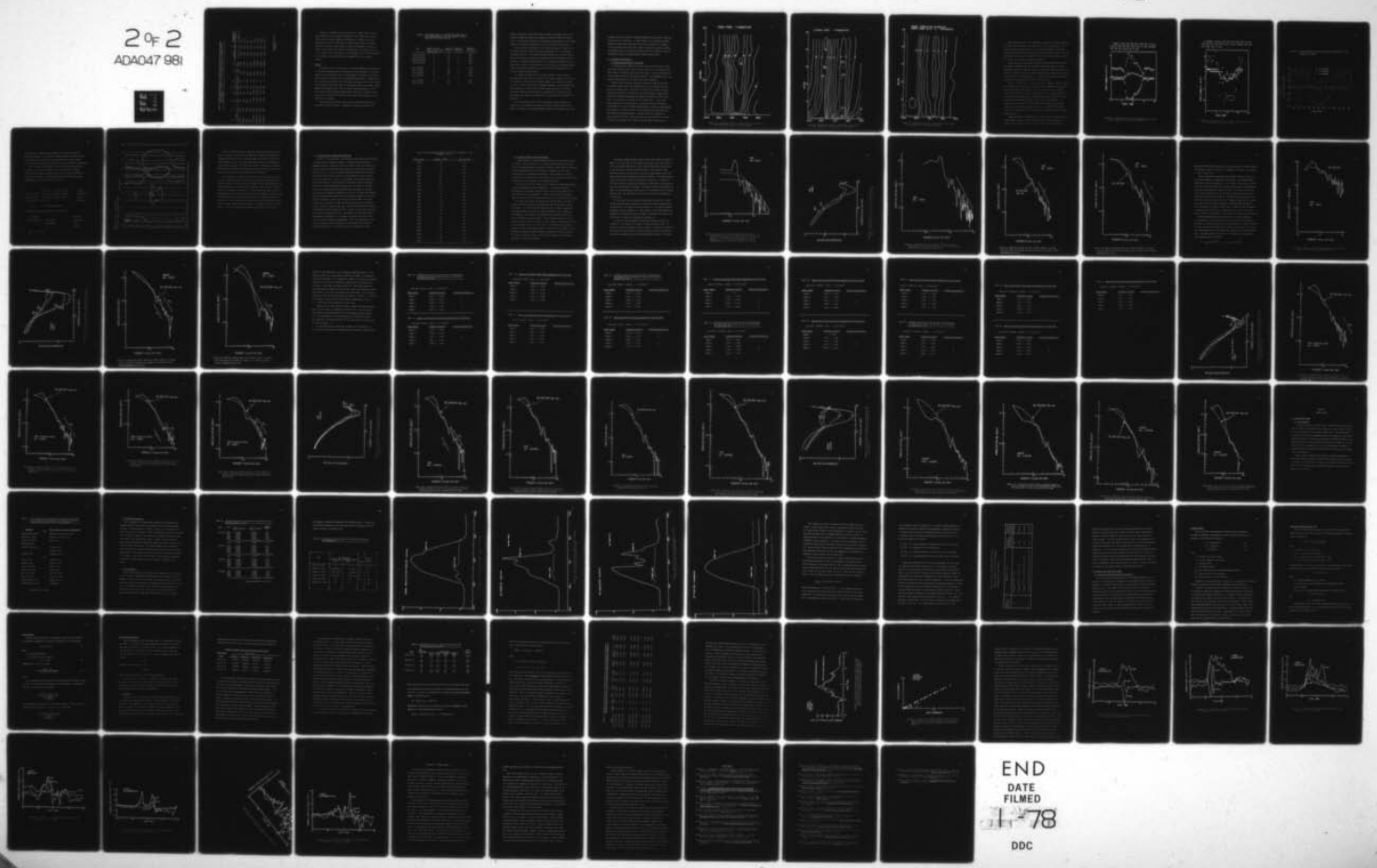

END
DATE FILMED
1-78
DDC

TABLE 18. CORRELATION AND REGRESSION STATISTICS FOR 384 CASES OF 30-MINUTE AVERAGED WIND PROFILES IN JANUARY, JUNE AND SEPTEMBER ABOVE THE SAKAERAT FOREST. [Y = A + BX]

Y	X	$\bar{Y}$	σ_y	$\bar{X}$	σ_x	A	B	R (Correlation)	F ratio	Standard Error of Estimate
UNITS →		[Y]	[Y]	[cm-sec^{-1}]	[cm-sec^{-1}]	[Y]	[Y/X]			[Y]
z_o(cm)	u(46)	466	214	429	139	79.3	0.900	0.586	200	173.5
z_o(cm)	u(32)	466	214	181	78	147.4	1.758	0.639	263*	164.8
d(cm)	u(46)	2761	102	429	139	2968	-0.483	0.659	293*	770
d(cm)	u(32)	2761	102	181	78	2945	-1.017	0.774	568*	649
ln[z_o(cm)]	u(46)	5.968	0.708	429	139	4.645	0.00308	0.607	223	0.563
ln[z_o(cm)]	u(32)	5.968	0.708	181	78	4.808	0.00641	0.704	374*	0.504
ln[d(cm)]	u(46)	7.923	0.037	429	139	7.997	-0.00017	0.656	289*	0.028
ln[d(cm)]	u(32)	7.923	0.037	181	78	7.988	-0.00036	0.770	556*	0.024

* Significant at the 5% level.

Finally, a preliminary analysis was made of a small sample of wind speed profiles in the clearing to determine to what extent these profiles can be fitted by simple algebraic relationships. Profiles of 30-minute averaged wind speeds for four days in January and two days in June were fitted, in the least squares sense, to linear and quadratic functions of height. Table 19 shows the results of these trials. The data at the top 6 or 7 levels in the clearing seem to be adequately fit by a linear relation and the winds at all levels seem to be adequately fit by a quadratic relation.

4. Summary

An analysis of the characteristics of wind and temperature distributions in a tropical evergreen forest in Thailand has been presented in this paper. Temperatures are generally cooler and wind speeds lower during the northeast monsoon season as compared with the southwest monsoon period. Conditions are more variable during January since the skies are clearer, the moisture content of the atmosphere above the forest is less and the radiational budget is more dynamic. The atmosphere just above the canopy therefore exhibits a much more complex thermal character during January than June or September with a large diurnal variation of stability which is also highly dependent on the proximity to the canopy.

Conditions during the warm, moist southwest monsoon generally show a much weaker diurnal variation. Cloudiness and atmospheric moisture are

TABLE 19. PRELIMINARY RESULTS OF FITTING WIND SPEED DATA IN THE CLEARED AREA TO LINEAR AND QUADRATIC PROFILE EQUATIONS FOR JANUARY AND JUNE

Date	Number of tower levels used starting from the top	Number of Profiles	Degree of Polynomial	Explained Variance (%)
June 20-21,1970	6	96	1	98.7
June 20-21,1970	7	96	1	98.1
June 20-21,1970	8	96	1	96.7
June 20-21,1970	8	96	2	98.2
Jan. 4-5,1970	6	96	1	79.5
Jan. 4-5,1970	7	96	1	79.8
Jan. 4-5,1970	6	96	2	82.9
Jan. 4-5,1970	8	96	2	83.9
Jan. 6-7,1970	6	96	1	97.9
Jan. 6-7,1970	7	96	1	97.5

greater during this season which tends to dampen the diurnal cycle in the radiation budget and, hence, the variation of stability above the canopy. There is a much higher frequency of near-neutral conditions above the canopy during this season than during the cool, dry northeast monsoon season.

For near neutral conditions in both monsoon periods, the winds in the microlayer above the forest canopy show a reasonable fit to a displaced logarithmic profile. The datum displacement height has an average value of about 27.6 meters but varies over a range of about 2(1/4) meters from the northeast to southwest monsoon periods. This seasonal variation is about 3 times larger than the standard deviation of the short period sample estimate during the southwest monsoon period and nearly 50 times larger than that for the northeast monsoon sample.

The roughness parameter for the canopy exhibits a strong seasonal variation with a mean value of 0.83 m for the January sample, 5.55 m for the June sample and 3.61 m for the September sample. The seasonal variation is about 2.7 times larger than the standard deviation in z_o during the short period samples of June but about 10 times larger than that for January. The canopy stress has a mean value of 1.3 dynes-cm^{-2} for January and the much larger mean values of 21.6 dynes-cm^{-2} for June and 13.7 dynes-cm^{-2} for September.

It is interesting to note that for the January cases for which the stability of the air above the canopy is much more variable and the wind speeds are smaller, the datum displacement height has its maximum value and

greatest consistency while the roughness parameter has its lowest value and least (relative) consistency. A pooled sample of the 30-minute averaged profiles of wind speed occurring in near-neutral conditions in January, June and September (some 384 cases) reveal a significant positive correlation between roughness parameter and wind speed and a significant negative correlation between datum displacement height and wind speed.

5. Supplemental Information

A. Thermal Characteristics for January

In discussing the stability of the air layer above the forest canopy during the January period in Part 2 of this Section, it was noted that the daily range of Richardson numbers was quite large. This was attributed to a more dynamic variability of thermal stability. To substantiate this, the thermal characteristics of the layer alone may be examined.

Figures (15) and (16) show time-height sections of temperature along both towers averaged over each 30-minute period of the day and over the days 1-14, January, 1970. The effect of the forest is evident in Figure (15) where an inversion just below the tree tops and lapse condition just above are established and persist throughout the morning and early afternoon. No such feature is evident in the clearing area. A weak early morning inversion in the trunk space of the forest tends to break down around 1000 local time but becomes reestablished in stronger fashion during the afternoon. At similar levels in the clearing, lapse conditions prevail during this afternoon period. Similar features are apparent in Figure (17) for 19-30 June, 1970 except that the perturbation at the level of the tree tops seemed to be weaker during the early morning period.

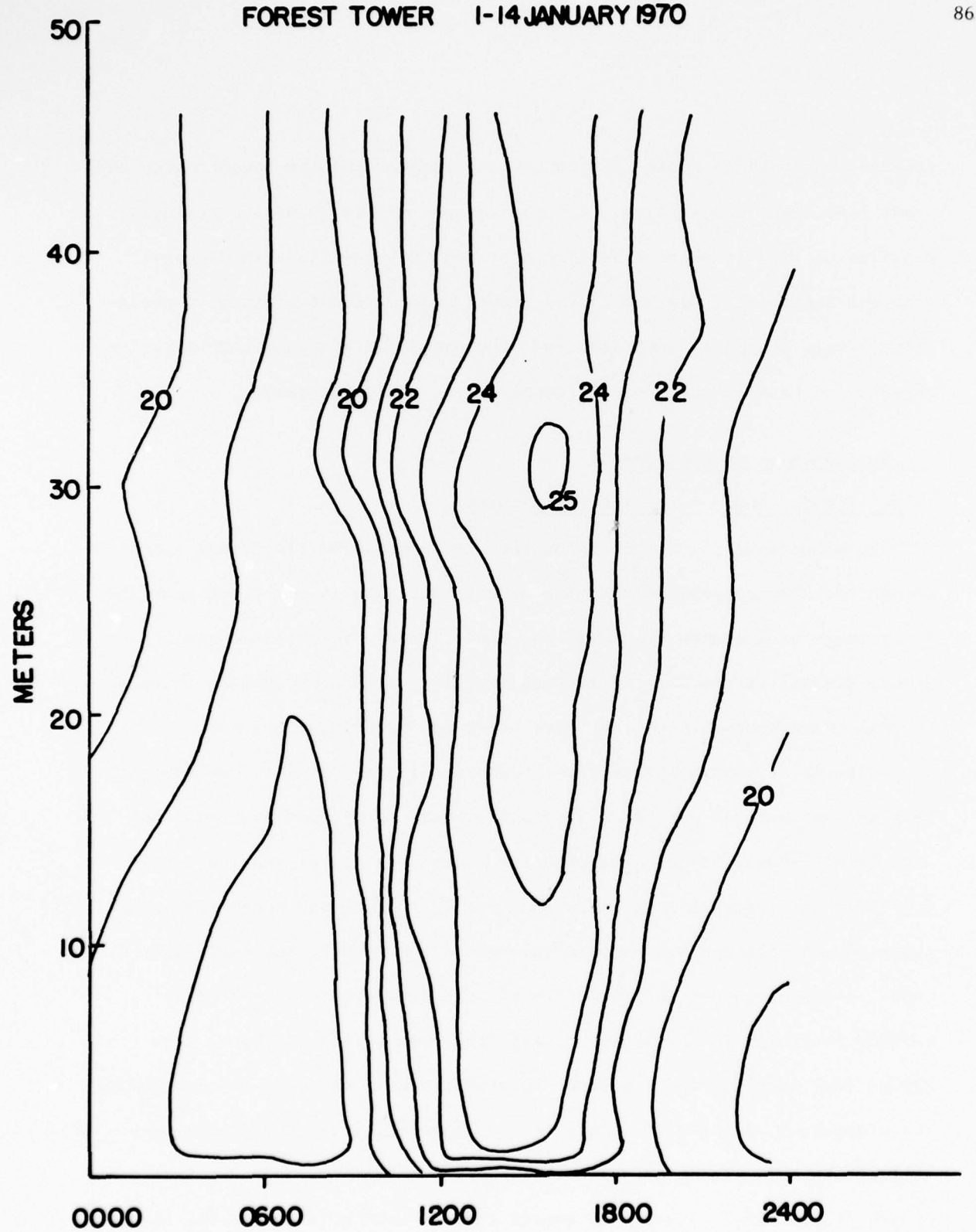

Figure 15. Time-Height Section of Temperature for the Tower in the Forest for an Average Day During January

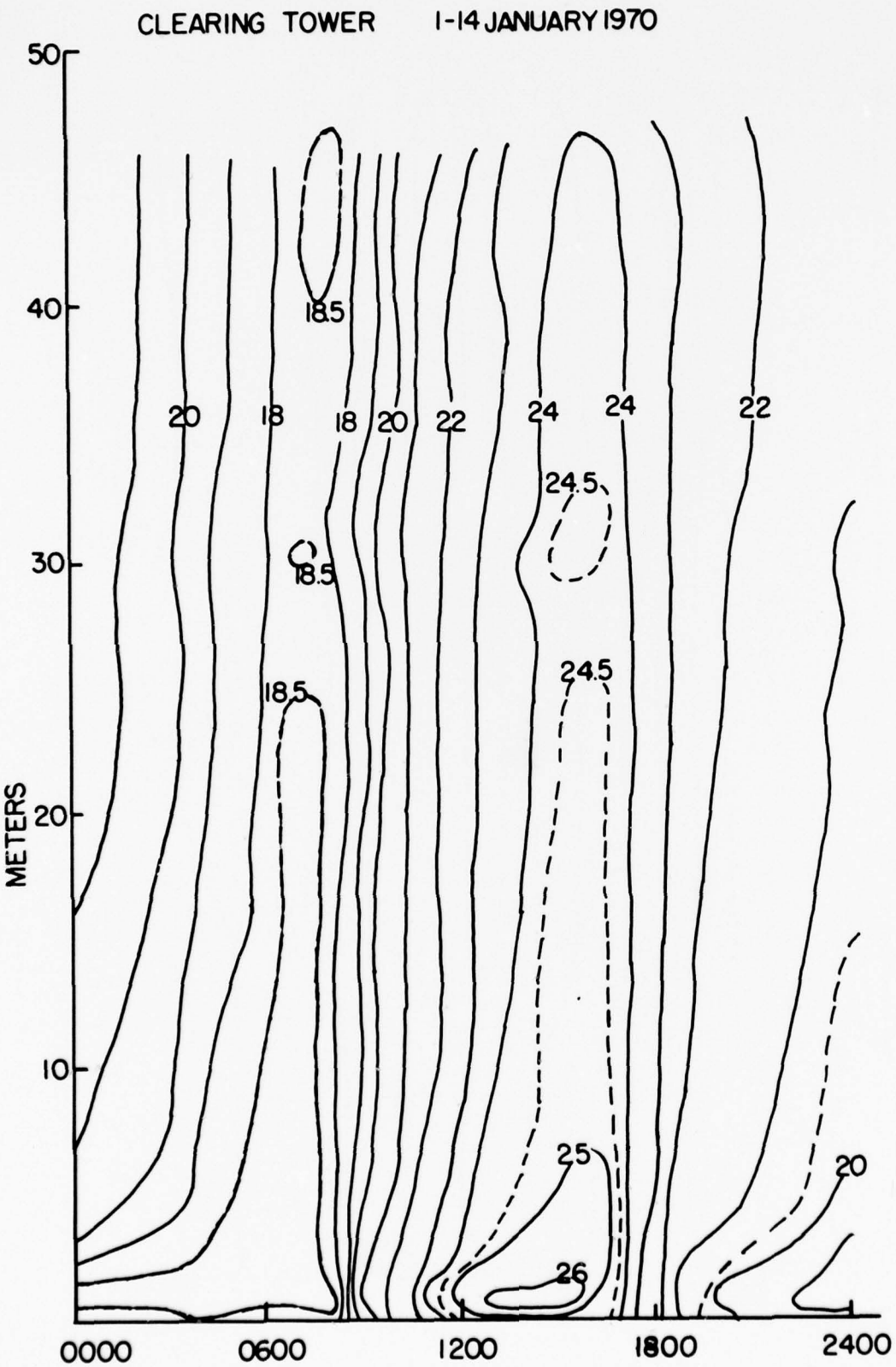

Figure 16. Time-Height Section of Temperature for the Tower in the Clearing for an Average Day During January

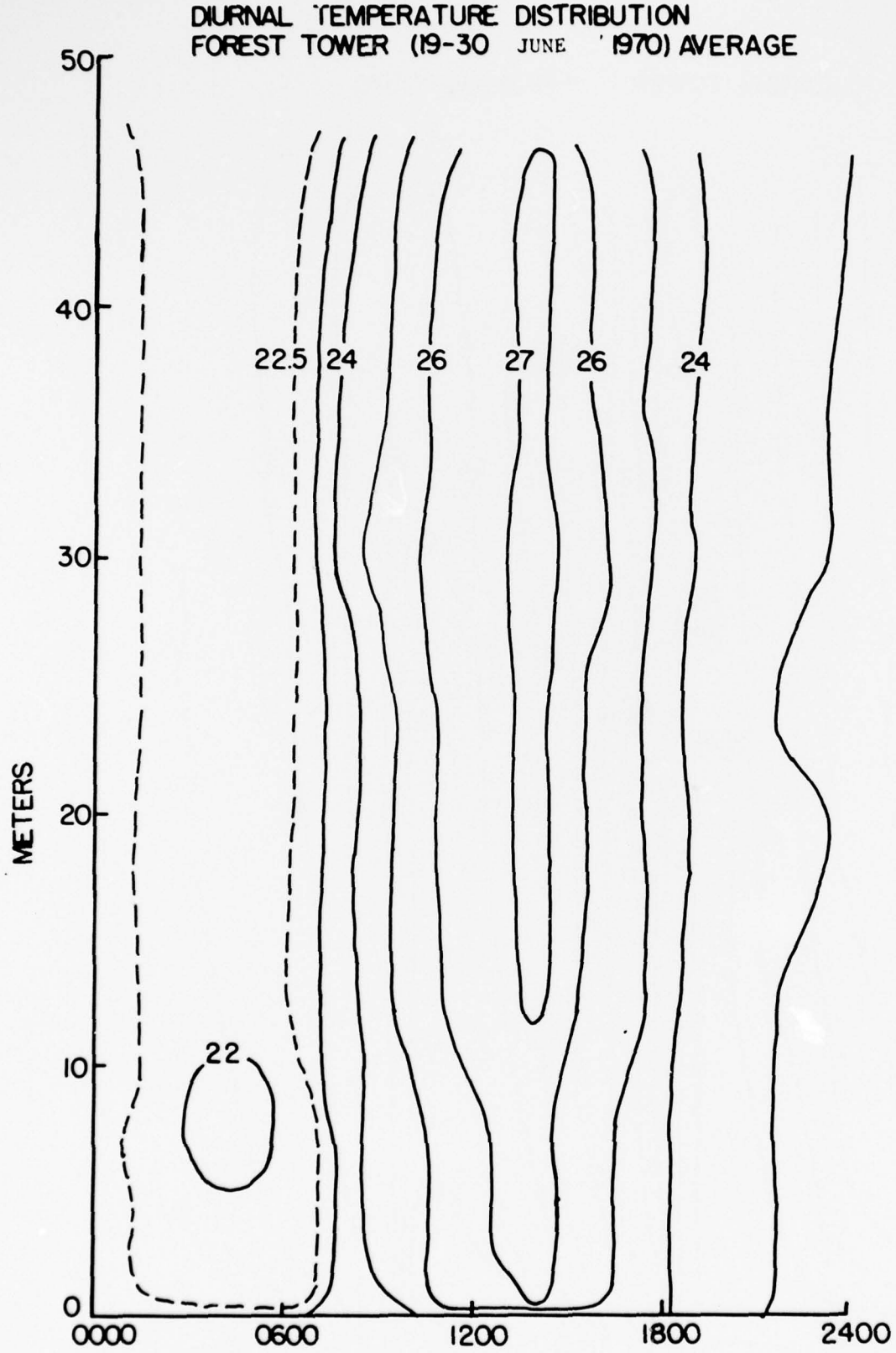

Figure 17. Time-Height Section of Temperature for the Tower in the Forest for an Average Day in June

Figure (18) shows the static stability $\sigma = [(g/c_p) - (\Delta T/\Delta z)]/\bar{T}$ computed for various layers defined by the top 6 levels of the forest tower. The values for the individual layers are most consistent during the nighttime hours 1730-0730 local time. During this period the values σ(25-30), σ(36-40), σ(40-46) are all within about $1 \times 10^{-4} m^{-1}$ with σ(25-30) consistently positive and σ(36-40) and σ(40-46) consistently negative.

During the day the stabilities undergo a rather well defined variation. For example, consistent with the warm layer development above the canopy during the daytime, σ(25-30) is positive in the stable lower portion of the layer with σ(30-32) and σ(32-36) highly negative in the unstable upper portion of this layer. In the higher layers near the top of the tower, σ(40-46) and σ(36-40) both show large stable values during the day.

Figure 19 shows values of static stability σ(32-46), σ(24-32), σ(16-24) as a function of time of day for the tower in the clearing. The distribution of temperature and stability at these heights are not as strongly distorted by the forest canopy as immediately above the canopy, hence, the values (and the ordinate scale of the diagram) are quite different than in the previous diagram for the forest tower stability distribution. The stability values σ(32-46), σ(24-32) undergo less diurnal variation than σ(16-24) and are generally within the range -2 to $+5 \times 10^{-5} m^{-1}$ throughout the entire 24 hour period. They generally show conditions nearest neutral during the day.

Figure (20) shows a distribution of values of static stability between levels (4-8m), (2-4m) and (1-2m) along the tower in the clearing. The layer next to the surface (1-2m) shows the largest diurnal variation of

FOREST. DOTS ARE FOR THE LAYER 36M TO 46M; CIRCLES ARE FOR THE LAYER 32M TO 36M; CROSSES ARE FOR THE LAYER 25M TO 30M.

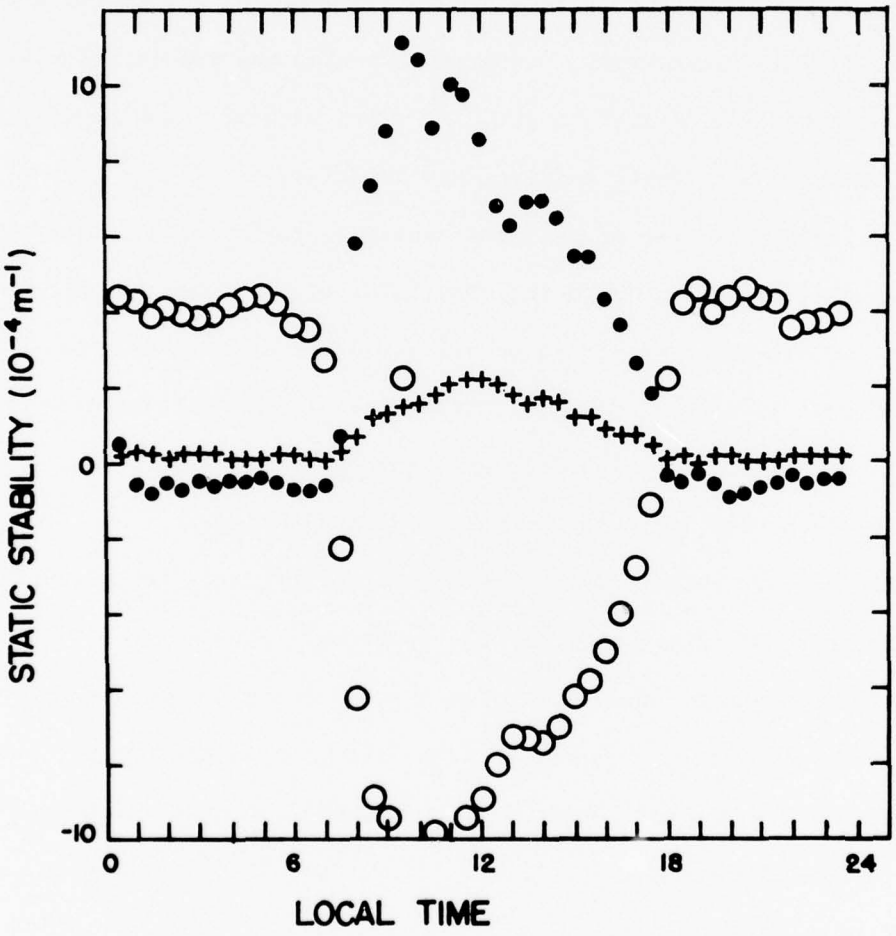

Figure 18. Diurnal Variation of Static Stability for Various Layers Above the Forest Canopy for January

CLEARING. CIRCLES ARE FOR THE LAYER 32M TO 46M; DOTS ARE FOR THE LAYER 24M TO 32M; CROSSES ARE FOR THE LAYER 16M TO 24M.

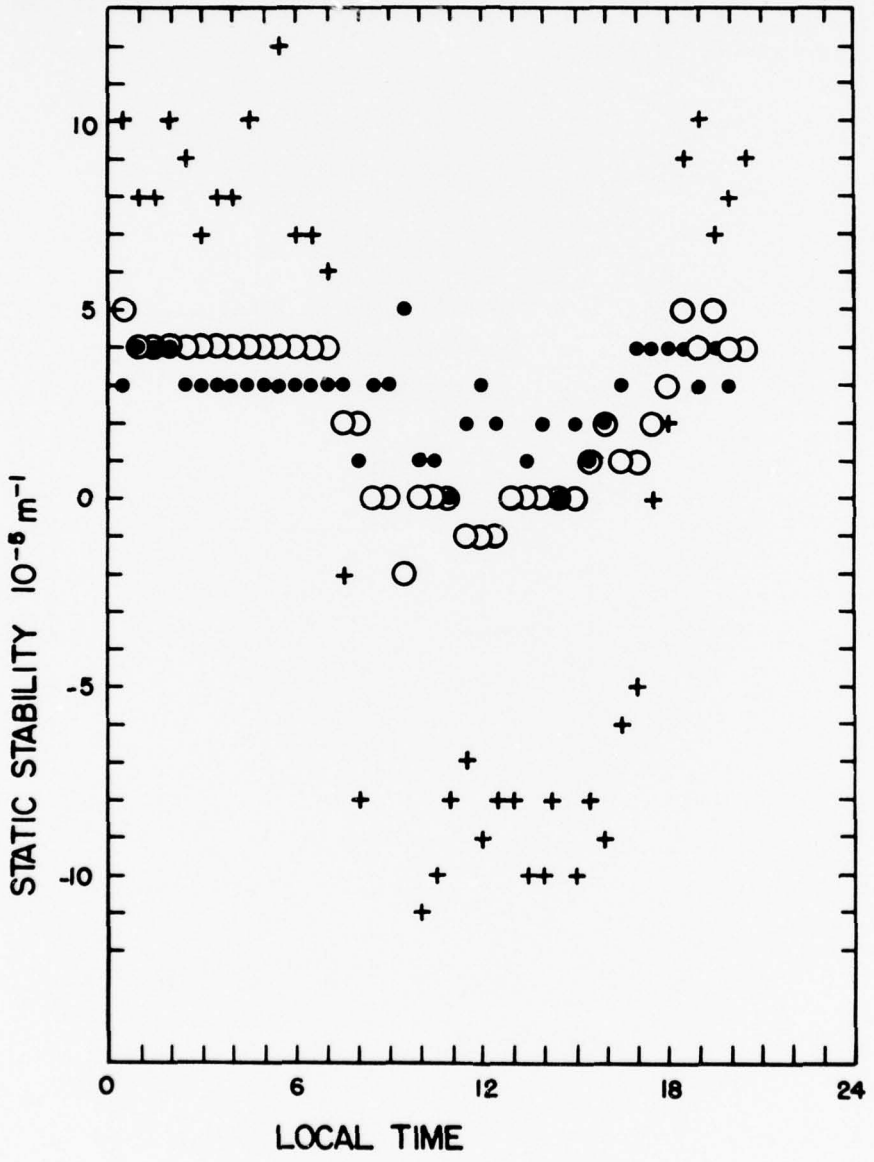

Figure 19. Diurnal Variation of Static Stability for Various Layers in the Clearing for January

FIGURE 20. DIURNAL VARIATION OF STATIC STABILITY AT LOW LEVELS IN THE CLEARING FOR JANUARY.

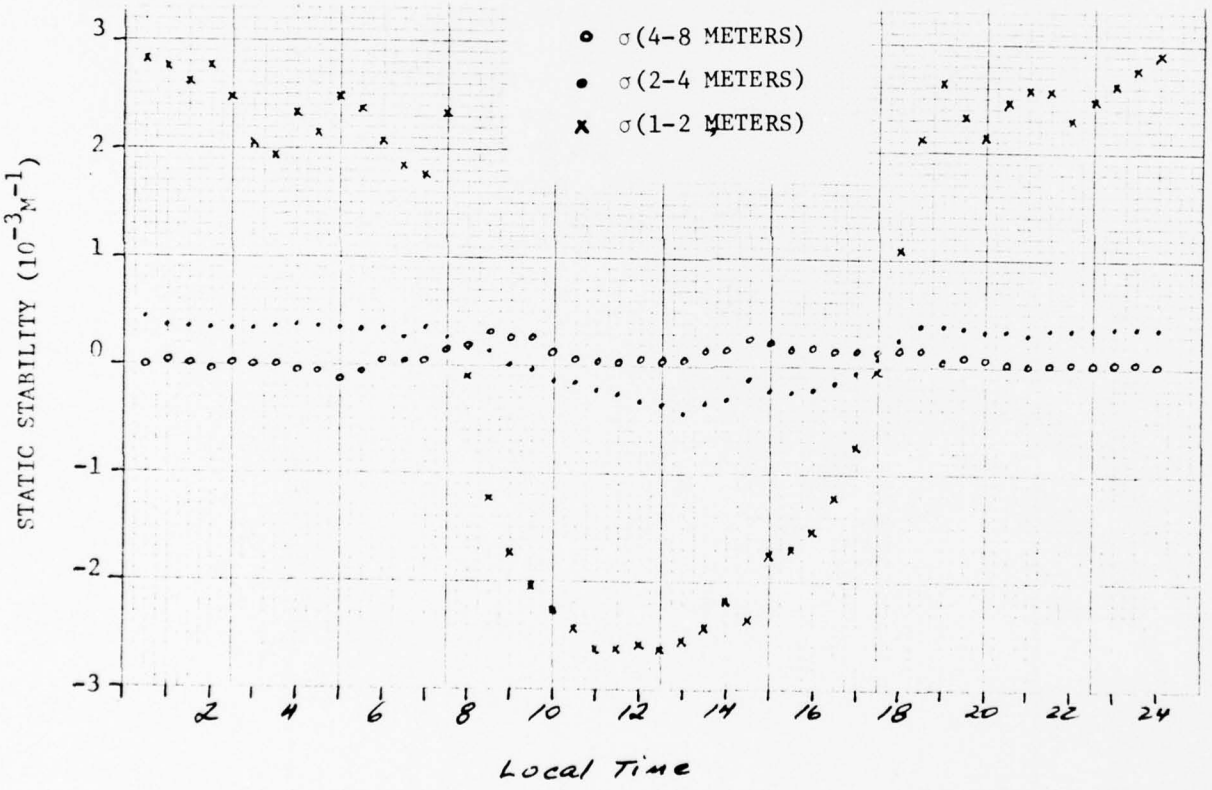

stability with a regime strongly coupled to the diurnal variation in surface temperature. In the layers (4-8m) and (2-4m) centered at 6m and 3m respectively, the stability is more uniform over the day although $\sigma(2\text{-}4)$ exhibits a diurnal cycle similar to $\sigma(1\text{-}2)$ but smaller in amplitude.

Fig. 21 shows a time-height section for two week averaged static stability in the forest for January. The section covers a typical diurnal variation from the ground to the top of the tower and shows the occurrence of unstable, near-neutral, stable and inversion conditions. Specifically, the criteria used in this plot is

	$(1/\theta)(\partial\theta/\partial z) \leq -3.333 \times 10^{-6} m^{-1}$	unstable
$-3.333 \times 10^{-6} m^{-1}$	$< (1/\theta)(\partial\theta/\partial z) \leq +6.667 \times 10^{-6} m^{-1}$	near-neutral
$+6.667 \times 10^{-6} m^{-1}$	$< (1/\theta)(\partial\theta/\partial z) \leq 30.000 \times 10^{-6} m^{-1}$	stable
$30.000 \times 10^{-6} m^{-1}$	$< (1/\theta)(\partial\theta/\partial z)$	inversion

where θ = potential temperature

These criteria correspond roughly to the following

$1.1(°K/100M)$	$\leq \Gamma$	unstable
$0.8(°K/100M)$	$\leq \Gamma < 1.1(°K/100M)$	near-neutral
0	$\leq \Gamma < 0.8(°K/100M)$	stable
	$\Gamma < 0$	inversion

where $\Gamma = -(\partial T/\partial z)$

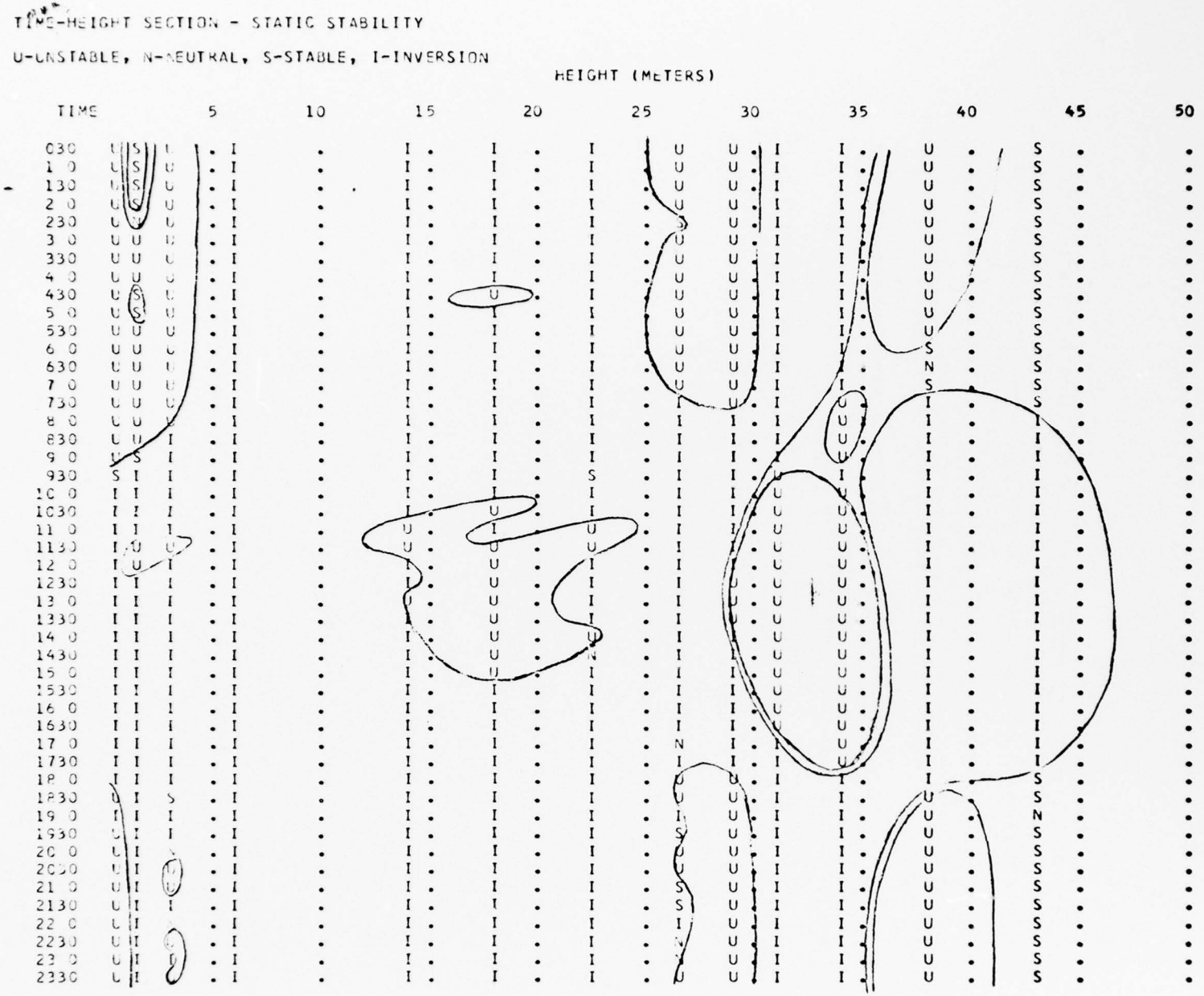

Figure 21. Time-Height Section of Static Stability in the Forest for an Average Day in January

As can be seen, near neutral conditions during this period were quite rare. The layer of air next to the forest floor shows strong inversion or isothermal conditions during the daylight hours from 10:00 to 19:00, then lapse conditions set in after sunset and develop large values during the night and early morning. The trunk space region is dominated by inversion and/or stable conditions with unstable conditions developing below tree-top level just before noon and continuing until mid-afternoon.

After sunrise, a warm layer centered on about the 30m level just above the tree tops develops and persists till the mid-afternoon gradually subsiding by sunset. The lower portion (~25-30m) of this layer maintains inversion conditions while the upper portion (~30-36m) exhibits lapse conditions which become unstable around 10:00. The above canopy jet tends to have its maximum speed in the portion of this layer showing significant lapse. During the night-time hours, the temperature at 30m shows a gradual cooling which establishes a thin unstable layer beneath and an inversion immediately above with a secondary unstable layer above that. At higher levels of the tower, stable or inversion conditions persist through virtually the entire day.

B. Wind Direction During January and June

In Part 3 of this Section, it was shown that the wind profile parameters - particularly the roughness parameter - varied considerably between different periods of the year. There are several factors which might contribute to these seasonal differences besides the prevailing wind speed as discussed in Part 3. One of the most prominent differences in the forest environment between January and June is the difference in the direction of the prevailing wind. June is in the middle of the southwest monsoonal flow while January is characterized by flow from the north or northeast. The upwind terrain characteristics during these two months is different with several cleared areas about 800-1000 meters northeast of the tower in the forest but generally unbroken forest area to the south and southwest. Also, the terrain slopes upward from the south and southwest to the towers with an inclination of about 1:40 or greater (ASRCT, 1969). The winds during June are generally stronger than during January but the direction is more variable in January than June. It was noted in Section II that the wind direction data was logged onto the "A-tapes" and that these tapes were not processed during this project. Nevertheless, limited wind direction information was available to us on computer printouts made from several A-tapes during the TREND field experiment. These are summarized in Table 20 which shows the diurnal variation of wind direction for January 4, 1970 and June 23, 1970. The wind direction is in degrees from north.

Table 20. Wind Direction (Degrees from North) for January 4, 1970 and June 23, 1970

Hour of Day	January 4, 1970	June 23, 1970
0000	47	262
0100	49	265
0200	63	258
0300	102	259
0400	344	263
0500	341	261
0600	346	258
0700	351	259
0800	13	260
0900	58	249
1000	53	247
1100	45	256
1200	59	252
1300	30	253
1400	36	241
1500	47	245
1600	69	234
1700	83	254
1800	87	262
1900	65	259
2000	42	254
2100	76	270
2200	88	274
2300	84	257

C. Spectral Analysis of Wind Speed Data

A limited amount of spectral analysis was done on wind speed data from the towers. The ultimate goal is to obtain spectral analyses (of kinetic energy and wind-temperature co-spectra) covering a large range of frequencies by using half-minute data for the highest frequencies and half-hourly averaged data for intermediate frequencies. These studies were started relatively late in the contract period and, thus, only kinetic energy spectra involving the lower frequencies are presently available.

The first step in these analyses was to develop an appropriate computer program for application to the TREND data. The Graduate Program in Meteorology has a spectral analysis routine using the Fast Fourier Transform (FFT) that has been adapted to a number of meteorological studies. Results using the FFT were compared with results of direct spectral estimates.

The time series chosen for analysis with the FFT were for 10 days in January and about 10 days in June using data from several levels along both towers. The FFT divides the time series into a number of equal and overlapping segments, obtains the spectral estimate of each segment and then averages. The length of the time series was 180 data points (that is, 180 30-minute averaged values). Since the method requires that the length of record should be a power of 2, the record is supplemented by zeroes up to 256 points which is the first power of 2 beyond 180. The number of lags was 127 (128 is the largest power of 2 which is less than 180). Using half-hourly averages as data, 180 values corresponds to 90 hours so that the largest frequency is about 3 days with this sample while the Nyquist frequency is $(1/2\Delta t)$=1 cycle/hour.

The kinetic energy spectral results from the FFT method are shown in Figure 22 for the tower in the forest for the period June 20-30, 1970. A "red" spectrum was computed as a first order linear Markov process based on one lag value of the autocorrelation series. This approach seems justified since the two lag value of the series approximates the one lag value squared [Gilman, Fuglister and Mitchell (1963)]. The autocorrelation values for levels 16m and 46m are plotted in Figure 23. In Figure 22 two "red" spectra are plotted to illustrate the difference in the manner by which the "red" spectra is defined. The dashed line was obtained using two lags in the autocorrelation function while the dot-dashed line was obtained using one lag. The chi-square test can be used to test the significance of each peak.

For the same record and using the same number of lags (127), direct spectral estimates were obtained and compared with spectra obtained from the FFT method. The results are shown in Figure 24 and exhibit features comparable to those of Figure 22. That portion of the spectrum above the frequency of 20 cycles/hour seems to follow a (-2) power law [and not the (-5/3) power law based on the Kolmogorov hypothesis].

In order to reduce computation and plotting time and increase the "stability" of the spectra, the number of lags was reduced to 50. The results are shown in Figures 25a,b and are similar in structure to Figure 24. On the basis of these results, it seems reasonable to deal with the half-hourly data by using direct Fourier transforms with 50 lags. The results

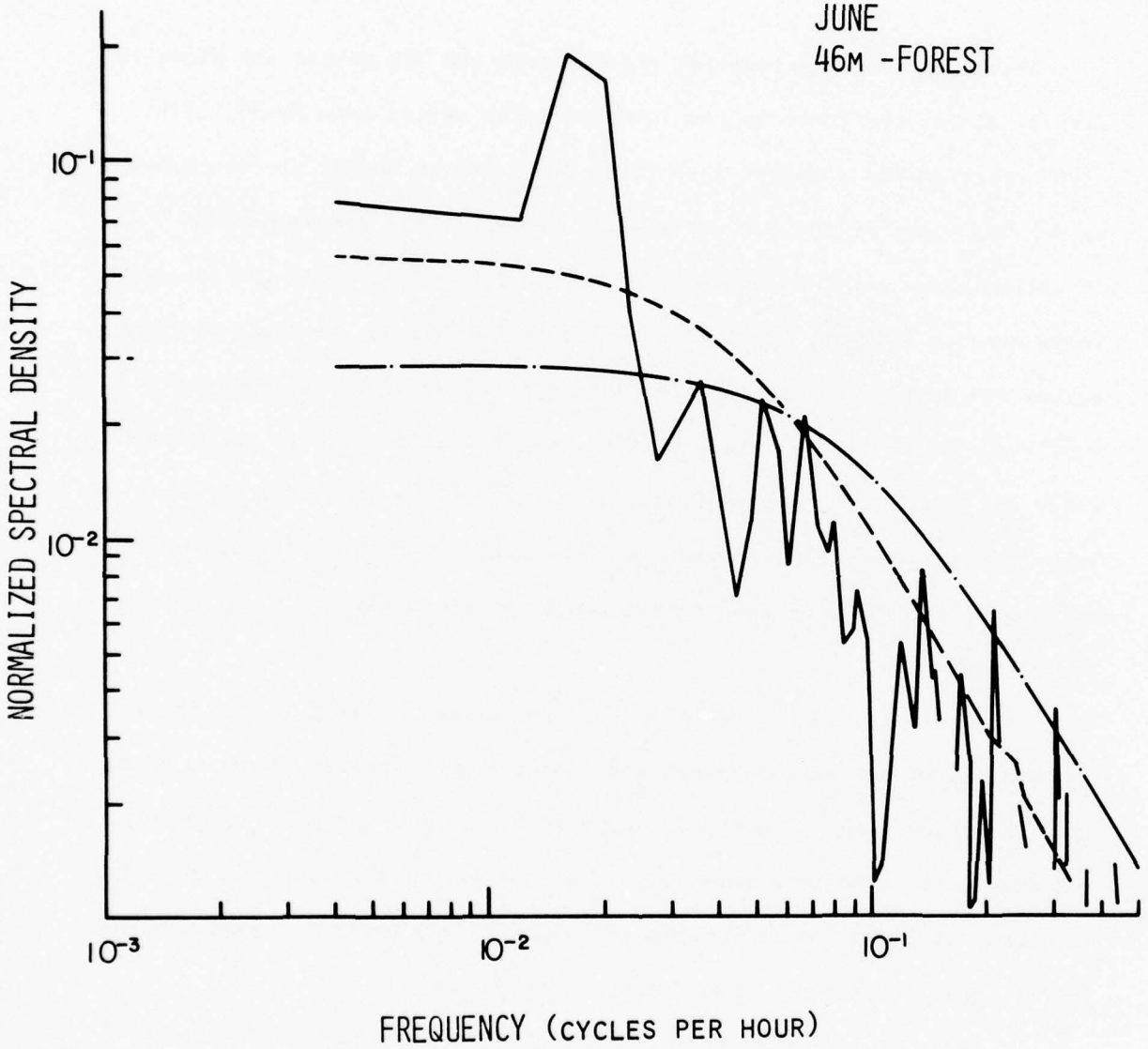

Figure 22. Normalized Spectral Density of Kinetic Energy at 46m Along the Tower in the Forest for June 20-30, 1970 Using the Fast Fourier Transform Method With 127 Lags. Dashed Curve is "Red Noise" Obtained With Two Lags; Dot-Dashed Curve is "Red Noise" Obtained With One Lag

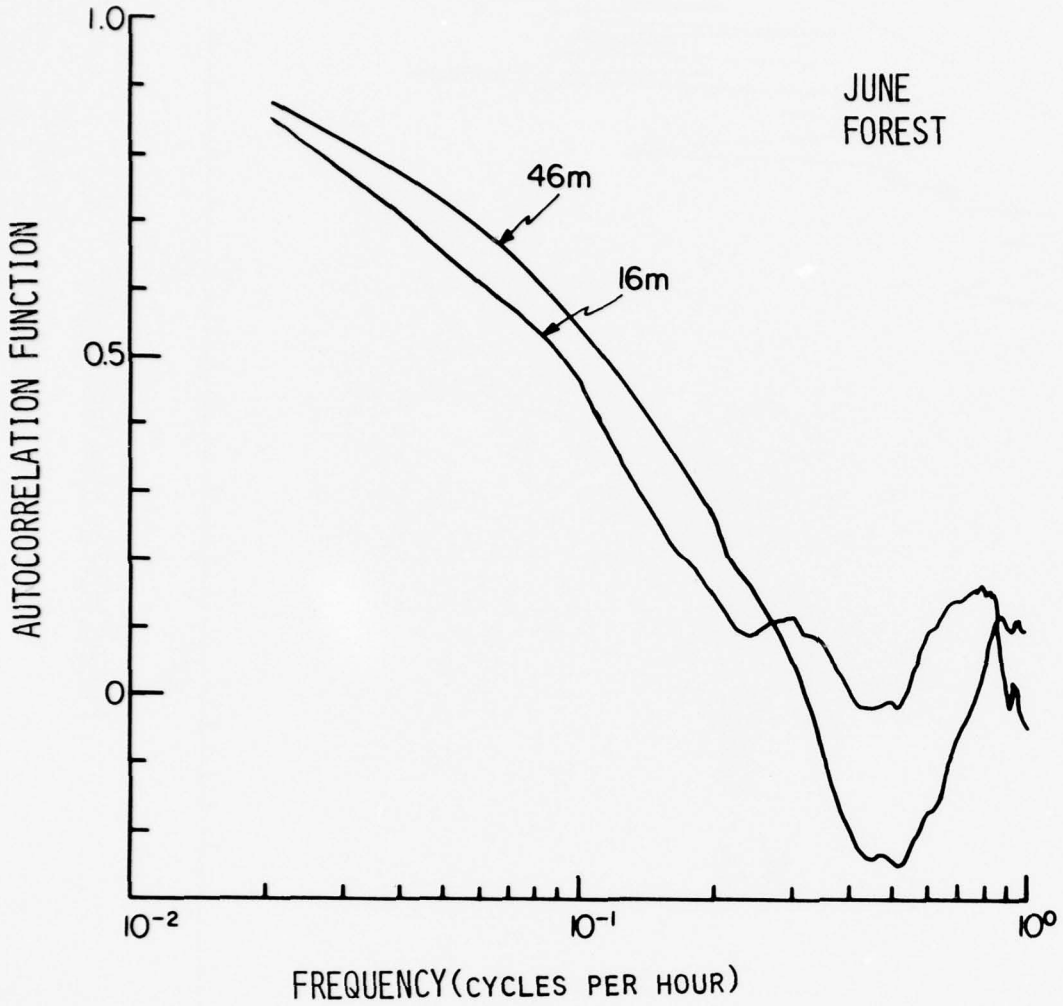

Figure 23. Autocorrelation Function for June 20-30, 1970 at the 16m and 46m Levels Along the Tower in the Forest Using 50 Lags.

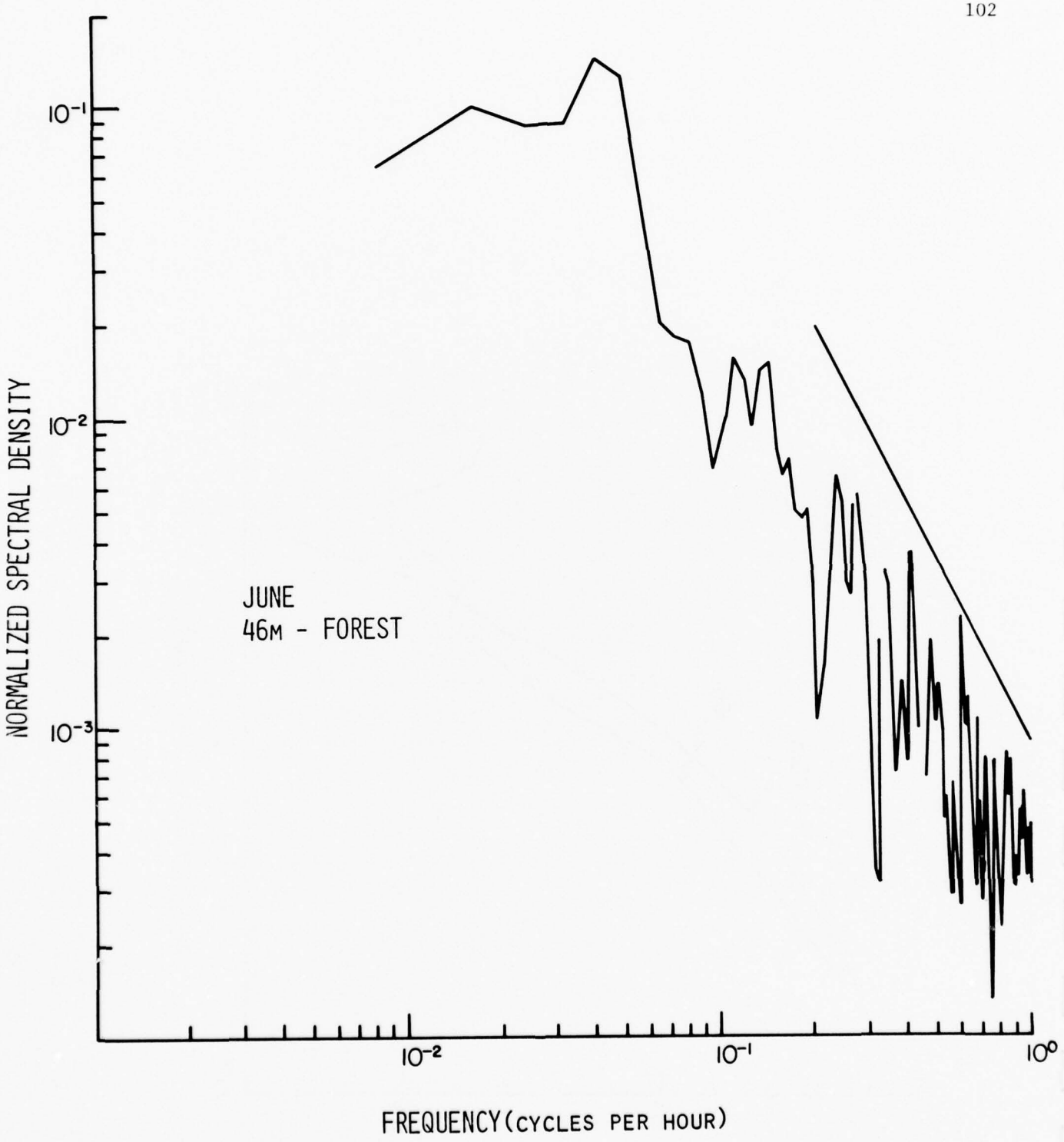

Figure 24. Normalized Spectral Density of Kinetic Energy at 46m Along the Tower in the Forest for June 20-30, 1970 Using Direct Fourier Transforms With 127 Lags

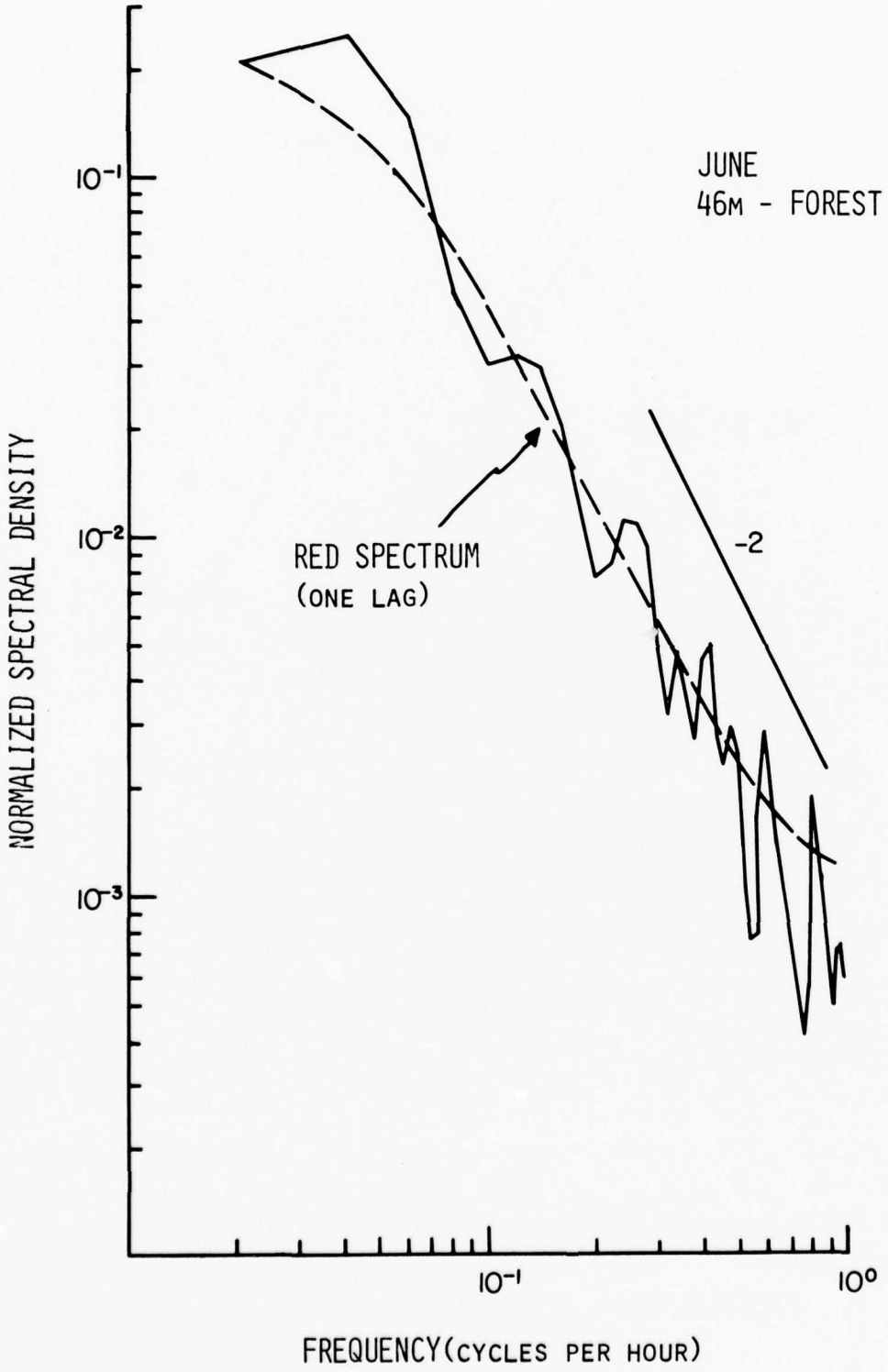

FIGURE 25a. NORMALIZED SPECTRAL DENSITY OF KINETIC ENERGY AT 46 METERS ALONG THE TOWER IN THE FOREST FOR JUNE 20-30, 1970 USING DIRECT FOURIER TRANSFORMS WITH 50 LAGS.

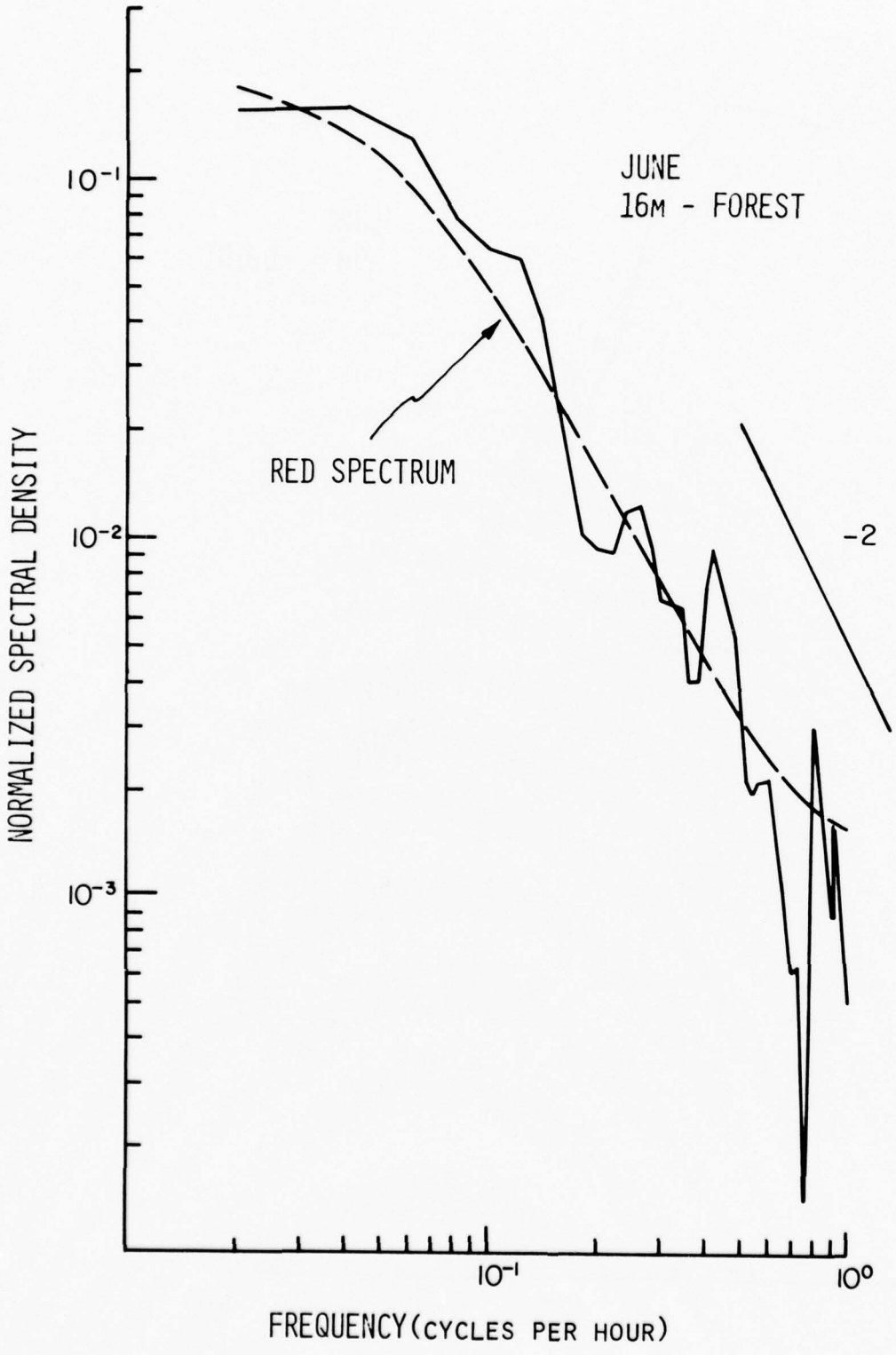

FIGURE 25b. NORMALIZED SPECTRAL DENSITY OF KINETIC ENERGY AT 16 METERS ALONG THE TOWER IN THE FOREST FOR JUNE 20-30, 1970 USING DIRECT FOURIER TRANSFORMS WITH 50 LAGS.

comprising Figure 25a were also plotted using the product of spectral density and frequency along the ordinate as is sometimes the custom. This display is shown in Figure 26.

Similar computations were done for data taken along the tower in the forest during January at levels 46m, 32m, 16m, 4m. The autocorrelation functions are plotted in Figure 27. It is readily evident that the levels within the canopy (4m, 16m) have different autocorrelation characteristics than those levels above the canopy (32m, 46m). The values drop off much faster and the computation of the red spectra using one lag in the auto-correlation function seems justified. Normalized spectral density for the 16m level is shown in Figure 28a. In the frequency range above 0.3 cycles/hour, the (-5/3) power law is indicated. Normalized spectral density for the 46m level is plotted in Figure 28b. It seems that the red spectra as computed here with one lag is inappropriate and that in this case it would be better to average over a few lags and then compute the red spectra.

Before preparing additional computations of spectral estimates, the variability of the time series was studied to test one of the basic hypotheses - that the data belong to the same population. Using the record for June, the data were divided into 5 samples of two days each. The mean and standard deviation of each sample were computed as well as the 10 day mean. Confidence limits for the mean of the population of each sample were computed using the "t"-test:

$$\bar{x} - t_{.05}\,[S/(n-1)^{1/2}] < \mu < \bar{x} + t_{.05}\,[S/(n-1)^{1/2}]$$

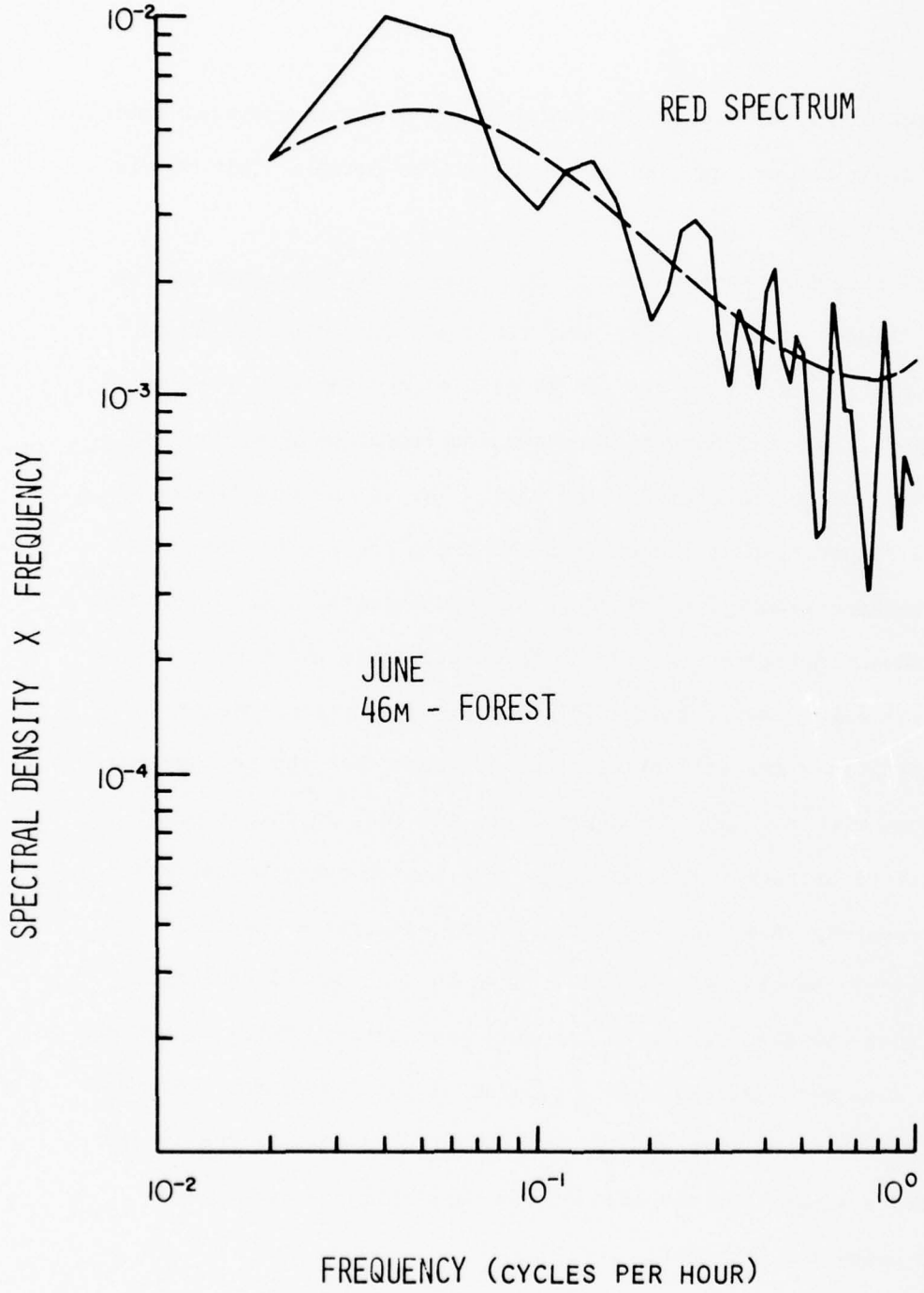

Figure 26. Product of Spectral Density and Frequency Corresponding to the 46m Level Data of Figure 25.

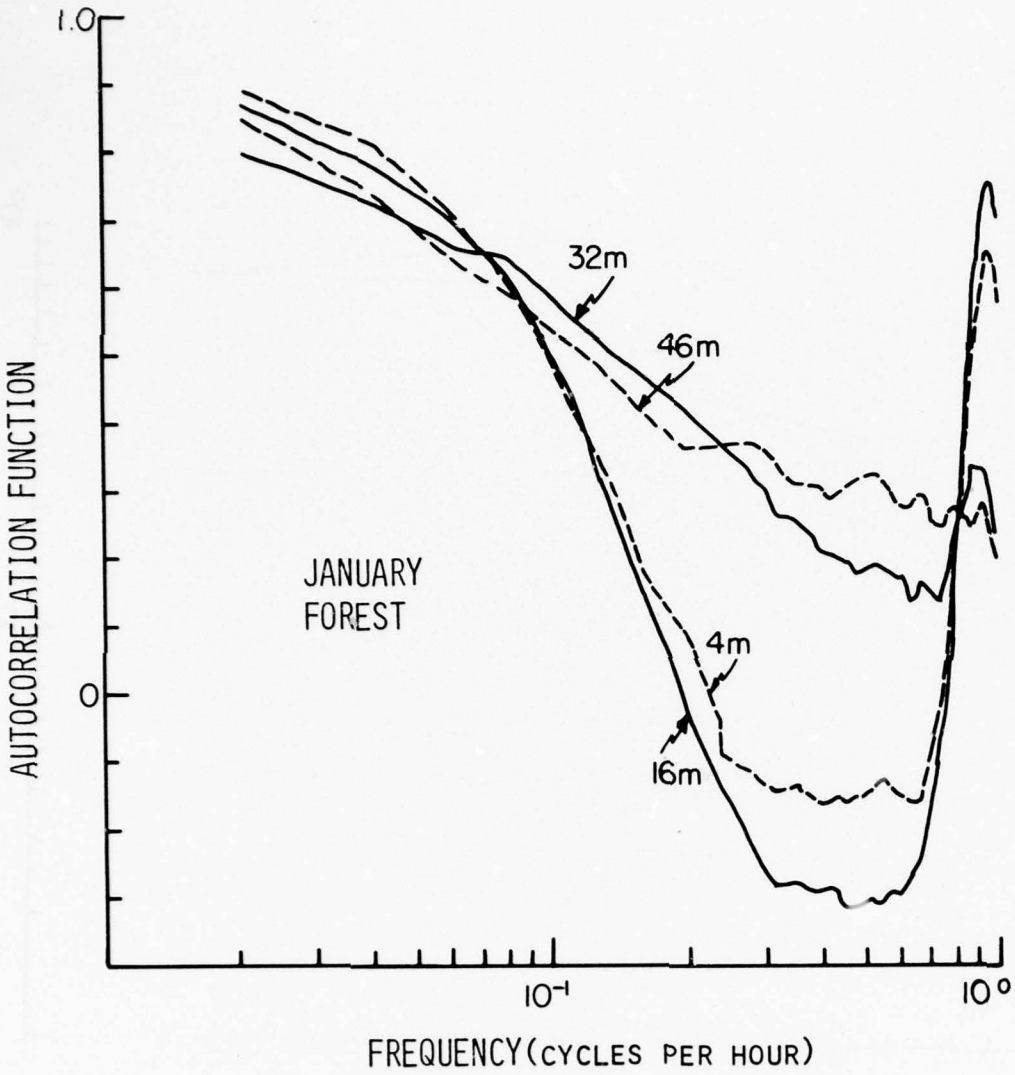

Figure 27. Autocorrelation Functions for January 4-14, 1970 at the 46m, 32m, 16m, 4m Levels Along the Tower in the Forest

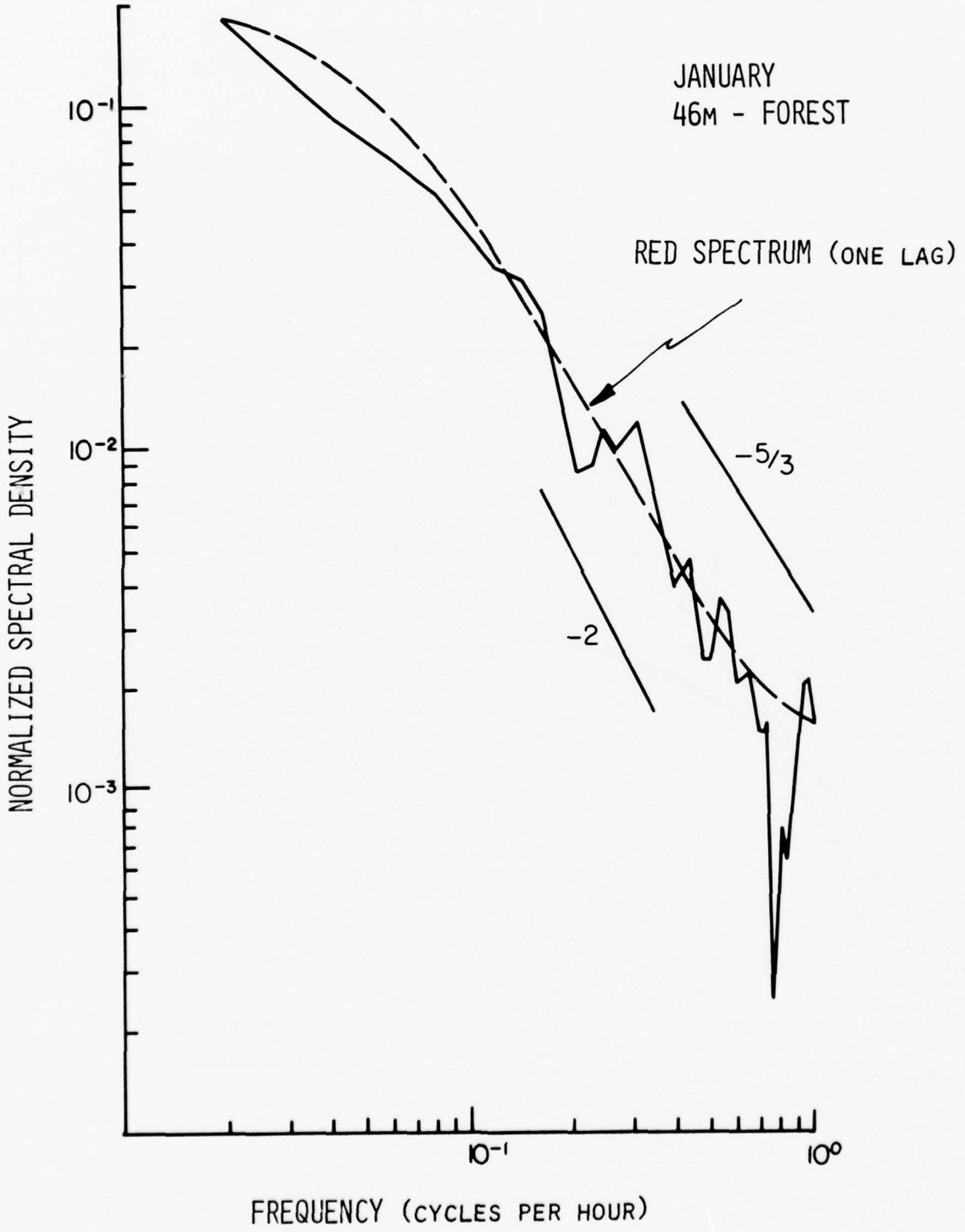

FIGURE 28a. NORMALIZED SPECTRAL DENSITY OF KINETIC ENERGY AT 46 METERS ALONG THE TOWER IN THE FOREST FOR JANUARY 4-14, 1970 USING DIRECT FOURIER TRANSFORMS WITH 50 LAGS.

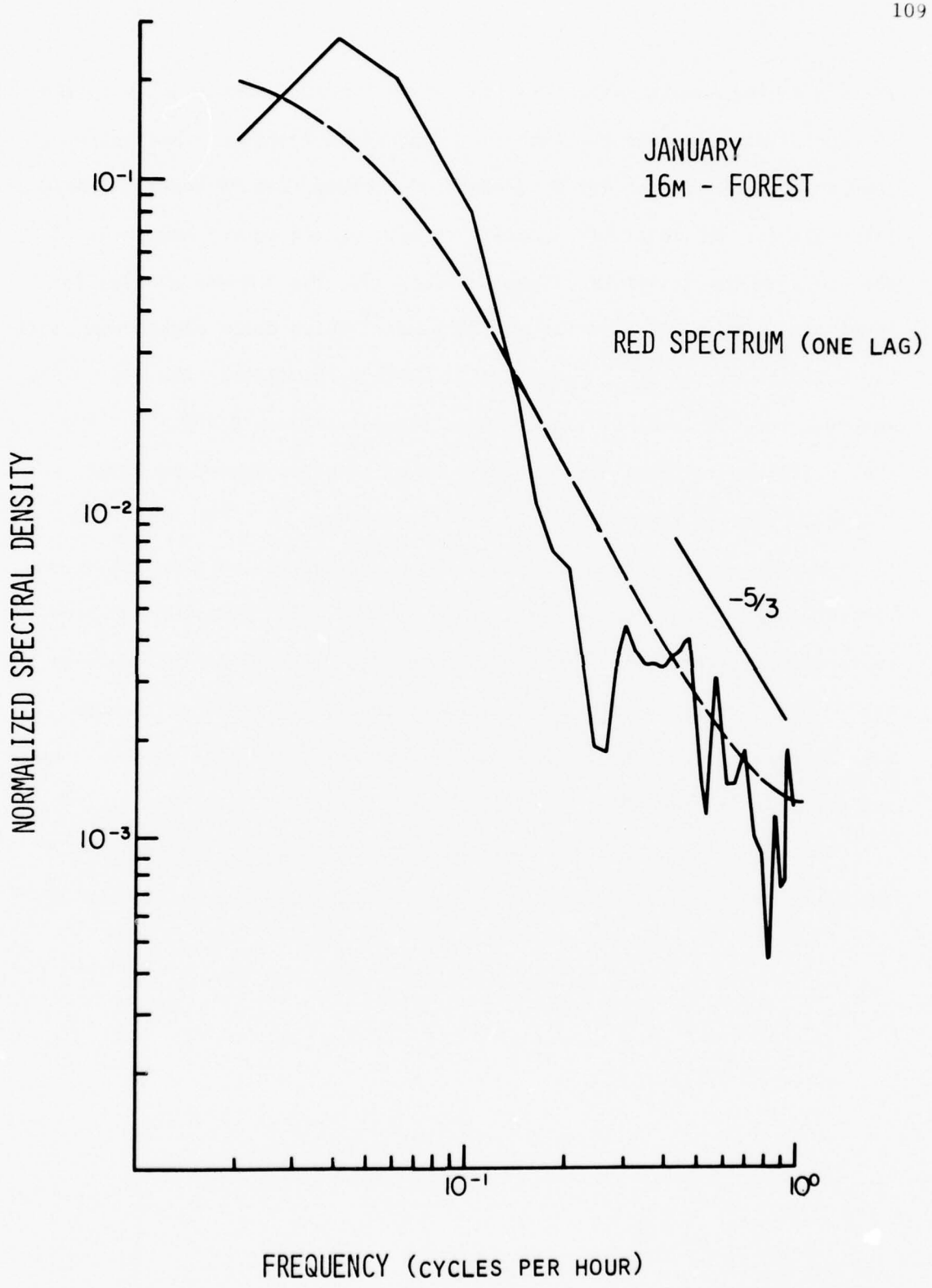

FIGURE 28b. NORMALIZED SPECTRAL DENSITY OF KINETIC ENERGY AT 16 METERS ALONG THE TOWER IN THE FOREST FOR JANUARY 4-14, 1970 USING DIRECT FOURIER TRANSFORMS WITH 50 LAGS.

where $\bar{x}$ is the sample mean, S is the sample standard deviation, μ is the population mean, n-1 is the number of degrees of freedom. The following results were obtained: For 95 degrees of freedom, t=1.99 and the confidence intervals for 95% level of significance appropriate to the 46m level of the tower in the forest are shown in Table 21. The ten day average for level 46m above the forest was μ=4.28 m-sec^{-1} which falls within the confidence limits of the first four samples but not the fifth. The confidence interval for 98% level of significance for sample 5 is $2.448 < \mu < 3.072$ and the confidence interval for the 99.9% level of significance is $2.311 < \mu < 3.209$ both of which exclude the 10 day mean.

Similar tests at other levels in both the forest and clearing during both June and January are summarized in Tables 22-35 . On the basis of these results, spectral estimates for the data taken along the tower in the forest during June for a shortened period of 8 instead of 10 days were computed. The autocorrelations are not much different, however, and are shown in Figure 29.

The autocorrelations and spectral estimates for both periods for the tower in the clearing were computed and are presented in Figures 30-34.

TABLE 21. Confidence Intervals for the 95% Level of Significance: Wind Speed Data at 46m Along the Tower in the Forest for June 20-30, 1970

Level 46m - Forest - June. $\mu = 4.28$ m-sec^{-1}

Sample Number	Confidence Interval	Criterion Satisfied (x)
Sample 1	$4.121 < \mu < 4.619$	x
Sample 2	$3.968 < \mu < 5.022$	x
Sample 3	$3.895 < \mu < 4.405$	x
Sample 4	$4.210 < \mu < 4.770$	x
Sample 5	$3.243 < \mu < 3.957$	

TABLE 22. Same as the Previous Table Except Appropriate to the 40m Level

Level 40m - Forest - June. $\mu = 3.72$ m-sec^{-1}

Sample Number	Confidence Interval	Criterion Satisfied (x)
Sample 1	$3.564 < \mu < 3.996$	x
Sample 2	$3.984 < \mu < 4.356$	
Sample 3	$3.377 < \mu < 3.823$	x
Sample 4	$3.641 < \mu < 4.119$	x
Sample 5	$2.866 < \mu < 3.474$	

TABLE 23. Same as the Previous Table Except Appropriate to the 36m Level

Level 36m - Forest - June. $\mu = 3.24$ m-sec^{-1}

Sample Number	Confidence Interval	Criterion Satisfied (x)
Sample 1	$3.092 < \mu < 3.468$	x
Sample 2	$3.461 < \mu < 3.779$	
Sample 3	$2.954 < \mu < 3.326$	x
Sample 4	$3.174 < \mu < 3.586$	x
Sample 5	$2.499 < \mu < 3.021$	

TABLE 24. Same as the Previous Table Except Appropriate to the 4m Level

Level 4m - Forest - June. $\mu = 0.43$ m-sec^{-1}

Sample Number	Confidence Interval	Criterion Satisfied (x)
Sample 1	$0.435 < \mu < 0.505$	x
Sample 2	$0.465 < \mu < 0.535$	
Sample 3	$0.411 < \mu < 0.489$	x
Sample 4	$0.345 < \mu < 0.415$	
Sample 5	$0.307 < \mu < 0.373$	

TABLE 25. Confidence Intervals for the 95% Level of Significance: Wind Speed Data at 46m Along the Tower in the Forest for January 4-14, 1970

Level 46m - Forest - January. $\mu = 2.28$ m-sec^{-1}

Sample Number	Confidence Interval	Criterion Satisfied (x)
Sample 1	$2.229 < \mu < 2.491$	x
Sample 2	$2.744 < \mu < 2.956$	
Sample 3	$1.802 < \mu < 2.018$	
Sample 4	$2.352 < \mu < 2.568$	
Sample 5	$1.734 < \mu < 1.946$	

TABLE 26. Same as Previous Table Except Appropriate to the 32m Level

Level 32m - Forest - January. $\mu = 0.55$ m-sec^{-1}

Sample Number	Confidence Interval	Criterion Satisfied (x)
Sample 1	$0.435 < \mu < 0.565$	x
Sample 2	$0.449 < \mu < 0.592$	x
Sample 3	$0.307 < \mu < 0.373$	
Sample 4	$0.519 < \mu < 0.662$	x
Sample 5	$0.745 < \mu < 0.875$	x

TABLE 27. Same as the Previous Table Except Appropriate to the 4m Level

Level 4m - Forest - January. $\mu = 0.27$ m-sec^{-1}

Sample Number	Confidence Interval	Criterion Satisfied (x)
Sample 1	$\mu = .2$	
Sample 2	$0.305 < \mu < 0.375$	
Sample 3	$0.256 < \mu < 0.305$	x
Sample 4	$0.269 < \mu < 0.331$	x
Sample 5	$0.240 < \mu < 0.280$	x

TABLE 28. Confidence Intervals for the 95% Level of Significance: Wind Speed Data at 46m Along the Tower in the Clearing for June 20-30, 1970

Level 46m - Clearing - June. $\mu = 5.9$ m-sec^{-1}

Sample Number	Confidence Interval	Criterion Satisfied (x)
Sample 1	$5.623 < \mu < 6.267$	x
Sample 2	$6.333 < \mu < 6.987$	
Sample 3	$5.294 < \mu < 6.086$	x
Sample 4	$5.788 < \mu < 6.572$	X
Sample 5	$4.531 < \mu < 5.549$	

TABLE 29. Same as the Previous Table Except Appropriate to the 32m Level

Level 32m - Clearing - June. $\mu = 5.13$ m-sec^{-1}

Sample Number	Confidence Interval	Criterion Satisfied (x)
Sample 1	$4.810 < \mu < 5.390$	x
Sample 2	$5.574 < \mu < 6.126$	
Sample 3	$4.655 < \mu < 5.325$	x
Sample 4	$4.983 < \mu < 5.637$	x
Sample 5	$3.949 < \mu < 4.831$	

TABLE 30. Same as the Previous Table Except Appropriate to the 16m Level

Level 16m - Clearing - June. $\mu = 3.76$ m-sec^{-1}

Sample Number	Confidence Interval	Criterion Satisfied (x)
Sample 1	$\mu = 3.468$	
Sample 2	$4.190 < \mu < 4.590$	
Sample 3	$3.475 < \mu < 3.965$	x
Sample 4	$3.595 < \mu < 4.065$	x
Sample 5	$2.845 < \mu$ (3.555	

TABLE 31. Same as the Previous Table Except Appropriate to the 2m Level

Level 2m - Clearing - June. $\mu = 2.35$ m-sec^{-1}

Sample Number	Confidence Interval	Criterion Satisfied (x)
Sample 1	$2.195 < \mu < 2.465$	x
Sample 2	$2.691 < \mu < 2.949$	
Sample 3	$2.253 < \mu < 2.567$	
Sample 4	$2.191 < \mu < 2.509$	x
Sample 5	$1.591 < \mu < 2.109$	

TABLE 32. Confidence Intervals for the 95% Level of Significance: Wind Speed Data at 46m Along the Tower in the Clearing for January 4-14, 1970

Level 46m - Clearing - January. $\mu = 2.95$ m-sec^{-1}

Sample Number	Confidence Interval	Criterion Satisfied (x)
Sample 1	$3.015 < \mu < 3.305$	
Sample 2	$3.650 < \mu < 3.870$	
Sample 3	$2.731 < \mu < 3.010$	x
Sample 4	$2.683 < \mu < 2.957$	x
Sample 5	$2.028 < \mu < 2.273$	

TABLE 33. Same as the Previous Table Except Appropriate to the 32m Level

Level 32 m - Clearing - January. $\mu = 2.95$ m-sec^{-1}

Sample Number	Confidence Interval	Criterion Satisfied (x)
Sample 1	$2.531 < \mu < 2.789$	
Sample 2	$3.070 < \mu < 3.270$	
Sample 3	$2.321 < \mu < 2.579$	
Sample 4	$2.330 < \mu < 2.571$	
Sample 5	$1.728 < \mu < 1.973$	

TABLE 34. Same as the Previous Table Except Appropriate to the 16m Level

Level 16m - Clearing - January. $\mu = 1.66$ m-sec^{-1}

Sample Number	Confidence Interval	Criterion Satisfied (x)
Sample 1	$1.682 < \mu < 1.918$	
Sample 2	$2.080 < \mu < 2.300$	
Sample 3	$1.419 < \mu < 1.681$	x
Sample 4	$1.401 < \mu < 1.679$	x
Sample 5	$1.124 < \mu < 1.356$	

TABLE 35. Same as the Previous Table Except Appropriate to the 2m Level

Level 2m - Clearing - January. $\mu = 0.83$ m-sec^{-1}

Sample Number	Confidence Interval	Criterion Satisfied (x)
Sample 1	$0.792 < \mu < 1.008$	x
Sample 2	$0.974 < \mu < 1.206$	
Sample 3	$0.584 < \mu < 0.816$	
Sample 4	$0.676 < \mu < 0.904$	x
Sample 5	$0.554 < \mu < 0.726$	

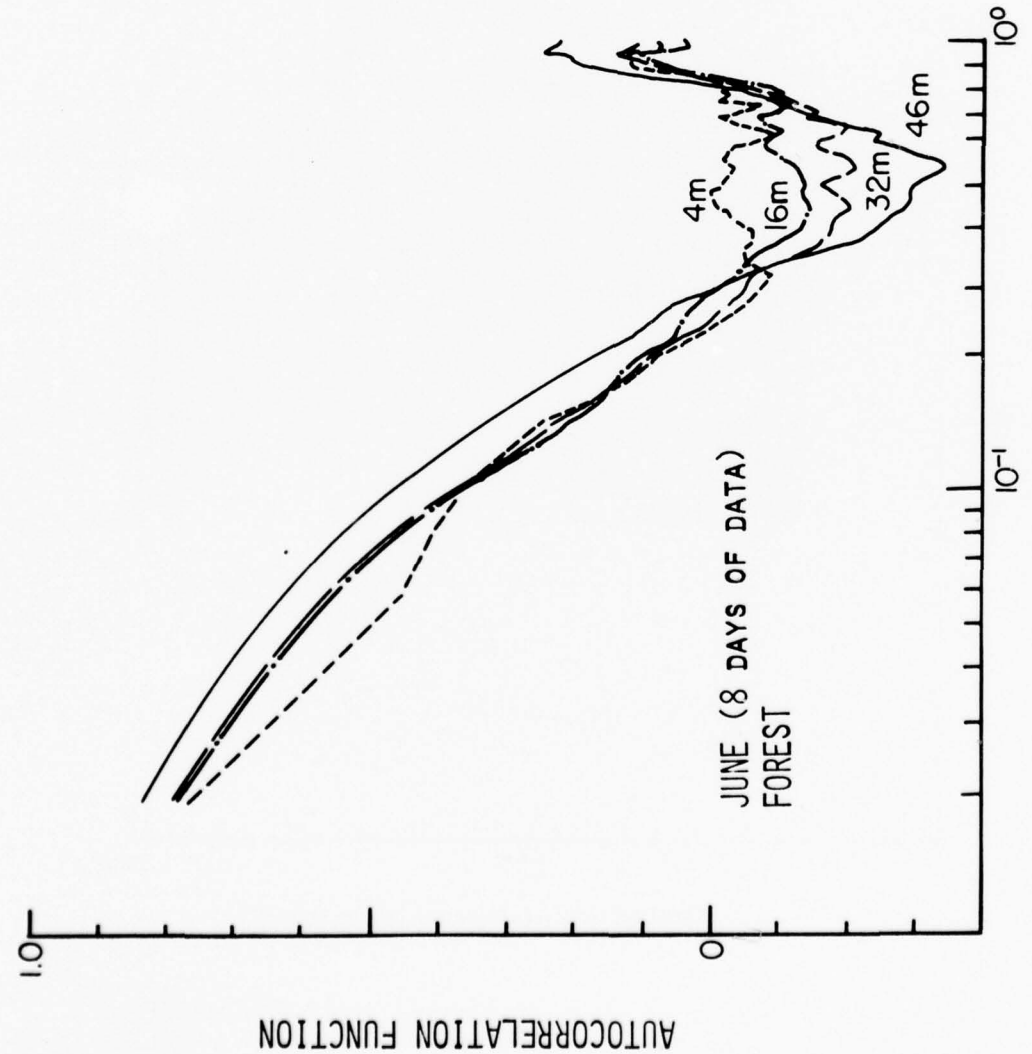

Figure 29. Autocorrelation Functions for Eight Days in June (June 20-28, 1970) at the 46m, 32m, 16m, 4m Levels Along the Tower in the Forest

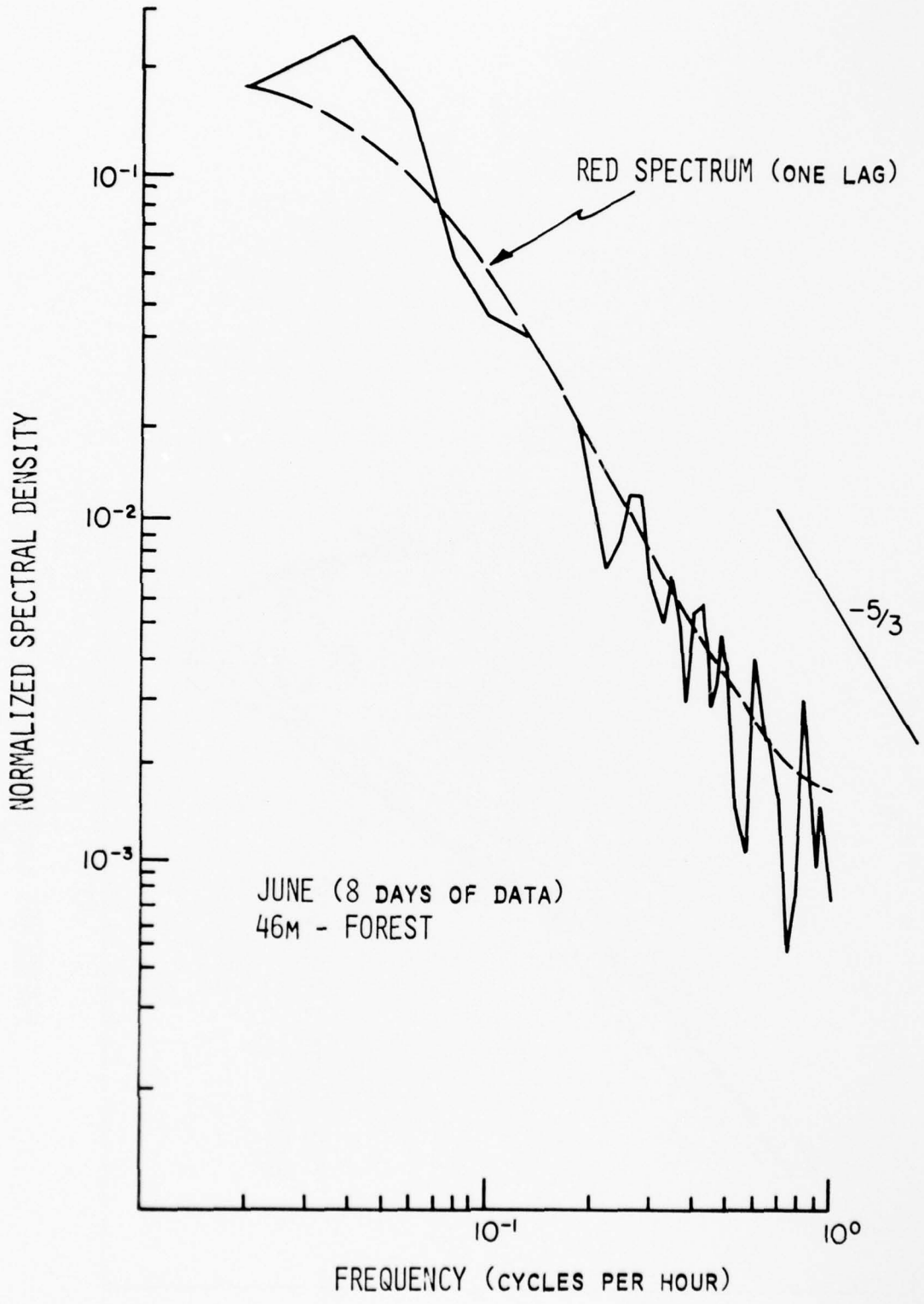

Figure 30a. Normalized spectral density of kinetic energy at 46 meters along the tower in the forest for an eight day period, June 20-28, 1970, using direct Fourier transforms with 50 lags.

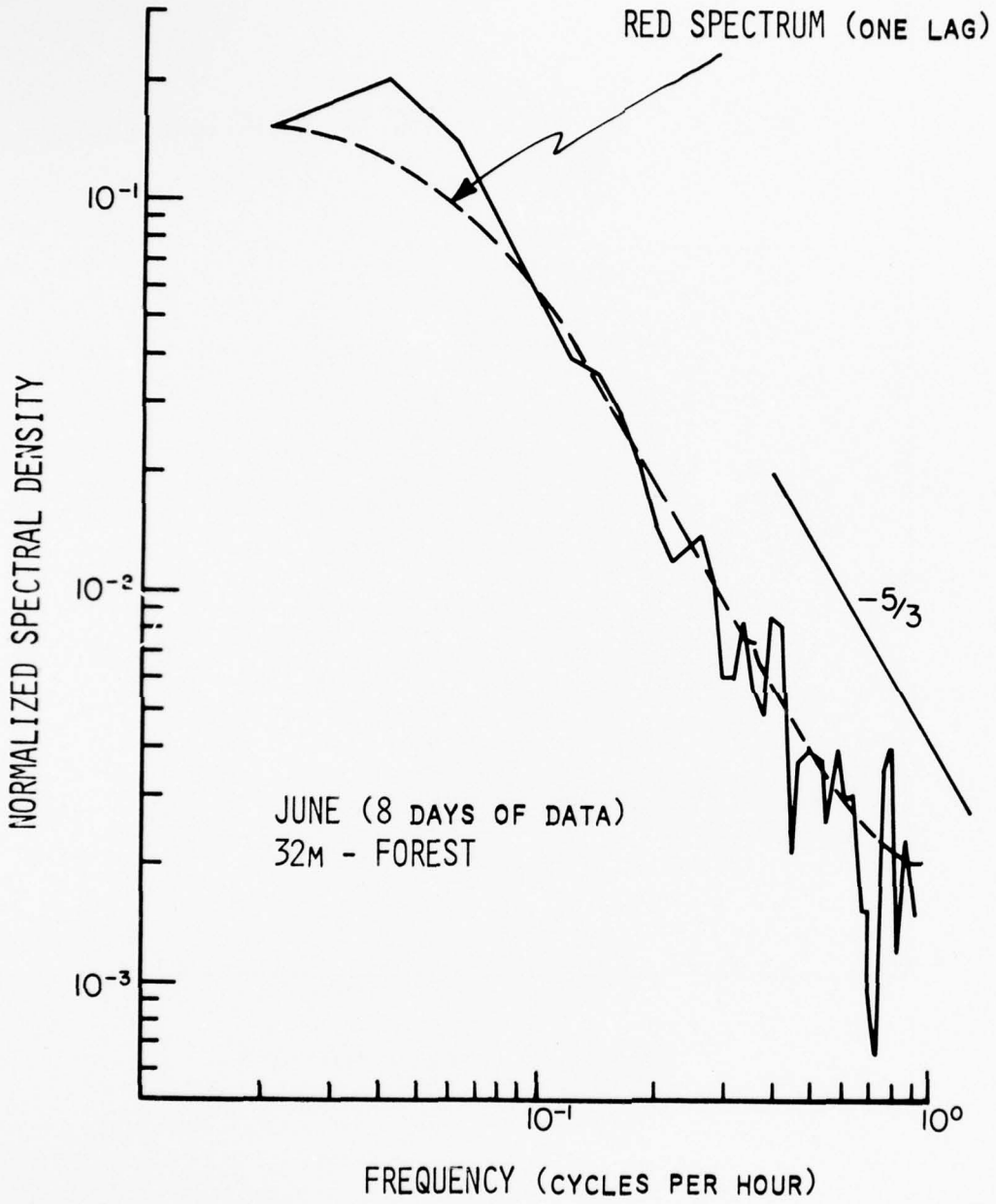

Figure 30b. Normalized spectral density of kinetic energy at 32 meters along the tower in the forest for an eight day period, June 20-28, 1970, using direct Fourier transforms with 50 lags.

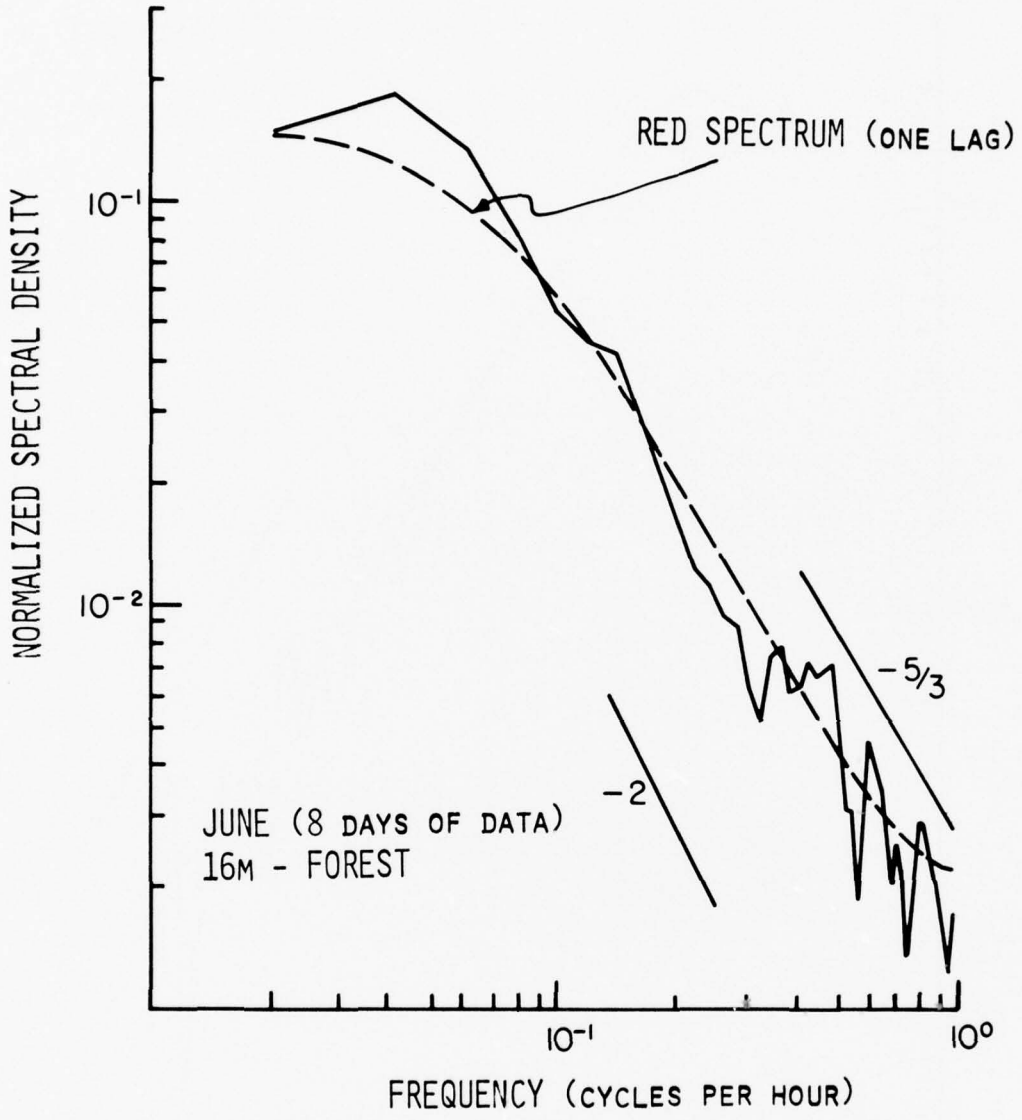

Figure 30c. Normalized spectral density of kinetic energy at 16 meters along the tower in the forest for an eight day period, June 20-28, 1970, using direct Fourier transforms with 50 lags.

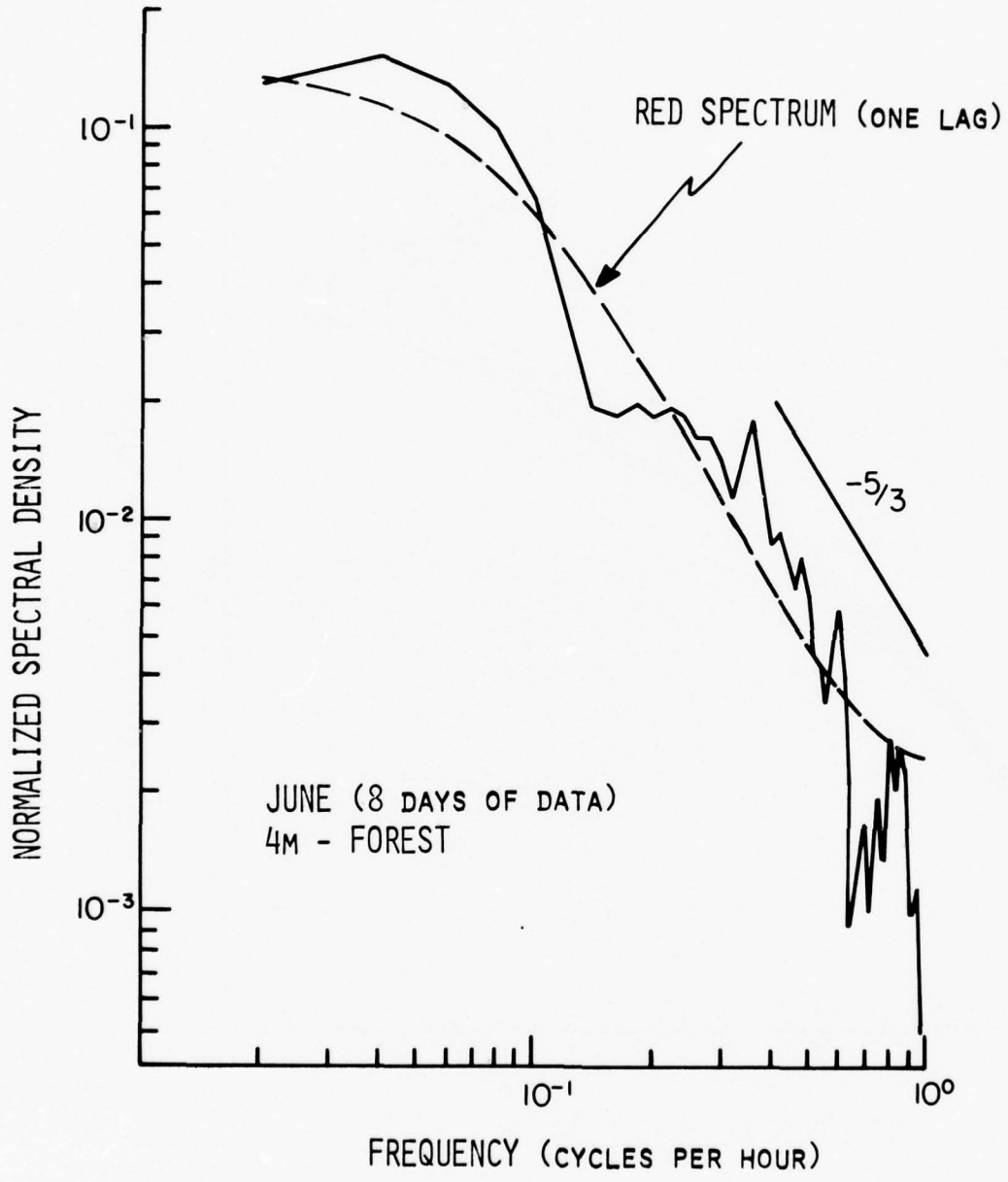

Figure 30d. Normalized spectral density of kinetic energy at 4 meters along the tower in the forest for an eight day period, June 20-28, 1970, using direct Fourier transforms with 50 lags.

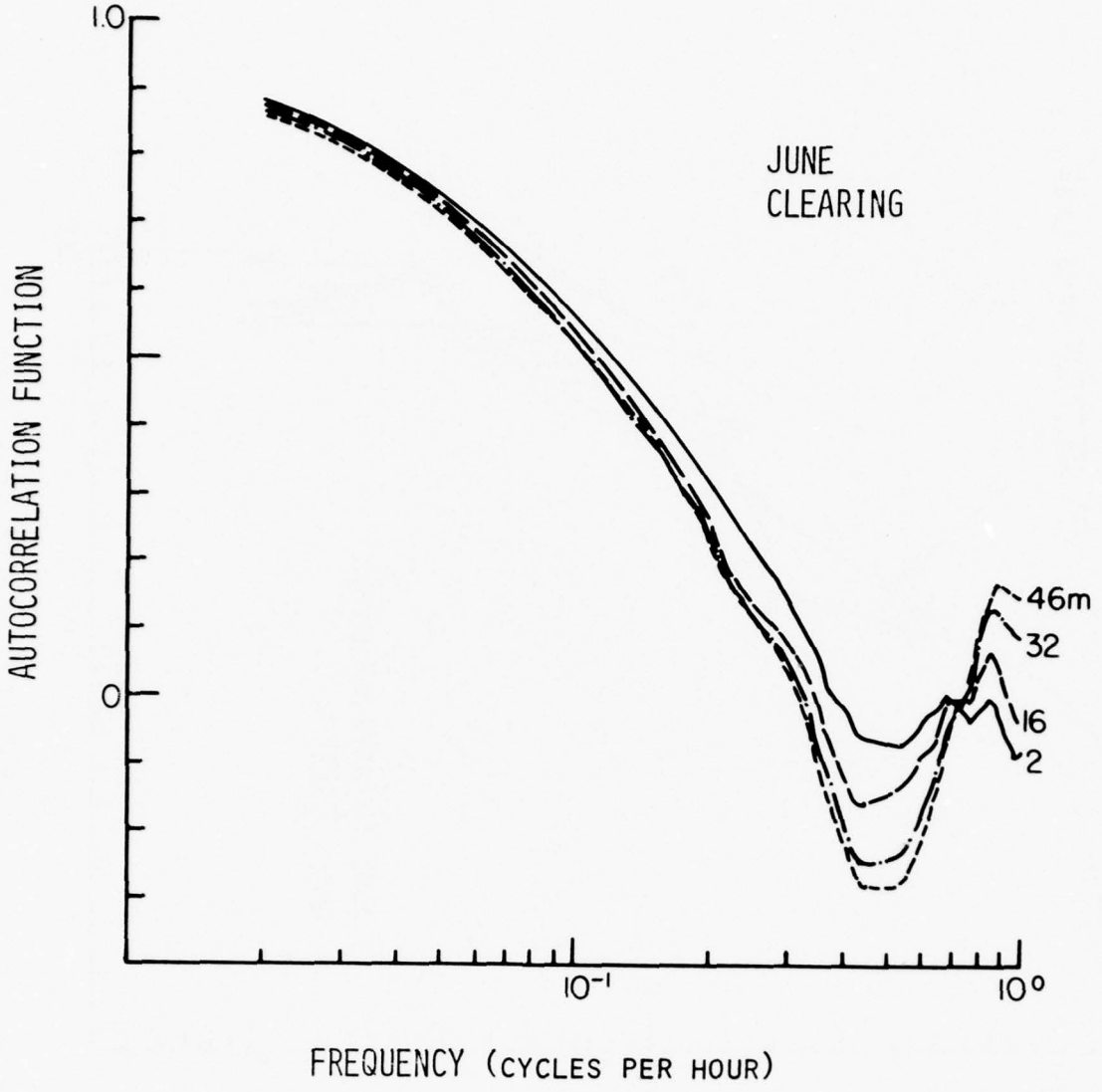

Figure 31. Autocorrelation function for June 20-30, 1970 at the 46m, 32m, 16m, and 4m levels along the tower in the clearing.

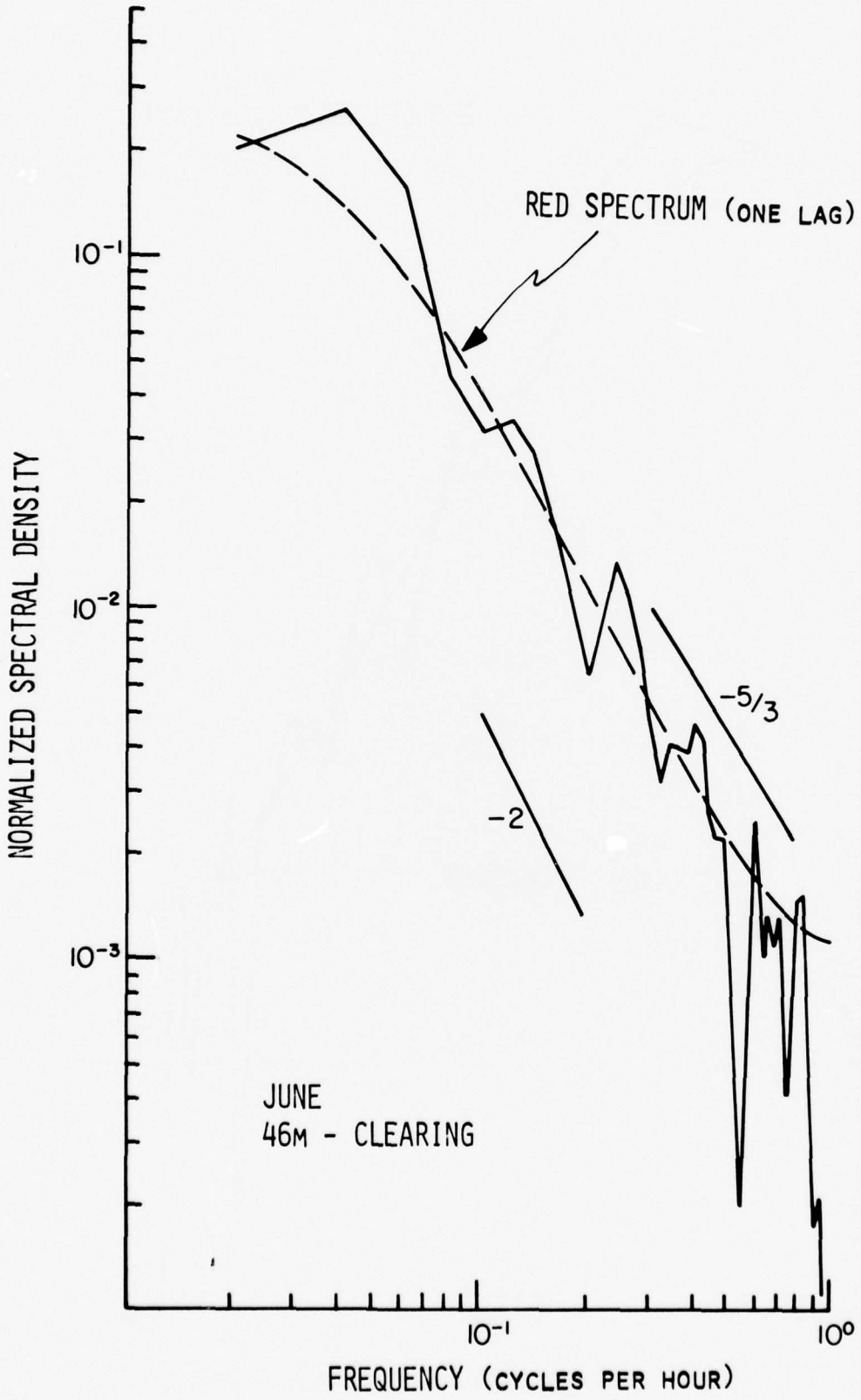

Figure 32a. Normalized spectral density of kinetic energy at 46 meters along the tower in the clearing for June 20-30, 1970 using direct Fourier transforms with 50 lags.

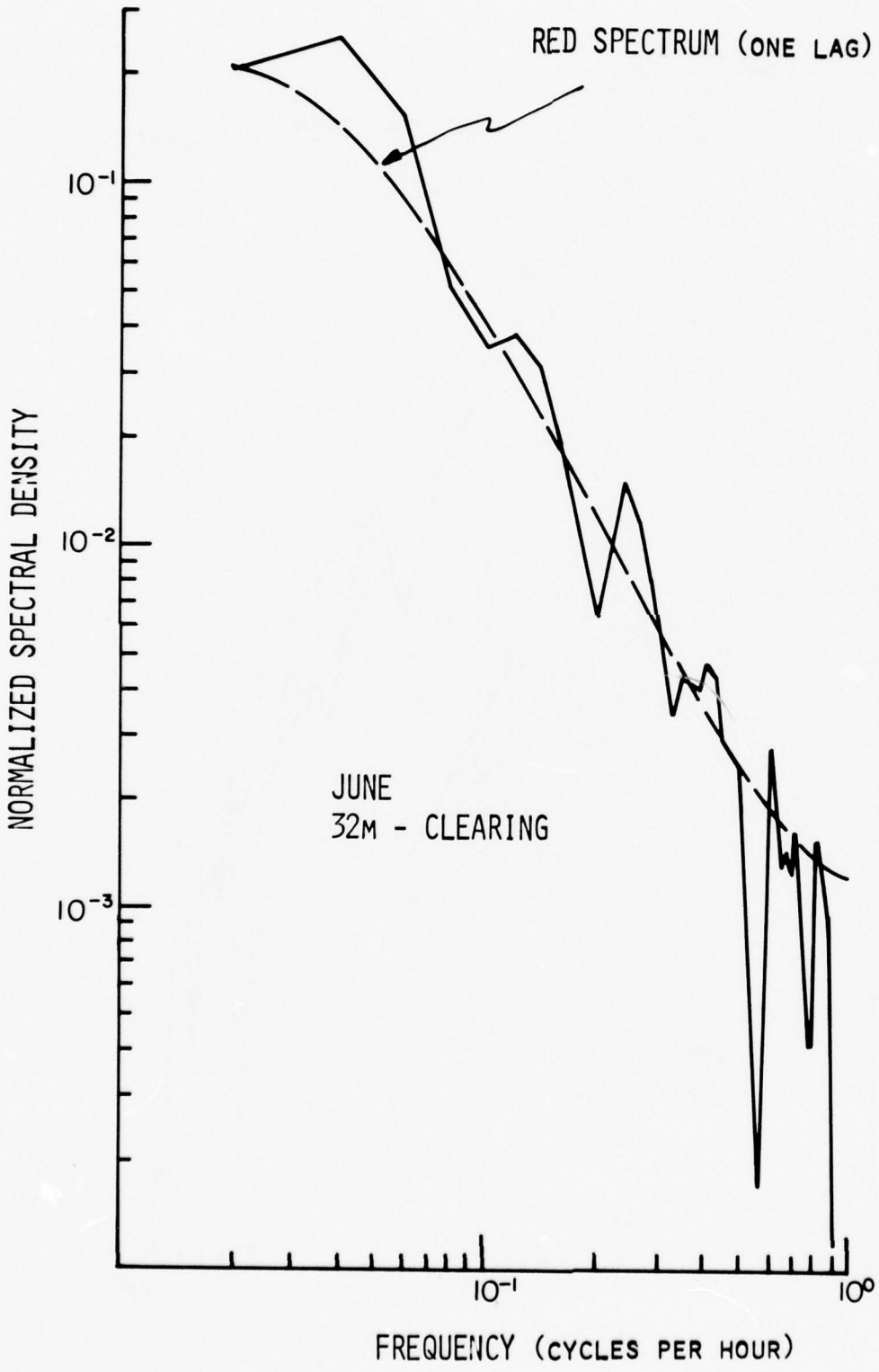

Figure 32b. Normalized spectral density of kinetic energy at 32 meters along the tower in the clearing for June 20-30, 1970 using direct Fourier transforms with 50 lags.

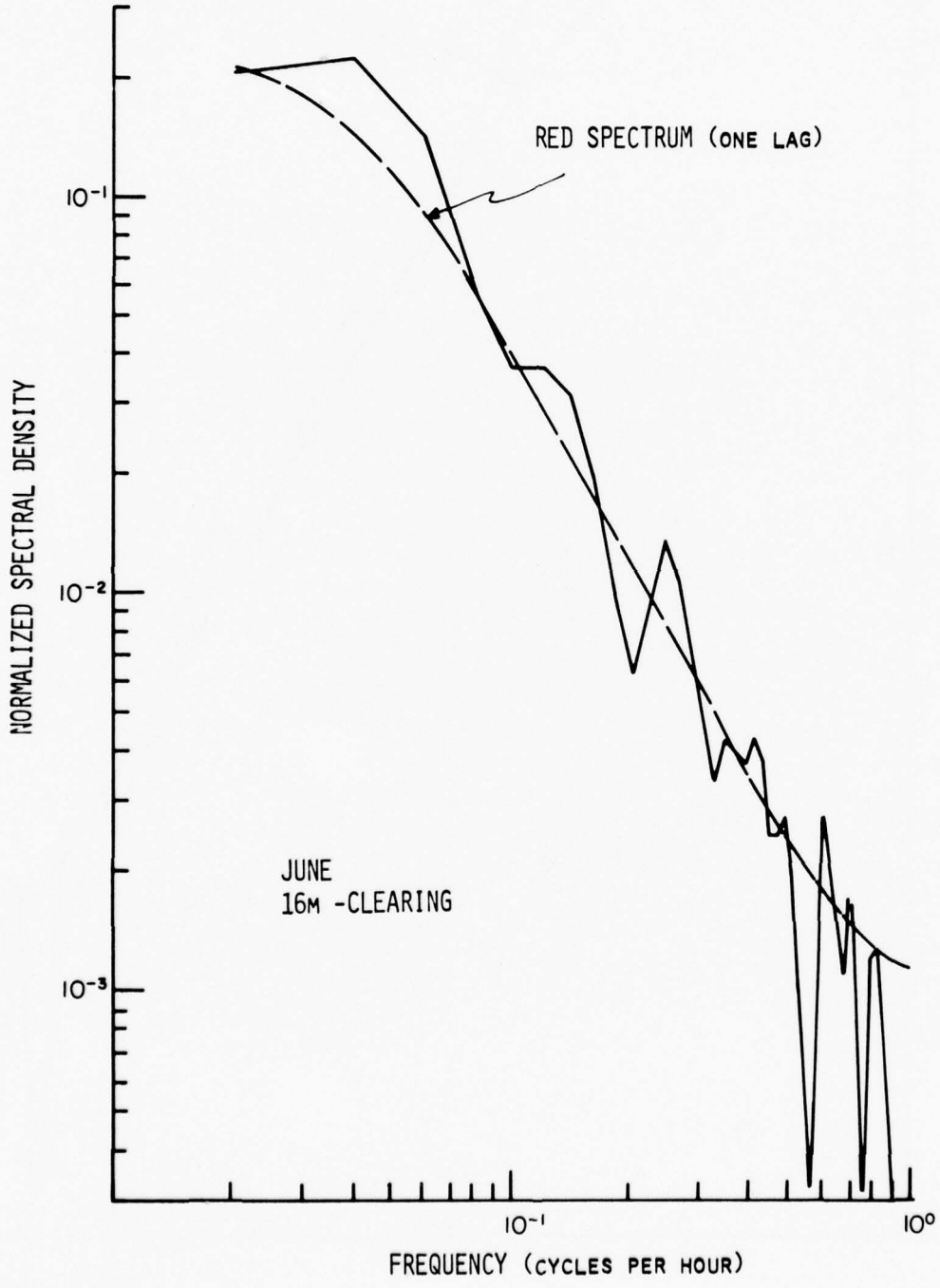

Figure 32c. Normalized spectral density of kinetic energy at 16 meters along the tower in the clearing for June 20-30, 1970 using direct Fourier transforms with 50 lags.

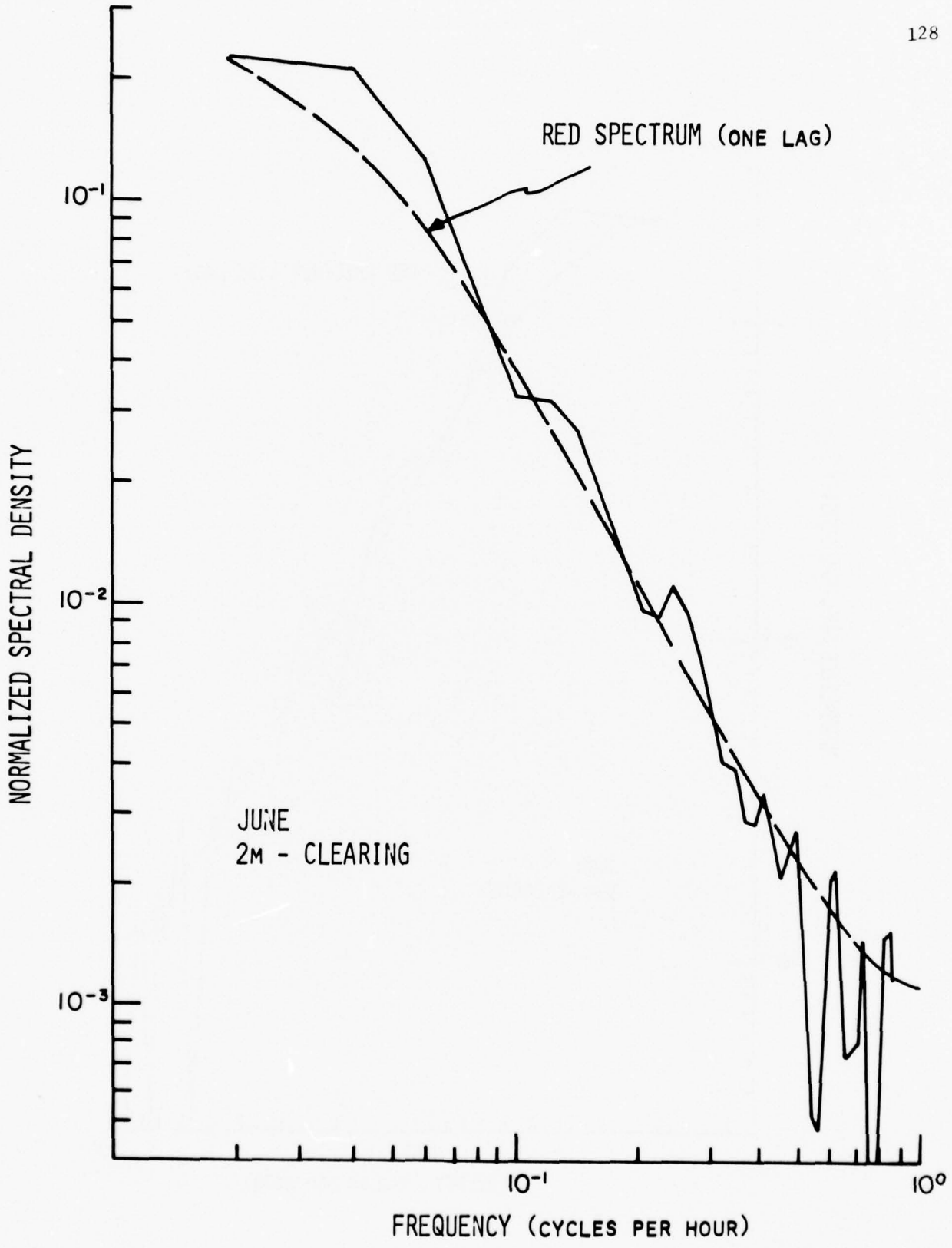

Figure 32d. Normalized spectral density of kinetic energy at 4 meters along the tower in the clearing for June 20-30, 1970 using direct Fourier transforms with 50 lags.

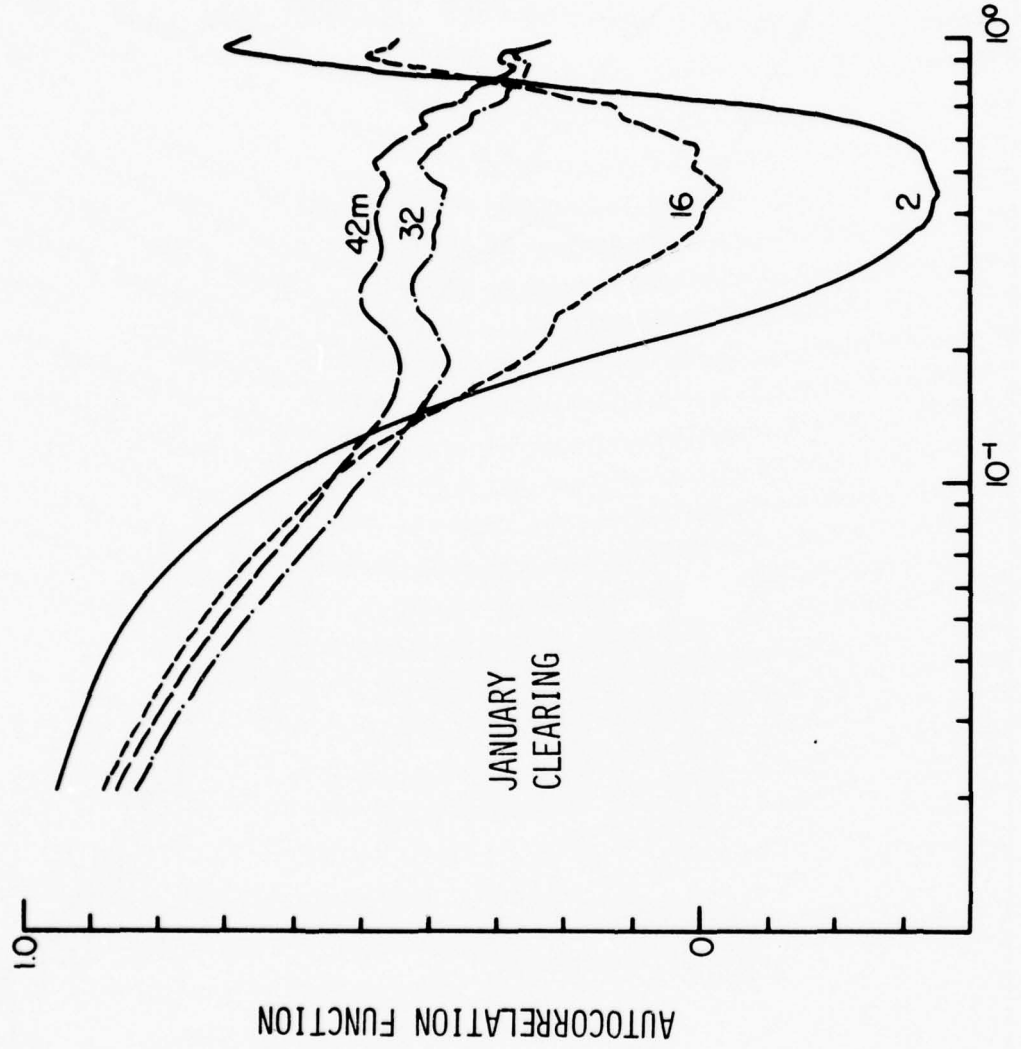

Figure 33. Autocorrelation functions for January 4-14, 1970 at the 46m, 32m, 16m, and 2m levels along the tower in the clearing.

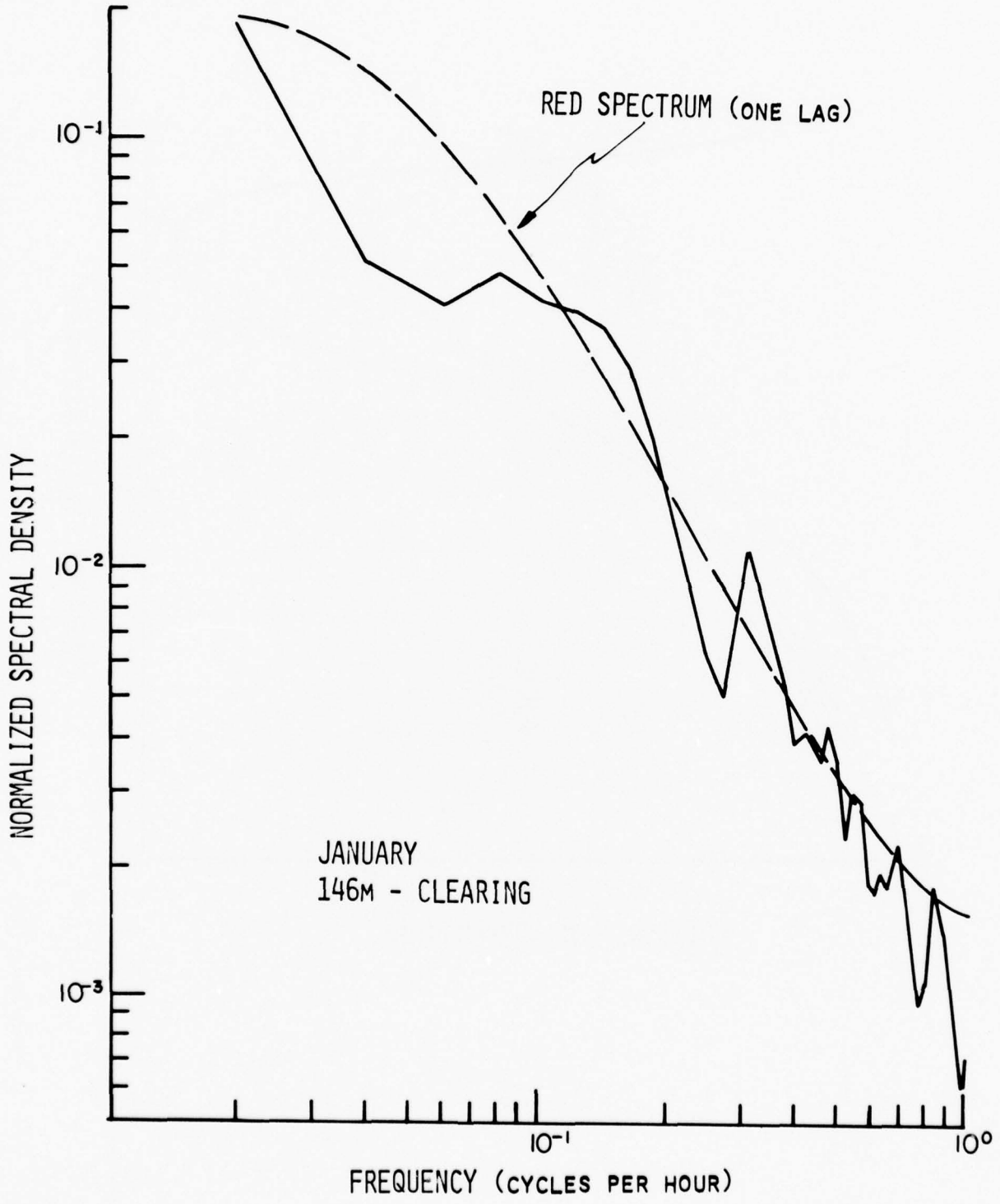

Figure 34a. Normalized spectral density of kinetic energy at 46 meters along the tower in the clearing for January 4-14, 1970 using direct Fourier transforms with 50 lags.

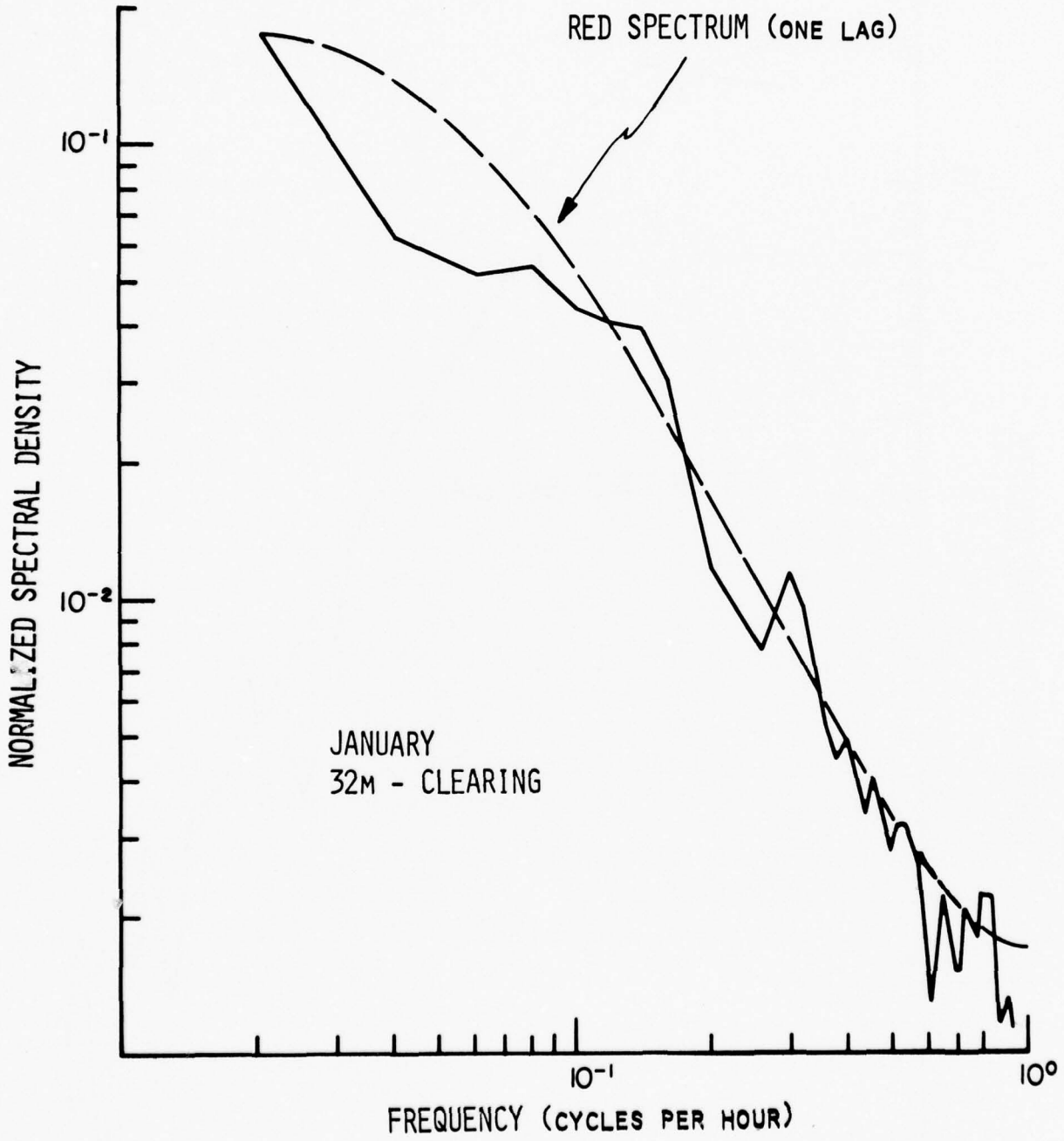

Figure 34b. Normalized spectral density of kinetic energy at 32 meters along the tower in the clearing for January 4-14, 1970 using direct Fourier transforms with 50 lags.

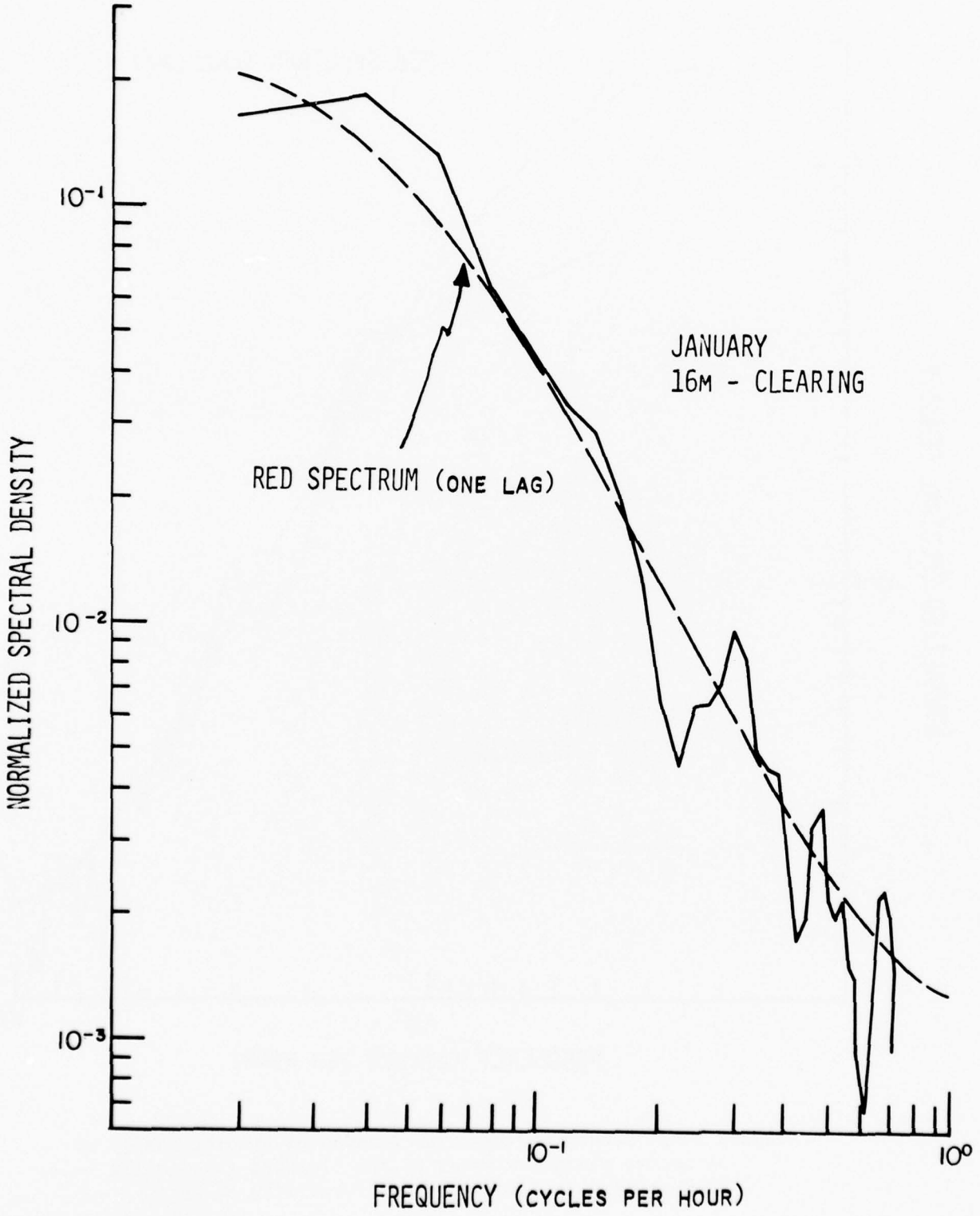

Figure 34c. Normalized spectral density of kinetic energy at 16 meters along the tower in the clearing for January 4-14, 1970 using direct Fourier transforms with 50 lags.

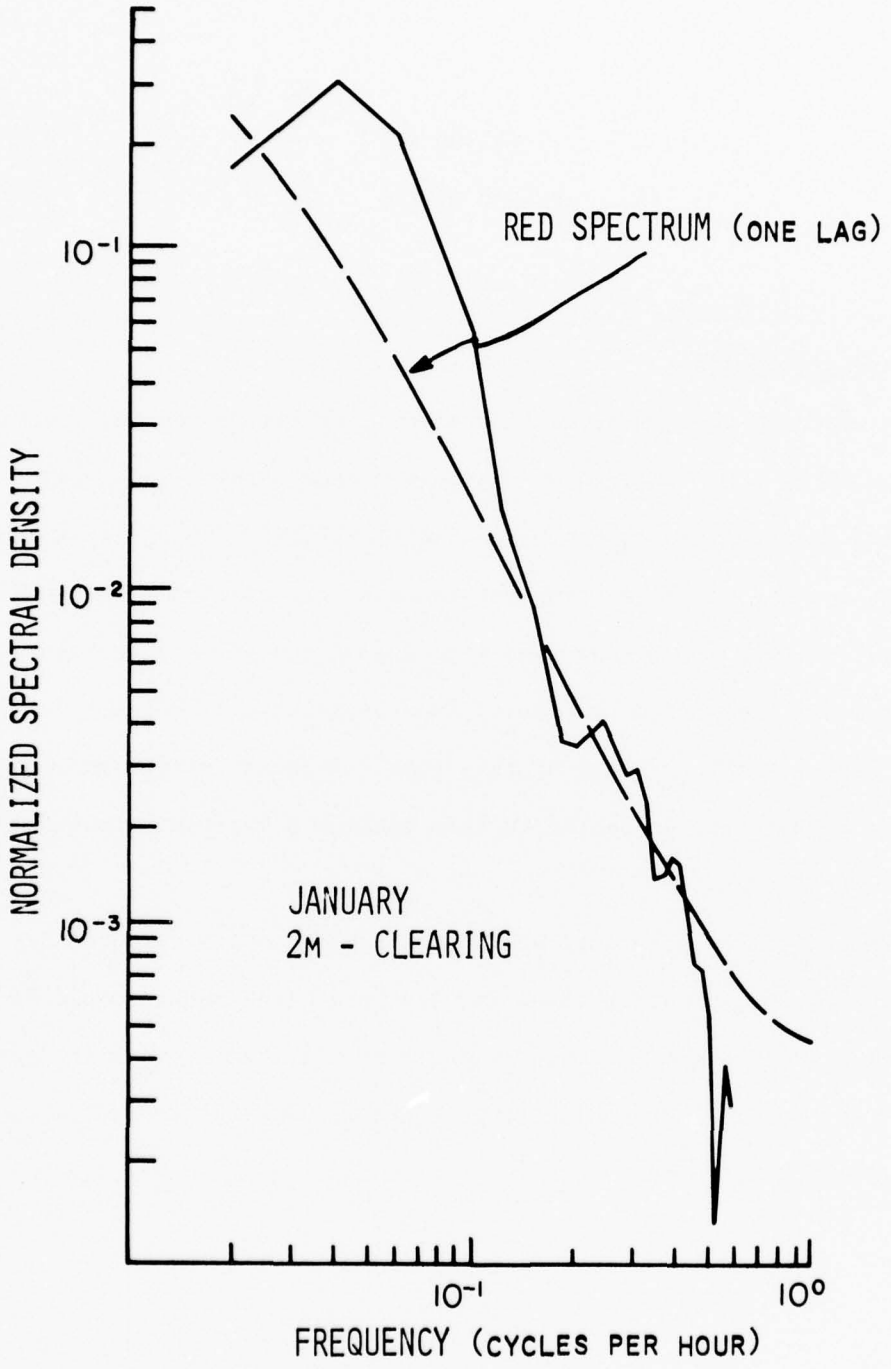

Figure 34d. Normalized spectral density of kinetic energy at 2 meters along the tower in the clearing for January 4-14, 1970 using direct Fourier transforms with 50 lags.

SECTION V

ENERGY FLUXES

1. Radiational Energy

A. Data Available

As noted in Section II of this report, radiation and dew point data from the TREND field experiment was logged onto A-tapes and none of these data were preprocessed into a readily usable form. Some limited amounts of radiation and dew point temperature data were available in the form of computer printouts of A-tape data made during the TREND experiment. Thus, extensive analyses of the radiation (and latent heat) budgets of the Thai forest area are not possible at this time. Representative samples of radiational data are presented in this section using the printout information at our disposal.

Table 36 gives a summary of the periods for which measurements of radiation fluxes, wind direction and dew point temperature could be taken from computer printout sheets. As noted in this table, (and in Section II), much of the recorded dew point temperature information is faulty due to malfunctioning sensors.

TABLE 36. Log of Periods for Which Radiation, Wind Direction and Dew Point Temperature Measurements are Available from Computer Printouts Made During the TREND Field Experiment

Radiation		Wind Direction, Dew Point Temperature
	1969	
February 6-23, 25-28		*February 6-15, 18-23, 26-28
March 1-13, 18-25		*March 1-4, 23-25, 27-31
April 1-13, 20-26		*April 1-5
September 29-30		
October 1-10, 11-12		*October 28-31
		*November 1-6
December 22-24		*December 22-24
	1970	
January 7-19		*January 3-21
February 5-24		*February 5-11
March 3-8, 14-29		*March 4-13
April 5-14, 20-30		*April 25-30
May 1-18, 20-31		*May 4-5, 27-31
June 1-4, 15-22		June 1-13, 22-30
August 14-22, 27-31		August 1-4, 25
September 4-18, 21-29		*September 4

* Faulty Dew Point Data.

B. Albedo Determinations

With a knowledge of incoming solar radiation one can estimate the outgoing stream by multiplying the incoming flux by the overall albedo, if known. Using measurements of both $R_s\downarrow$ and $R_s\uparrow$, one can estimate the albedo from the ratio $[R_s\uparrow/R_s\downarrow]$. With a representative value for the albedo for the forest, we reduce by one the number of radiative fluxes that must be measured for an energy balance survey. Table 37 shows estimates of albedo made from radiation measurements during the daytime in each of four different months of the year. The overall average value of albedo for these determinations is about 14% but varies from about 11% to 17% in the sample tested. There appear to be some consistent differences with season in the sample. Since the forest top is not a rigid surface, one expects variations in albedo related to the environmental conditions in the forest.

C. Net Radiation

Table 38 and Figures 35-38 represent the information on the net radiation in a number of characteristic days during spring, summer and winter. December 23, 1969 and April 21, 1969 are clear days and seem to be perfect for energy balance study; however, no humidity data were available for these days. The required corrections to the incoming and outgoing radiations were made for the August 11-13, 1970 data, since the Funk black body temperatures necessary to make these corrections were on the printouts.

TABLE 37. Albedo Estimates for a Tropical Dry Evergreen Forest for Selected Seasonal Periods

DATE	TIME	$R_s\downarrow$ (cal-cm^{-2}-min^{-1})	$R_s\uparrow$ (cal-cm^{-2}-min^{-1})	ALBEDO (%)
3/21/70	0930	0.7420	0.0996	13.4
	1030	0.8663	0.1065	12.3
	1330	1.0370	0.1153	11.1
	1430	0.8853	0.1046	11.8
	1530	0.3959	0.0497	12.6
			Average	12.2
	1630	0.0927	0.0180	19.4
6/15/70	0930	0.2734	0.0346	12.7
	1030	0.5203	0.0654	12.6
	1330	0.5088	0.0614	12.1
	1430	0.6902	0.0847	12.0
	1630	0.3297	0.0456	13.8
			Average	12.6
	1730	0.0806	0.0144	17.8
9/22/70	0930	0.5594	0.0863	15.4
	1100	0.8424	0.1150	13.7
	1400	1.2116	0.1408	11.6
	1500	0.7195	0.0854	11.9
	1600	0.1164	0.0195	16.7
			Average	13.9
12/22/69	0930	0.6975	0.1215	17.4
	1030	0.9227	0.1481	16.0
	1330	0.9982	0.1539	15.4
	1430	0.8092	0.1295	16.0
			Average	16.2

Overall Average ------- 14.1%

The numbers in parenthesis represent the corrected values. It seems that the difference between corrected and uncorrected net radiation values is within the limits of possible error.

TABLE 38. Net Radiation (Langleys/day) for Several Days During the TREND Experiment

DATE	NET RADIATION		%	Hours of
	Forest top (Ly/d)	Forest floor (Ly/d)	FF/FT	Sunshine
April 21, 1969	441	43	9.75	10.5
August 11, 1970	288 (288.6)	16 (16.7)	5.5	> 8
August 12, 1970	306 (306.9)	21 (20.1)	6.8	> 8
August 13, 1970	287 (287)	15 (14.5)	5.2	> 8
August 30, 1970	317	29	9.1	10.2
December 23, 1969	353	-18		8.9

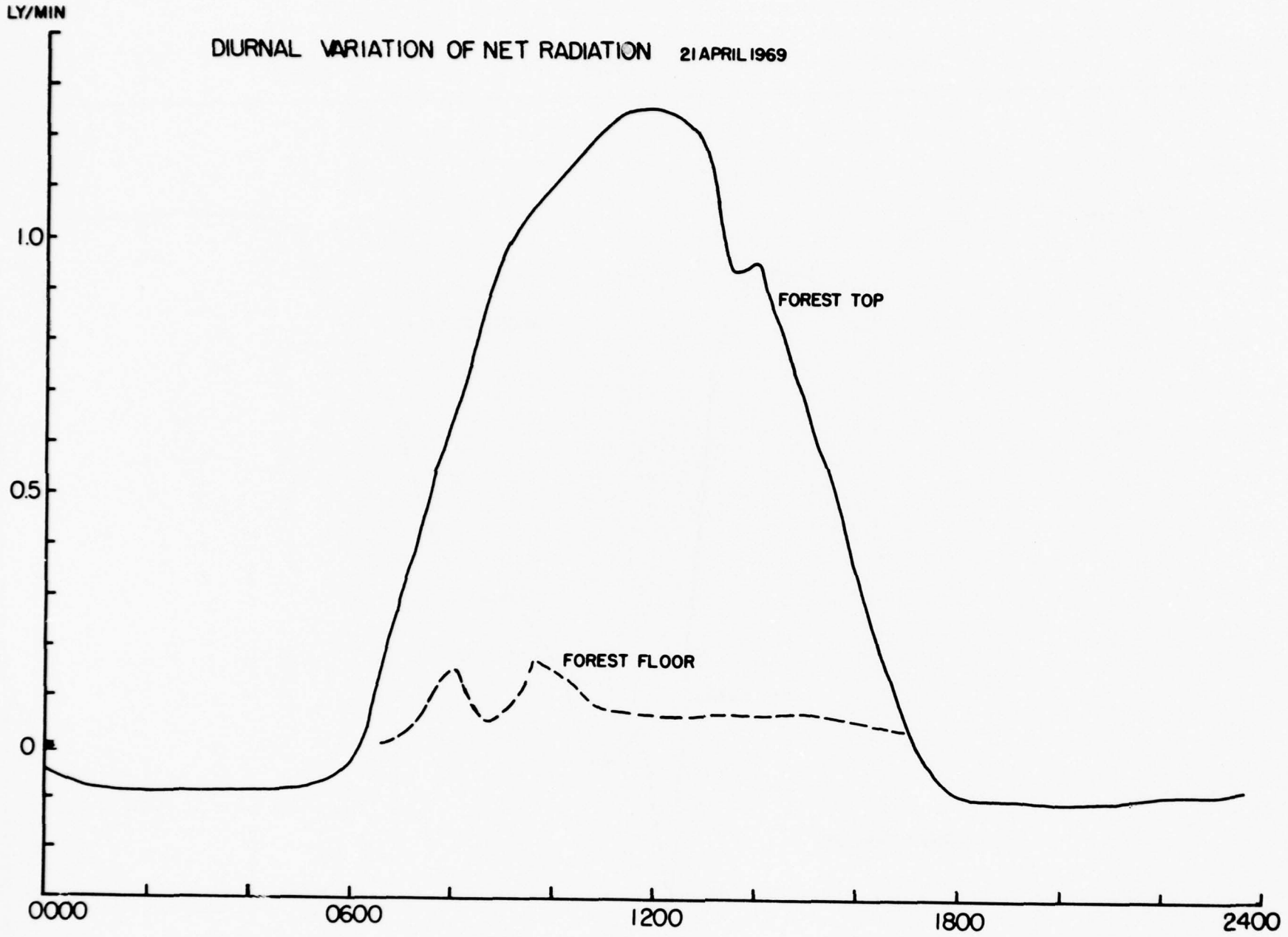

Figure 35. Diurnal variation of net radiation above the forest and at the forest floor for April 21, 1969.

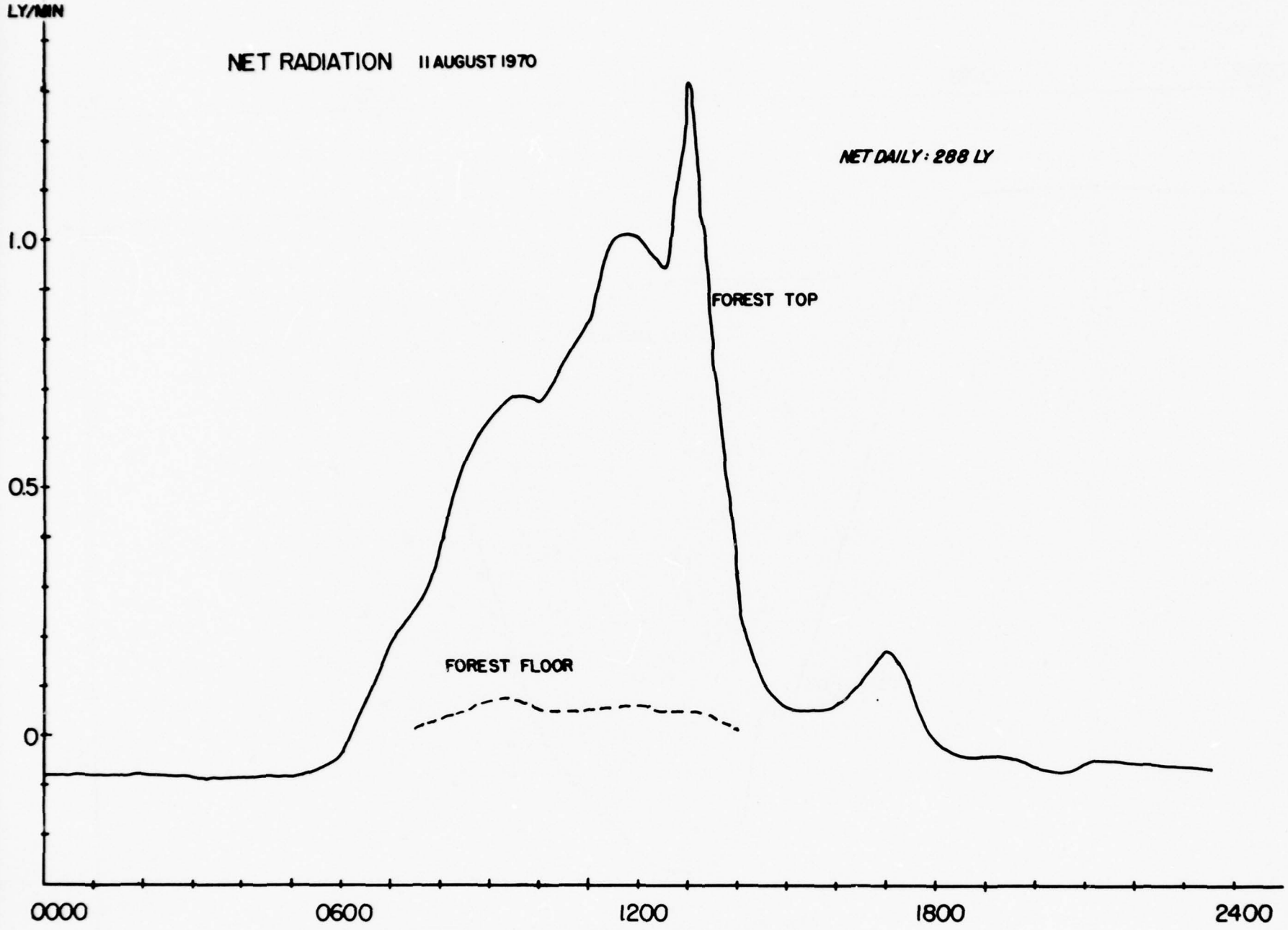

Figure 36. Diurnal variation of net radiation above the forest and at the forest floor for August 11, 1970.

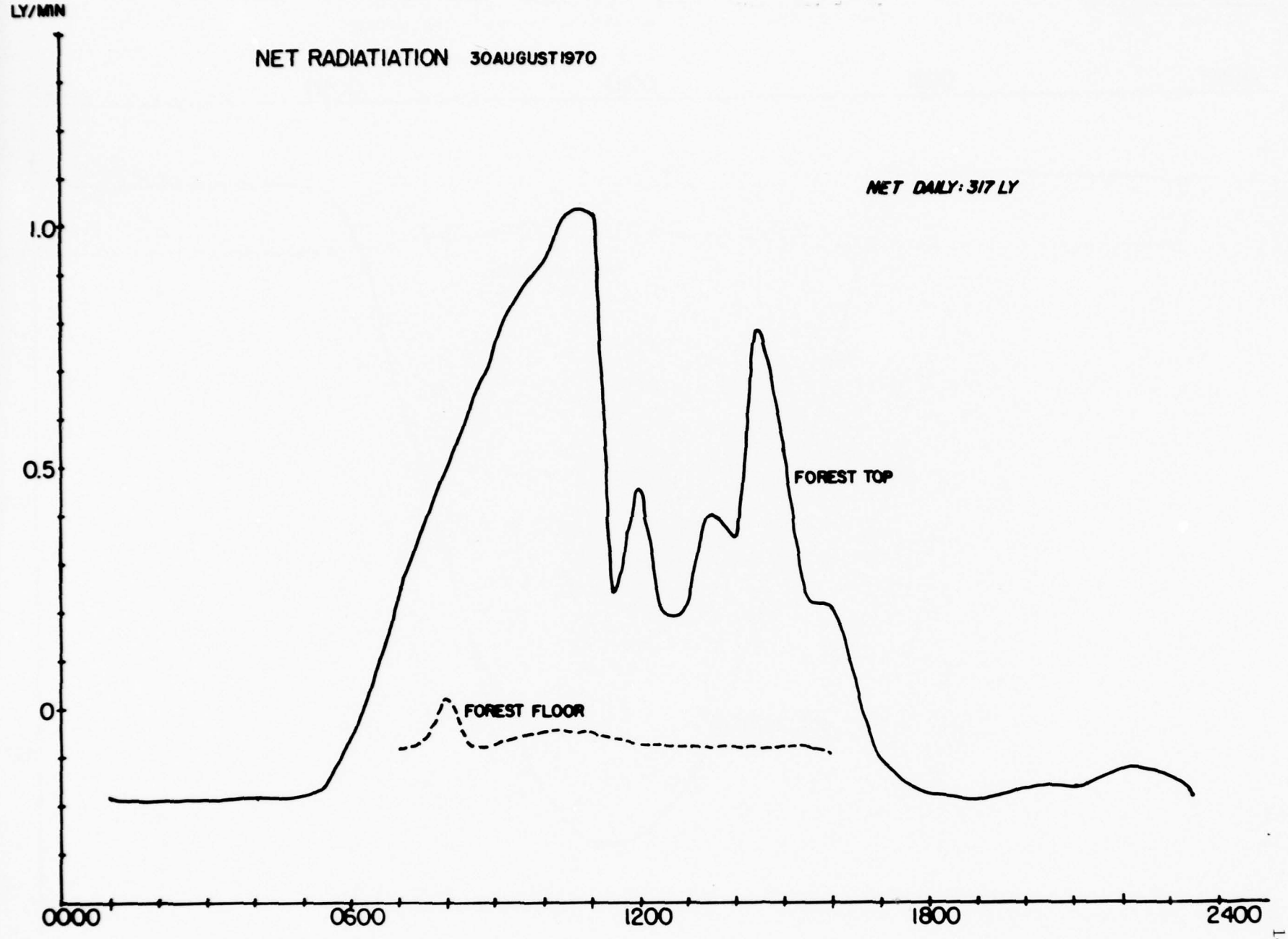

Figure 37. Diurnal variation of net radiation above the forest and at the forest floor for August 30, 1970.

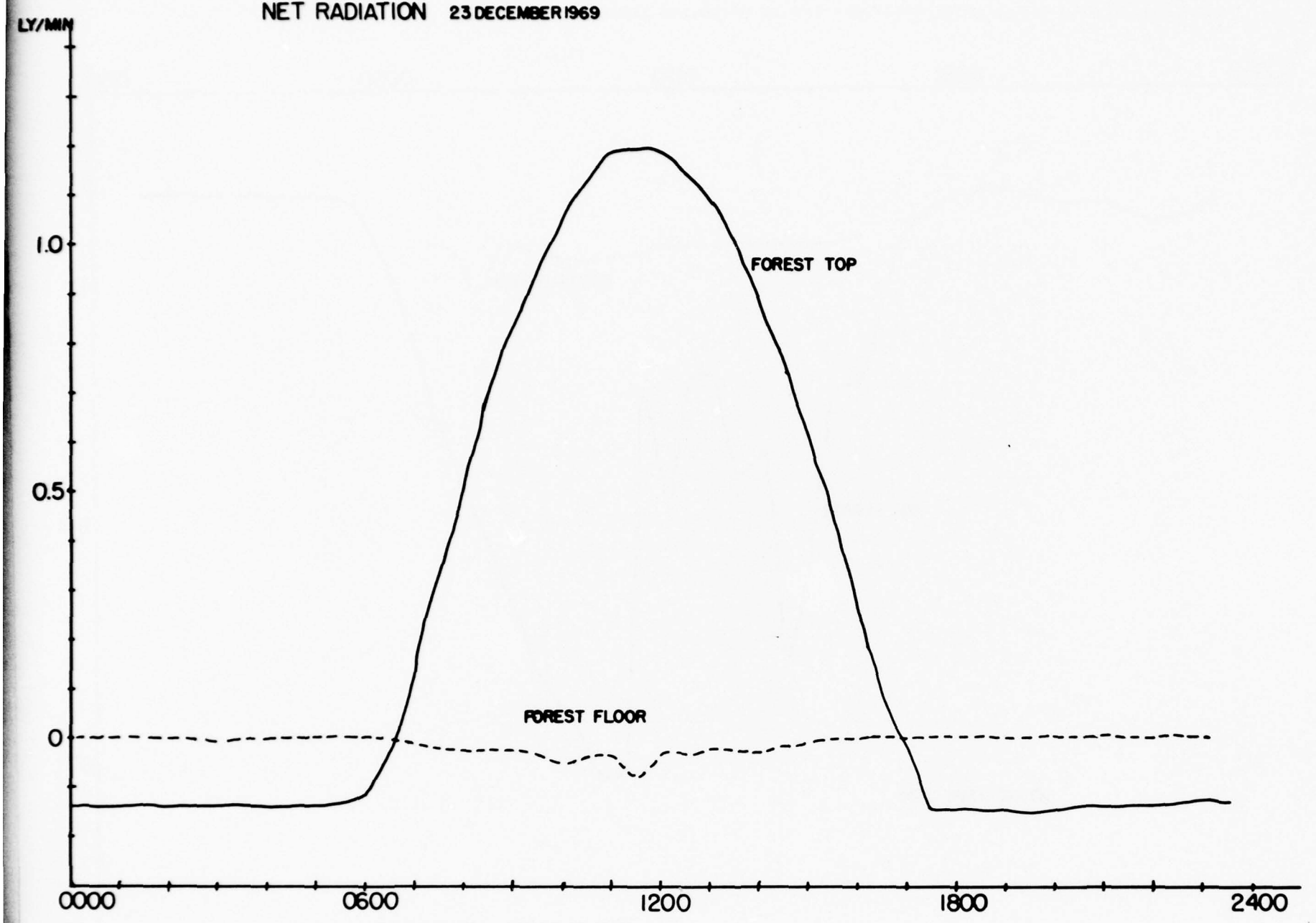

Figure 38. Diurnal variation of net radiation above the forest and at the forest floor for December 23, 1969

Some attempts were made to parameterize the net radiation flux in terms of various temperatures measured simultaneously along the towers. For energy balance studies, direct measurements of radiation are, of course, much more desirable than any parameterization but since the record of radiational data is quite limited, it is of interest to search for empirical estimators of such quantities. It is also true that a parameterization of radiational fluxes should incorporate information on cloud cover, humidity, etc., but once again, the motivation was to test parameterizations involving only temperature since there is far more temperature and wind speed information for these studies than any other kind.

The initial test was to search for a simple correlation between the net infra-red radiation flux and the temperature in the forest canopy, T_c(°K) [actually, the estimator used was σT_c^4; σ=Stephan-Boltzmann constant]. Radiation and temperature data were selected during nighttime hours between 2230 and 0530 for the dates June 19, 20, 21, 22, 1970. For the resulting sample of 45 measurements we found the regression relation as follows:

$$(R_L)_{net} = 0.1777(\sigma T_c^4) - 0.1047$$

where the radiation is in cal-cm^{-2}-min^{-1}, T_c is the absolute temperature at the 30 meter level of the tower and is taken to represent the canopy temperature. The correlation coefficient was only 41.9% and the standard error of estimate was 0.00178 cal-cm^{-2}-min^{-1}. Since this correlation was

rather weak, the data were submitted to a stepwise screening regression algorithm with several (admittedly interdependent) temperature predictors to discover which were the most significant predictors and how great a correlation could be obtained using temperature predictors alone. The predictors used were as follows:

$P_c=(\sigma T_c^4)$; T_c= canopy temperature [temperature at the 30 meter level]

$P_s=(\sigma T_s^4)$; T_s= temperature at the forest floor

$P_a=(\sigma T_a^4)$; T_a= average temperature for the layer 0 m to 46 m height

$P_t=(\sigma T_t^4)$; T_t= average temperature for the top layer 30m to 46m height

During the nighttime hours for clear sky conditions, the net infra-red radiation is generally negative; that is, more energy is radiated upward by the surface and/or forest than is received from the atmosphere above. The first variable selected by the stepwise regression scheme was, consequently, the forest floor temperature, T_s, which turned out to be a more powerful predictor than the canopy temperature. Of the four temperature predictors mentioned above, the above-canopy average temperature, T_t, should be most representative of the radiating characteristics of the atmosphere above the forest and, hence, of the incoming infra-red radiation. Indeed, the second predictor selected by the stepwise regression scheme was T_t. The third and fourth predictors were, respectively, T_a and T_c. The regression equations corresponding to the four steps of the stepwise regression scheme are given in Table 39 . Our interpretation of these results is that

TABLE 39. STEPWISE REGRESSION EQUATIONS FOR NET INFRA-RED RADIATION IN TERMS OF TEMPERATURES IN VARIOUS LAYERS OF THE FOREST.

Number of Predictors	Regression Equation	Multiple Correlation Coefficient (%)	Standard Error of Estimate
1	$(R_L)_{net}=0.2238P_s - 0.1341$	47.2	0.00173
2	$(R_L)_{net}=0.4776P_s -0.2336P_t -0.1474$	52.6	0.00169
3	$(R_L)_{net}=-0.1798P_s -2.655P_t +3.011P_a -0.1028$	73.8	0.00136
4	$(R_L)_{net}=-1.701P_s -4.373P_t +2.531P_a +3.650P_c -59.00$	75.1	0.00135

temperature quantities alone are not sufficiently powerful as predictors and that one should select only T_s and T_t and test other non-temperature predictors (relative humidity, cloud cover, etc.) for their ability to reduce variance. Also, the constant terms in each of the equations above are rather large which indicates that the time mean value of the (radiating temperature) predictors are rather significant in determining the net radiation. In fact, this has a great deal to do with the resulting algebraic signs which precede the various predictor terms in Table 39 . While the regression equations could be linearized and the means extracted, one cannot be too encouraged at the prospects of parameterizing radiational fluxes in terms of temperature alone especially when one recalls the large variability of cloudiness and humidity during the various monsoon periods.

2. Sensible and Latent Heat Fluxes

A. Outline of Possible Estimating Procedures

One of the most interesting aspects of the TREND experiment was the potential for estimating all components of the complete energy and moisture balance of a tropical evergreen forest for many periods during the complex monsoon cycle. As the reader is by now aware, it was not feasible to completely achieve this goal during this phase of the tropical environmental study due largely to the rawness of the original data and certain sensor malfunctions. With the large amount of temperature and wind speed data, it was possible to make some estimates of sensible heat flux and limited latent heat flux estimates. Before presenting these results, it is of interest to review briefly several alternative procedures for making such estimates.

Gradient Method

One of the better known methods for indirect flux determination utilizes the gradient of temperature, specific humidity and velocity as expressed in the following relations:

$$H = - C_p \rho K_n (dT/dz) \quad (1)$$

$$E = - \rho K_w (dq/dz) \quad (2)$$

$$\tau = \rho K_m (du/dz) \quad (3)$$

where

H - sensible heat flux (ly/min)

E - rate of evaporation ($gr/cm^3 sec$)

τ - shearing stress

ρ - air density (g/cm^3)

K_m - eddy diffusivity for horizontal momentum (cm^2/sec)

C_p - specific heat of air (cal/gdeg)

K_h - eddy diffusivity for heat (cm^2/sec)

Equation (3) is introduced here to point out the assumption of similarity between the vertical flux equations of momentum, heat and moisture.

In order to bring the previous relations into operative status it is the practice to make some assumptions and modifications about the relation of the turbulent transfer coefficients. According to Pasquill (1949) they are identical only under stable and neutral conditions. Swinbank (1955) has shown that K_h/K_w increases with increasing instability. Taylor (1960), after analyzing Swinbank's data and the data of Rider (1954) comes to the conclusion that both factors are identical. Uncertainty remains only under very unstable atmospheric conditions. Investigations by Crawford (1965) favor the identity of both factors.To employ this method, one must make direct use of estimated values of diffusivities.

Bowen Ratio Method (Bowen, 1926)

One of the methods which avoids direct use of the eddy diffusivity factors but uses only their quotients is the Bowen ratio method. The Bowen ratio is defined as:

$$\beta = H/LE = \gamma(K_h/K_w)\left(\frac{T_s - T_a}{e_s - e_a}\right)$$

where

L - latent heat of evaporation

T_s, T_a - surface and air temperature

e_s, e_a - vapor pressure at surface and in air

γ - psychrometer constant (0.485 mmHg $\cdot$ $^{o}C^{-1}$)

Assuming identity of transfer coefficients K_h, K_w and using the heat budget equation adjusted to the air/forest interface, one may write,

$$R + S + EL + H = 0$$

where

R - the net radiation at top of forest

S - heat gained or lost by vegetation soil and photosynthesis

EL,H - as before

If $B = 1/\beta$, the energy balance equation may be solved to yield

$$Q = -(R + S)/(1 + B)$$

and

$$EL = -(R+S)B/(1 + B)$$

This method has been used by many investigators and has been shown to give reliable measurements in many agricultural situations (Tanner, 1968; Albrecht, 1937; Sverdrup, 1951).

Profile Method

Another classical approach to estimating fluxes of heat and moisture is assumption of adiabatic conditions and integration of the following:

$$K_w = K_m = ku^*z \tag{4}$$

where

k - von Karman constant

u* - friction velocity defined as

$$u^* = (\tau/\rho)^{1/2} \tag{5}$$

Combining (3), (4) and (5) yields

$$u^* = \frac{k(u_2 - u_1)}{\ln[(z_2-d+z_o)/(z_1-d+z_o)]} \tag{6}$$

where

u_1, u_2 are wind speeds measured at two heights above the canopy z_1 and z_2, and d is the zero plane displacement (explained later). Substituting (6) into (4) and then into (2) yields

$$E = \frac{-\rho k^2(u_2 - u_1)(q_2 - q_1)}{[\ln(\frac{z_2-d+z_o}{z_1-d+z_o})]^2}$$

which is known as the Thornwaite and Holzman equation. If (6) and (4) are substituted into equation (1) instead of (2), one obtains

$$H = \frac{-C_p\rho K^2(u_2 - u_1)(T_2 - T_1)}{[\ln(\frac{z_2-d+z_o}{z_1-d+z_o})]^2}$$

Eddy Correlation Method

Vertical transport of heat and water vapor in the atmosphere is mostly turbulent. If we define q' as the instantaneous deviation of q from its mean value at the point, the product q'w'(w' - the vertical component of the wind speed) is the deviation of the instantaneous water vapor flow from its mean value. The evaporation is found by averaging over time the quantity

$$E = \rho \overline{w'q'}$$

Similarly for sensible heat flux:

$$H = C_p \rho \overline{w'T'}$$

Where the overbar represents the averaging operation.

This best method of estimation is difficult to apply to the TREND data since there are no direct observations of vertical velocity and the only values of specific humidity available are values related to thirty minute averaged values of dewpoint temperature.

B. Results

From Table 36 it is clear that very little dew point temperature data is available for computational purposes. [A large amount of the dewpoint temperature data appearing in the computer printouts of A-tape data are values of order 10^{-3}°C !] Values of Bowen's ratio were computed for four days in June using data at the 32m and 36m levels along the tower in the forest which was not obviously and absurdly faulty by virtue of its magnitude.

Computations were made for each half-hour period and then averaged over six-hour periods of each day. Resulting values are shown in Table 40.

TABLE 40. Bowen's Ratio for Four Days in June, 1970

Bowen Ratio	Time of Day			
Date	0:00-6:00	6:00-12:00	12:00-13:00	13:00-24:00
June 23, 70	.3729-03	-.1468-01	.4620-02	.9214-03
June 24, 70	-.2253-02	-.7589-02	-.5274-02	-.5352-03
June 25, 70	.6290-03	-.1788-01	-.4522-02	.1124-02
June 26, 70	.6101-03	.8557-03	.1583-03	-.7583-03

The values shown in Table 40 are extremely small and fluctuate in sign. According to the stability statistics given in Section IV, the layers above the forest canopy are frequently near neutral conditions so that a Bowen ratio would be the ratio of two small and variable energy fluxes. It is not clear that the ratios appearing in Table 40 are very revealing. To further document the situation on these four days, however, six-hour totals of rainfall at the top and floor of the forest were computed. The rainfall totals are shown in Table 41 where it may be seen that rain indeed fell during each of the 16 six-hour periods. Also, the fraction of the daily total rainfall which reached the floor of the forest varied from a high of 93% on June 26, 1970 to a low of about 49% on June 23, 1970. The rain gauge at the forest floor actually collected more water than fell as rain for 3 of the six-hour periods shown in Table 41.

Having performed determinations of roughness parameter and datum displacement level for a large sample of wind profiles during January, June and September, the sensible heat flux [and, perhaps, the latent heat flux] may be calculated using the Thornthwaite-Holzman equations given in the previous subsection. Such calculations were carried out for the periods in January, June and September noted in Table 17 and will be presented shortly. Before presenting these results, attention is drawn to the fact that there was a wide variability in the values of z_o and d calculated using Stearn's method for the three periods. While the Thornthwaite-Holzman equation is linear in the wind and temperature information, it is highly non-linear in z_o and d. In computing, say, sensible heat flux from this equation, one faces a choice of using some average, representative values of z_o and d in the equation or using "instantaneous" values of these parameters determined from the actual profile from which the heat flux is computed. If the variability of these "site parameters" was sufficiently small, one would feel reasonably comfortable in using average values in heat flux computations. Table 17 of Section IV gives evidence that such is not the case here. This issue is quite relevant to micrometeorological studies since some methods for estimating z_o and d yield only one pair of estimated values and the investigator has no choice but to use this pair in all heat flux computations.

One can get an estimate of how bad the situation might be by performing an error analysis of the heat flux equation of Thornthwaite and Holzman.

TABLE 41. Rainfall at Forest Top (FT) and Forest Floor (FF) for Four Days in June, 1970

Date	Rainfall (mm)	Time of day				Daily Total
		0 - 6	6 -12	12-18	18-24	
June 23, 70	FT	6.6	5.7	6.0	6.9	25.2
	FF	2.4	3.0	3.6	3.3	12.3
June 24, 70	FT	4.8	5.7	3.3	6.9	20.7
	FF	2.7	3.0	2.7	3.3	11.7
June 25, 70	FT	7.5	2.1	3.0	4.2	16.8
	FF	2.7	2.7	3.0	2.7	11.1
June 26, 70	FT	6.6	41.1	6.0	9.3	63.0
	FF	2.3	41.4	11.1	2.7	58.5

If one defines ΔH as the error incurred in calculating the heat flux due to errors, Δz_o and Δd, in estimating the roughness and datum displacement height, then one may write

$$\Delta H = (\partial H/\partial z_o)\ \Delta z_o + (\partial H/\partial d)\Delta d$$

The maximum relative error is obtained by dividing both members of this equation by H and summing absolute values:

$$(\Delta H/H) = \left|(1/H)(\partial H/\partial z_o)\ \Delta z_o\right| + \left|\ (1/H)(\partial H/\partial d)\ \Delta d\ \right|$$

The relative derivative terms may be calculated from the heat flux equation. Carrying this out one may write

$$(\Delta H/H) = C\ [|(\Delta z_o/z_o)| + |(\Delta d/z_o)|]$$

where

$$C = [2\ z_o(z_2-z_1)]\ /\ [Y_1\ Y_2\ \ln\ (Y_2/Y_1)]$$

$$Y_1 = z_1 - d + z_o\ ;\quad Y_2 = z_2 - d + z_o$$

Thus, the error effect involves only z_o, d, and the pair of levels used in the computation. One may <u>estimate</u> the error effect from the variability of z_o and d shown in Section IV in the following way: if one uses average values $\bar{z}_o$ and $\bar{d}$ for z_o and d and standard deviations in z_o and d for Δz_o, Δd, then $(\Delta H/H)$ represents a measure of the discrepancy involved in calculating H using average rather than instantaneous values of the profile parameters. That is, the quantity $(\Delta H/H)$ calculated in this manner becomes an estimate of the error limits encompassing 2/3 of the values of $[H(\bar{z}_o, \bar{d})-H(z_o,d)]/H(\bar{z}_o,\bar{d})$. Table 42 gives values of $(\Delta H/H)$ appropriate to the statistics of z_o, d for the periods in January, June and September summarized earlier. It is seen that the non-linear error effect is actually a damping effect. For example, for the sample covering September 9-11, 1970 using the levels 40m and 46m, the standard deviations of z_o and d relative to $\bar{z}_o$ are 35.4% and 21.3% respectively, yet the coefficient C = 0.397 (which is a damping of error since C < 1) and the discrepancy $(\Delta H/H)$ = 22.5%. Thus, even though the errors in z_o and d are additive in this

TABLE 42. Estimates of Relative Error in Sensible Heat Flux Calculated Using the Thornthwaite-Holtzman Equation with Mean Values of Displacement Height and Roughness Parameter.

Period	z_2(m)	z_1(m)	$\bar{d}$(m)	$\bar{z}_o$(m)	Δd(m)	Δz_o(m)	$(\Delta d/\bar{z}_o)$	$(\Delta z_o/\bar{z}_o)$	C	$(\Delta H/H)$
Jan. 8-10, 1970	46	40	29.53	0.826	0.05	0.47	0.061	0.569	0.119	0.075
June 20-26, 1970	46	40	27.17	5.55	0.70	1.72	0.126	0.308	0.526	0.228
Sept. 9-11, 1970	46	40	28.09	3.61	0.75	1.10	0.213	0.354	0.397	0.225
Jan. 8-10, 1970	40	36	29.53	0.826	0.05	0.47	0.061	0.569	0.183	0.115
June 20-26, 1970	40	36	27.17	5.55	0.70	1.72	0.126	0.308	0.684	0.297
Sept. 9-11, 1970	40	36	28.09	3.61	0.75	1.10	0.213	0.354	0.542	0.307
Jan. 8-10, 1970	36	32	29.53	0.826	0.05	0.47	0.061	0.569	0.345	0.217
June 20-26, 1970	36	32	27.17	5.55	0.70	1.72	0.126	0.308	0.913	0.396
Sept. 9-11, 1970	36	32	28.09	3.61	0.75	1.10	0.213	0.354	0.792	0.449

approach, the corresponding relative error in H is less than the error in determining z_o alone. It is encouraging that errors in determining z_o and d are damped by the Thornthwaite-Holzman equation. Nevertheless, the entries in Table 42 suggest that one may incur large discrepancies in calculating H using mean values of z_o and d as opposed to instantaneous values. The coefficient C is larger in June than September and January for all three layers shown and generally increases with decreasing height of the layer. Due to larger variability in z_o and d in September compared with June, however, the discrepancy in H is larger in September than June. The value of C is minimum in January so that even though the variability of z_o is largest in this month, the discrepancy in H is smallest.

To obtain an empirical estimate of the effect of using period mean profile parameters, values of sensible heat flux were computed for June 23, 1970 from the TREND profile data using the Thornthwaite-Holzman formula with period average values of z_o and d, and then using "instantaneous" values of z_o and d. The result is shown in Figure 39. The differences are small when the heat flux is small but of increasing importance as the flux becomes large. Generally speaking, however, the two methods give compatible results. The observed differences at each half-hour interval during June 23, normalized to the heat flux value calculated with the half-hourly values of z_o and d, [that is, $(\Delta H/H)$ observed] were compared with a theoretical estimate of the discrepancy calculated as indicated previously but using z_o, d, $\Delta z_o = z_o - \bar{z}_o$, and $\Delta d = d - \bar{d}$, for each half hour period [that is, $(\Delta H/H)$ estimate]. The relation between the two is shown in Figure 40. Most of the values lie on a straight line indicating that most of the discrepancy between the curves in

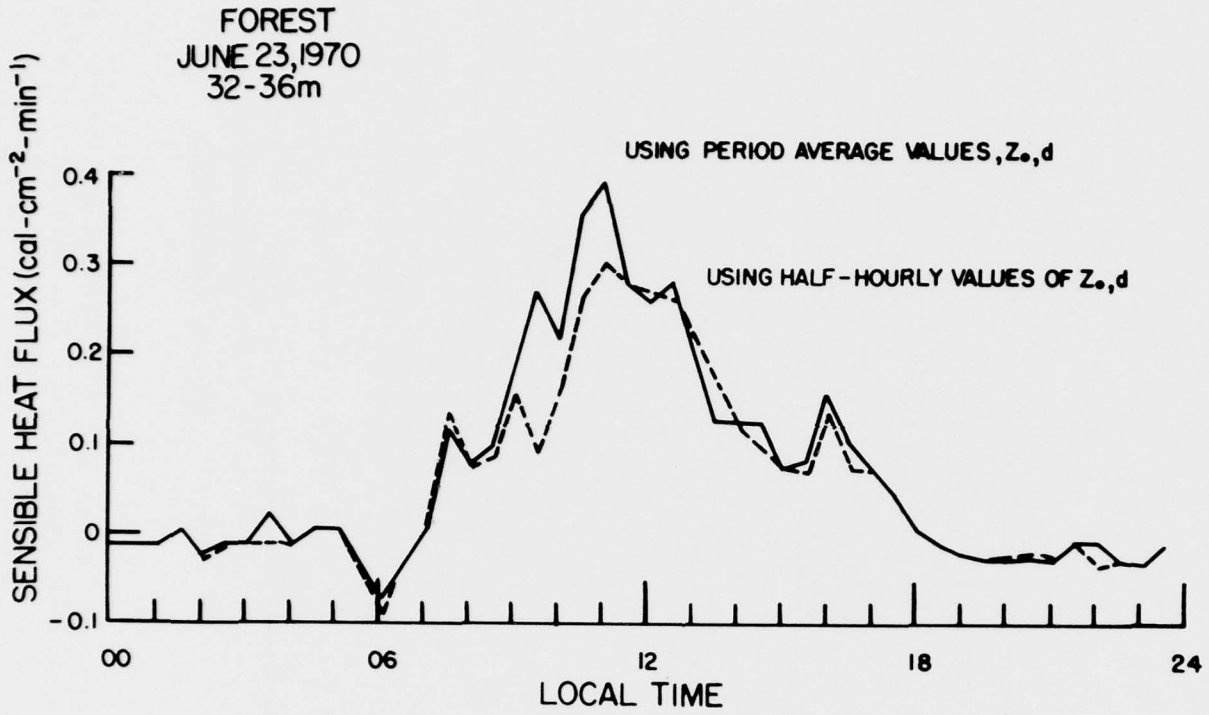

Figure 39. Sensible heat flux for June 23, 1970 for the layer 32-36 meters above the forest canopy computed using the Thornthwaite-Holzman equation with average and instantaneous values of roughness and displacement height.

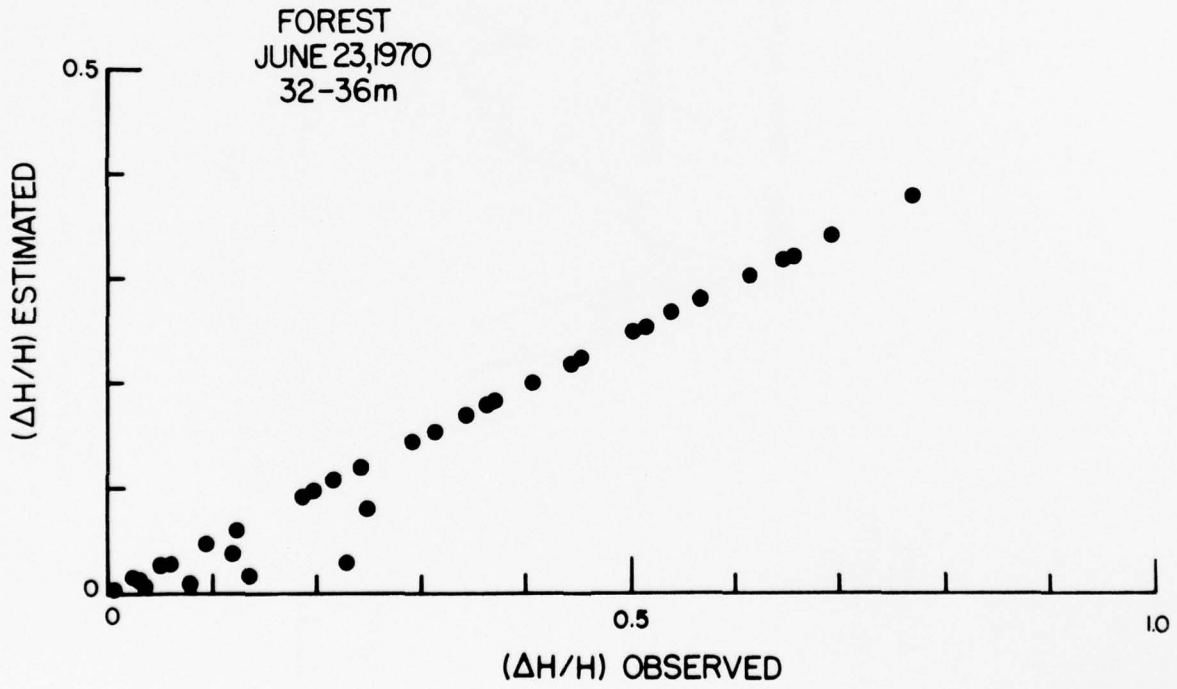

Figure 40. Comparison of estimated and observed discrepancy between sensible heat flux calculations using average and instantaneous values of roughness and displacement height.

Figure 39 may be attributed to the variation in roughness parameter and displacement height throughout the period. The slope of the relationship shown in Figure 40 is not unity, however, which indicates that the discrepancy between the two methods of calculation is actually less than that predicted by the theoretical error analysis.

Finally, Figures 41a, b, 42a, b, 43a, b show values of sensible heat flux for two days each of the months of January, June and September, 1970. Computations were made using mean values of the profile parameters for the three periods for each of three layers above the forest canopy. The characteristic temperature structure above the canopy in January, which was discussed in conjunction with Figure 10a, yields strong upward sensible heat flux from the canopy during the day through the layer 32-36m but variable or downward fluxes through the higher layers due to the tendency for inverted temperature structure in these higher layers. The total transport upward from the canopy was larger for January 8, when there were nine hours of sunshine falling on the canopy than for January 6 when there were only 1. 1 hours of sunshine on the canopy. The sensible heat flux in June tends to be positive through all the layers during the day with slight downward flux at night in the layer immediately above the forest canopy. Both days were partly cloudy with June 20 experiencing more than three but less than eight hours of sunshine at canopy level but June 21 had only a half-hour of sunshine on the canopy during the day. Note that the scales of Figures 42a and b are different and that the total transport was much smaller on June 21. Both days had intermittent rainfall which further tended to interrupt the daytime surge of sensible heat flux from the canopy. The two days in September for which Figures 43a, b were prepared had little sunshine and significant rainfall. While the sensible heat flux tends to be upward during the daytime hours, the values are small and the variability large.

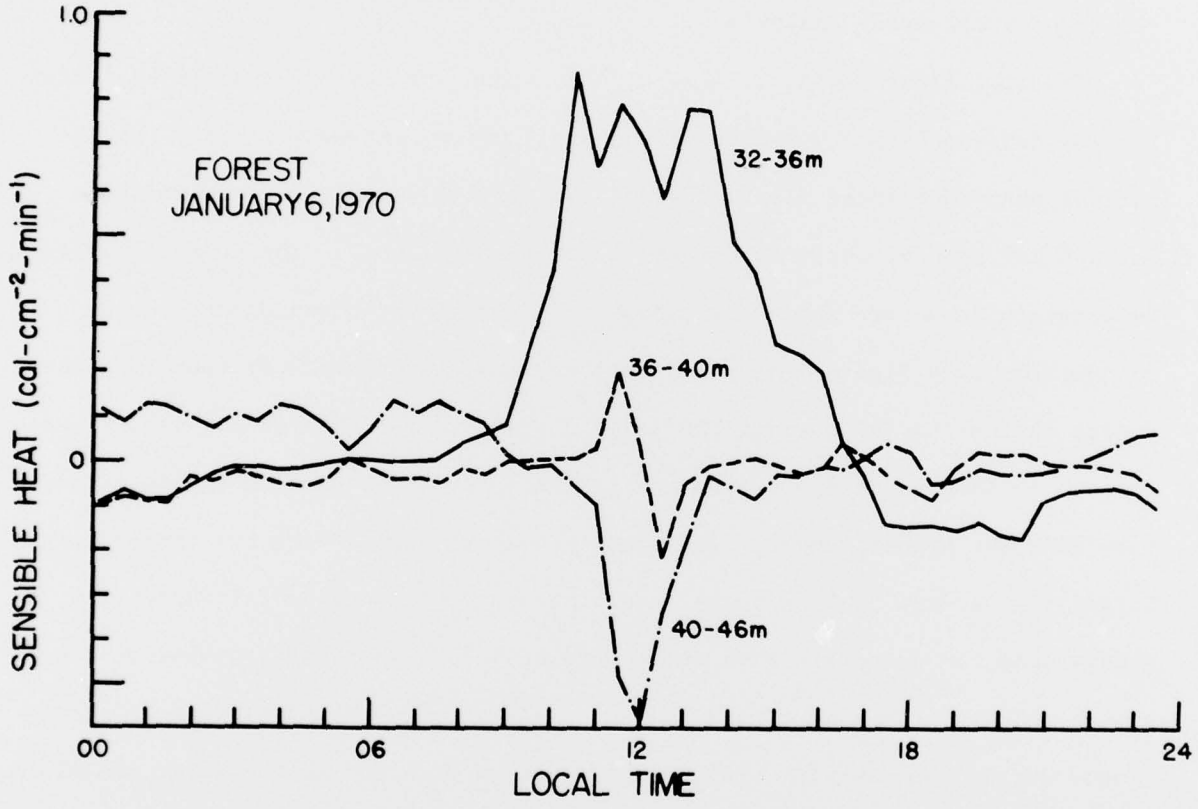

Figure 41a. Sensible heat flux through various layers above the forest for January 6,1970.

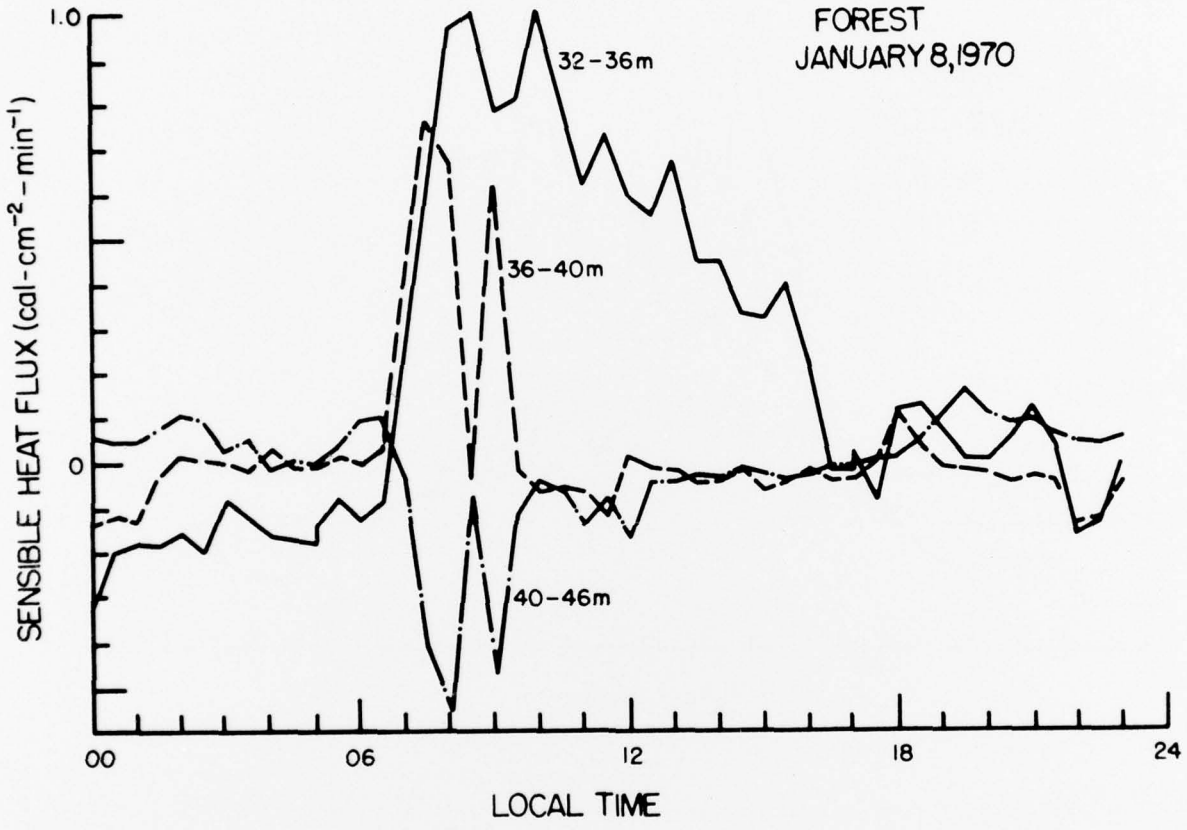

Figure 41b. Sensible heat flux through various layers above the forest for January 8, 1970.

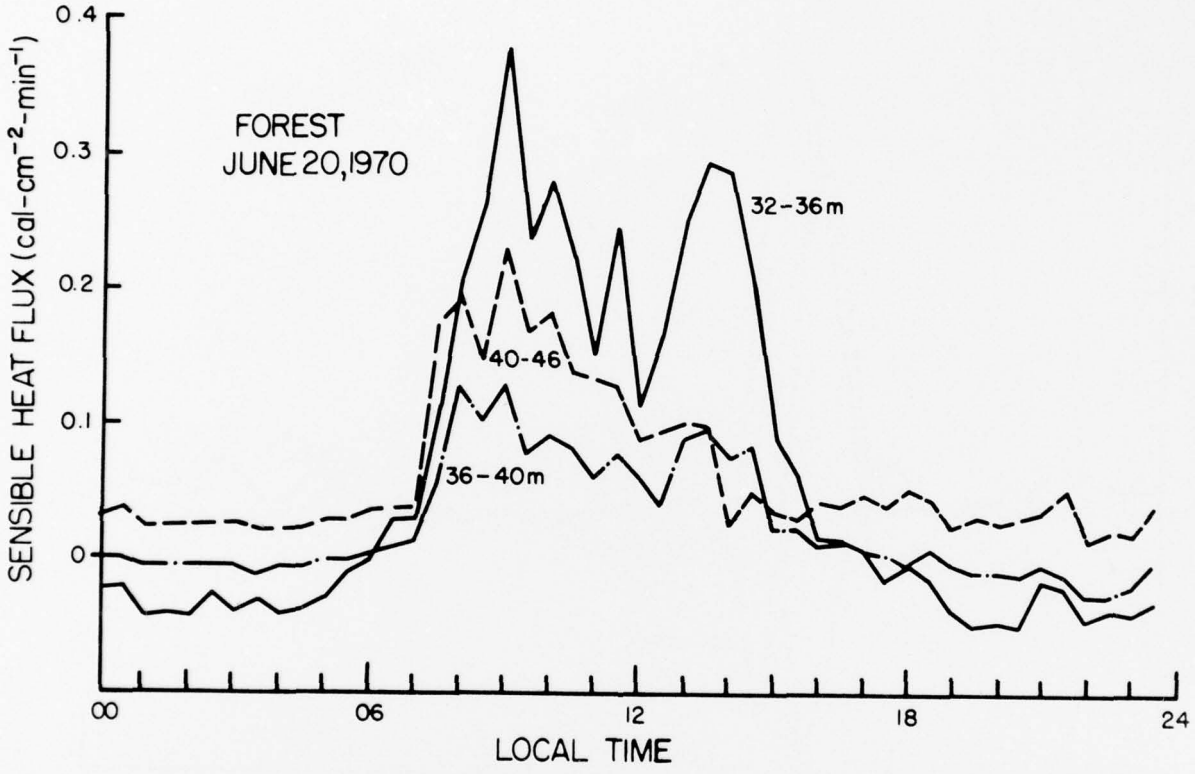

Figure 42a. Sensible heat flux through various layers above the forest for June 20, 1970.

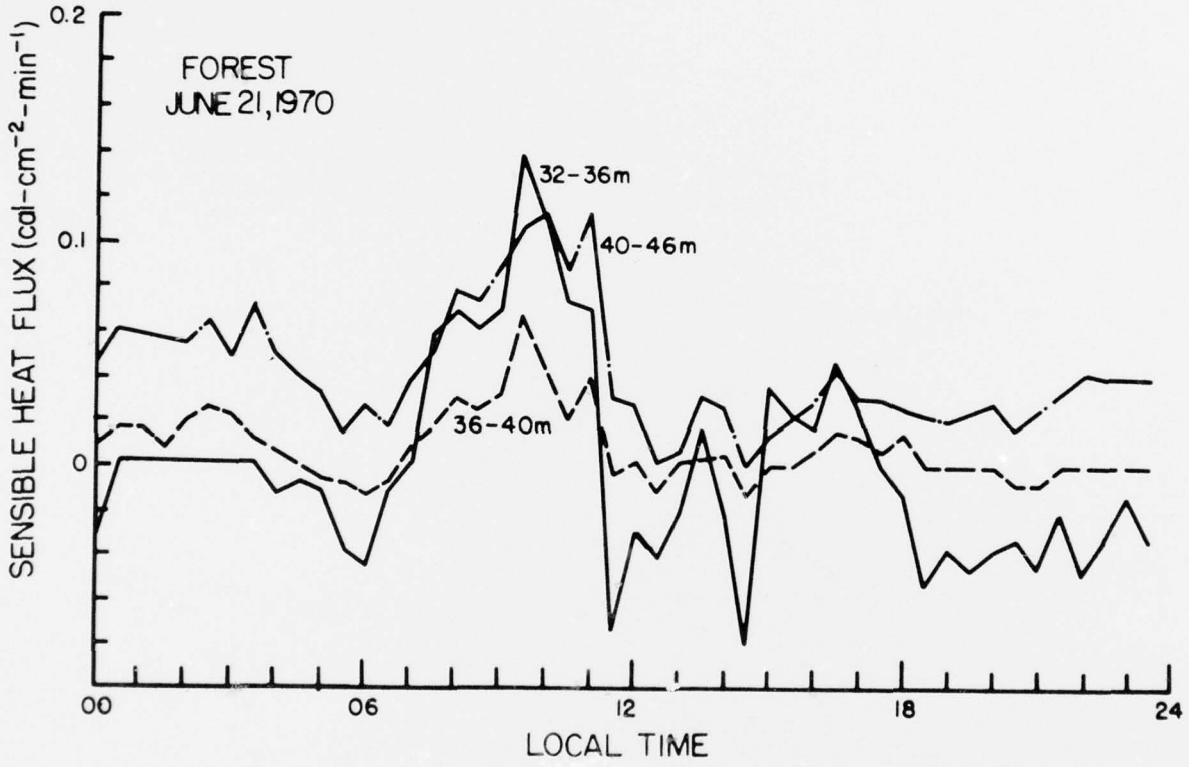

Figure 42b. Sensible heat flux through various layers above the forest for June 21, 1970.

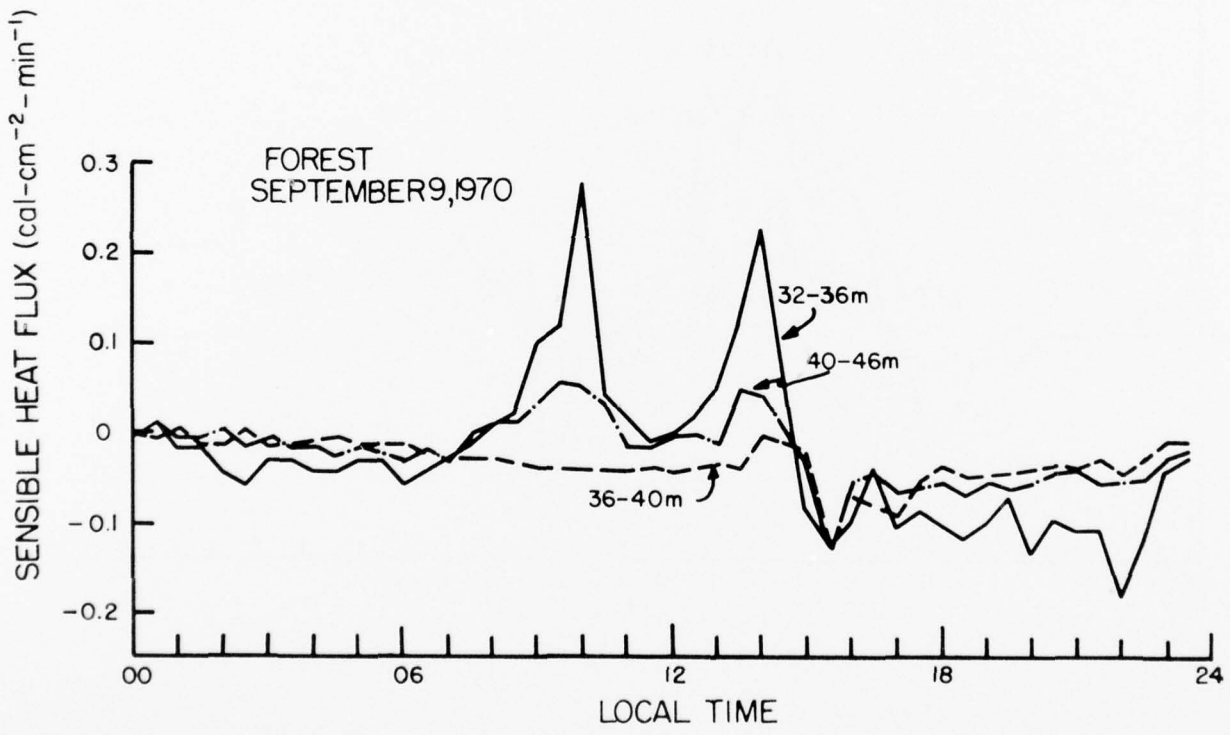

Figure 43a. Sensible heat flux through various layers above the forest for September 9, 1970.

Figure 43b. Sensible heat flux through various layers above the forest for September 10, 1970.

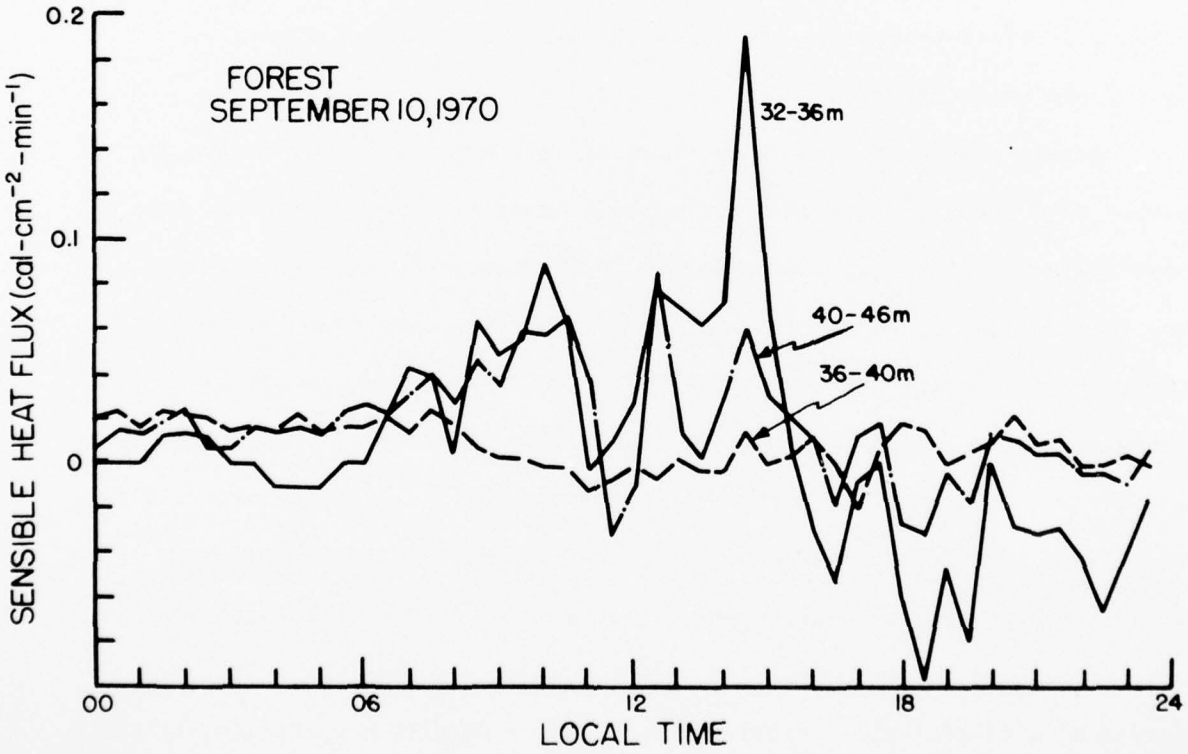

Figure 43b. Sensible heat flux through various layers above the forest for September 10, 1970.

SECTION VI - GENERAL SUMMARY

This report has documented the major results of work done at the University of Maryland over the two year period June, 1972 - August, 1974 under Contract DAAK02-72-C-0287 to the U. S. Army Engineer Topographic Laboratory, Ft. Belvoir, Virginia. The general objective of this work has been to extract scientific information from various raw meteorological data materials collected during Project TREND (Tropical Environmental Data). Project TREND was a large U. S. Army sponsored interdisciplinary scientific field program in the Sakaerat Forest of Thailand conducted during the years 1967-70.

Certain ground station meteorological data were collected during the period Nov. 1967 to Sept. 1970 and certain other micrometeorological data were collected along two towers in the forest area during about the last two years of the field experiment. At our disposal were measurements of temperature, relative humidity, precipitation, evaporation, hours of sunshine, solar radiation, infra-red radiation, profiles of wind, temperature and dew point temperature in the forest canopy and in a cleared area within the forest area, and profiles of temperature beneath the ground at both sites. As the original data tapes logged at the TREND experimental site were in very rough form when they were turned over to the University of Maryland, a considerable effort was required to develop computer processing techniques which would produce a usable data source for scientific analysis. This report documents the condition of the raw data and summarizes the

current usability and availability of TREND Project micrometeorological data.

Data from the TREND project have been analyzed to yield a coherent depiction of the climatological conditions at the Thai forest site. A comparison was made of climatological conditions in the Sakaerat Forest with conditions at a number of locations in Southeast Asia. Locations chosen for comparison generally yield a depiction of the monsoonal cycles on the eastern and western coasts and at low, middle and higher latitudes in the interior of the Southeast Asian land mass. It is found that the local effects of the large scale monsoon system in this area of the world are a strong function of orography and windward proximity to the tropical waters in which the area is nested and that mesoscale variations in, say, precipitation may be quite dramatic in Southeast Asia.

The influence of the tropical forest on the nature of the vertical profiles of wind and temperature have been given in this report. Using profile data on a frequency of once per thirty minutes, careful estimates of forest roughness, datum displacement height and frictional stress have been made for three periods of the year: January (during the cool, dry, northeast monsoon season); June (in the middle of the warm, moist, southwest monsoon season); September (during the month of maximum precipitation, also in the southwest monsoon season). These estimates have been compared with similar information for other types of crop canopy. Spectral analyses of these data have also been carried out for periods of about 10 days in

length during January and June.

Certain elements of the energy budget of the tropical forest were studied. These studies were somewhat limited because of difficulties with extracting usable radiation and dew point temperature data from the original TREND experiment data tapes and certain instrumental malfunctions during the field experiment. Estimates of sensible heat flux were made and are presented. Some calculations of latent heat flux and Bowen's ratio were made using the dew point temperature measurements from the TREND project. Information on incoming and reflected solar radiation fluxes and on the albedo of the Sakaerat Forest are presented. Diurnal variations of net radiation above the forest canopy and at the floor of the forest are given for several days distributed through the year.

Certain aspects of the research initiated during this project will be continued. In particular, attention will be given to the following: extending the survey of wind and temperature profile characteristics of the tropical forest region to include diabatic conditions; estimation of sensible heat fluxes under near-neutral and diabatic conditions for several periods of the year; analysis of other components of the energy budget including conductive heat flux into the soil; extension of spectral analyses of wind and temperature data to higher frequencies by utilizing the once per half-minute profile data; and further attempts to extract usable radiation and dew point information from raw A-tapes for various periods of the year. Sufficient success in these endeavors would provide a comprehensive survey of the energy budget of the tropical forest region which would be of wide interest to environmental scientists.

BIBLIOGRAPHY

Albrecht, F.: "Messgeraete des Waerme-haushaltes au der Erdoberflaeche als Mittel der bioklimat. Forschung", Meteorol. Z. 54, 471, 1937.

Allen, L. H., Jr. (1968: "Turbulence and Wind Speed Spectra within a Japanese Larch Plantation", Journal of Applied Meteorology, Vol. 7, pp. 73-78.

Anstey, R. L. (1966): CLOTHING ALMANAC FOR SOUTHEAST ASIA; Technical Report 66-20-ES, Earth Sciences Division, U. S. Army Nat ick Laboratories, Nat ick, Massachusetts, 1966.

ASRCT (1969): Mesometeorological Network Installation and Instrumentation at ASRCT Sakaerat Experiment Station (Nhakon Ratchasima), Report #5, Cooperative Research Program No. 27, U. S. Army Nat ick Laboratories, Nat ick, Massachusetts (USA).

Baynton, H. W., Hamilton, H. L., Jr., Sherr, P. E., Worth, J. J. B., "Temperature Structure in and Above a Tropical Forest", Quart. J. Roy. Met. Soc. Vol. 91, 1965.

Belt, G. H. (1969): "Estimation of Sensible Heat and Momentum Fluxes in a Boundary Layer of a Pine Plantation (Abstract)", Bulletin of the American Meteorological Society, Vol. 50, pp. 469.

Bowen, J. S., "The Ratio of Heat Losses by Conduction and by Evaporation from any Water Surface", Phys. Rev. 27, 779, 1926.

Crawford, T. V. (1965), "Moisture Transfer in Free and Forced Convection", Quarterly Journal of the Royal Meteorological Society, Vol. 91, (387), pp. 18-27.

Gilman, D. L., F. J. Fuglister and J. M. Mitchell, Jr. (1963): "On the Power Spectrum of 'Red Noise' ", Journal of the Atmospheric Sciences, Vol. 20, pp. 182-184.

Landsberg, H. E. (1966): INTERDIURNAL VARIABILITY OF PRESSURE AND TEMPERATURE IN THE COTERMINOUS UNITED STATES; U. S. Weather Bureau Technical Paper No. 56, (Washington, D. C.) 53 pp.

Landsberg, H. E. (1970):THE ASSESSMENT OF HUMAN BIOCLIMATE - A REVIEW; World Meteorlogical Organization Bulletin, (Geneva) 56 pp.

Leonard, R. E., and C. A. Federer (1973): "Estimated and Measured Roughness Parameters for a Pine Forest", Journal of Applied Meteorology, Vol. 12, pp. 302-307.

Lettau, H. H. (1957): "Computation of Richardson's Numbers Classification of Wind Profiles and Determination of Roughness Parameters", Exploring the Atmosphere's First Mile, Vol. I (ed. by Lettau and Davidson) Pergamon Press, N. Y. and London, pp. 337-72.

Lettau, H. (1970): Final Report, Contract DAAG17-C-0095, U. S. Army Nat ick Laboratories, (Nat ick, Massachusetts) 49 pp.

Lenschow, D. H. and W. B. Johnson (1968): "Concurrent Airplane and Balloon Measurements of Atmosphere Boundary Layer Structure Over a Forest", Journal of Applied Meteorology, Vol. 7, pp. 79-89.

Pasquill, F., 1949. "Eddy diffusion of Water Vapor and Heat Near the Ground", Proc. Roy. Soc. London A 198:116-140.

Rauner, Y. L. (1960): "Teploroi Balans Lesa", Iza. Akad. Nauk SSSR, Ser. Geogr., No. 1, pp. 45-59.

Rider, N. E., 1954. "Eddy Diffusion of Momentum, Water Vapor and Heat near the Soil", Phylos. Trans. A 246:481-501.

Smith, W. L. (1966): NOTE ON THE RELATIONSHIP BETWEEN TOTAL PRECIPITABLE WATER AND SURFACE DEW POINT; Journal of Applied Meteorology, Vol. 5, pp. 726-727.

Stanhill, G. (1969): "A simple Instrument for the Field Measurement of Turbulent Diffusion Flux", Journal of Applied Meteorology, Vol. 8, pp. 509-513.

Stearns, C. R. (1970): "Determining Surface Roughness and Displacement Height", Boundary-Layer Meteorology, Vol. 1, pp. 102-11.

Sverdrup, H. V.: "Evaporation from the Oceans", Compendium of Meteorology, 1071, Boston, 1951.

Swinbank, W. C., 1955, "An Experimental Study of Eddy Transports in the Lower Atmosphere", C.S.I.R.O. Div. Met. Phys. Techn. Paper 2.

Szeicz, G., et al. (1969): "Aerodynamic and Surface Factors in Evaporation", Water Resources Research, Vol. 5, pp. 380-394.

Tajchmann, S. (1967): Energie und Wasserhaushalt Verschiedener Pflanzenbestande bei Munchen, Univ. Munchen Meteor. Inst. Wiss. Mitt., No. 12, 95 pp.

Tanner, C. B., and M. Fuchs, 1968, "Evaporation from Unsaturated Surfaces: A Generalized Combination Method". J. Geophy. Res., 73:1299-1304.

Taylor, R. J., 1960, "Similarity Theory in the Relation Between Fluxes and Gradients in the Lower Atmosphere", Quart. J. Roy. Met. Soc. 86:67-78.

Thornthwaite, C. W. and Holzman, B. 1939, "The Determination of Evaporation From Land and Water Surfaces; Mon. Weath. Rev., 6, pp. 4-11.

Yule, G. U. and M. G. Kendall (1950): AN INTRODUCTION TO THE THEORY OF STATISTICS, C. Griffin Publishers (London).